

Josip Juraj Strossmayer University of Osijek
University of Dubrovnik
Ruđer Bošković Institute
University Postgraduate Interdisciplinary Doctoral Studies
Molecular Biosciences

Katarina Šunić Buljanić

**Metabolic, Biochemical, and Physiological Response of Winter Wheat
(*Triticum aestivum* L.) to Biotic Stress Caused by Infection with *Fusarium*
Species**

PhD Thesis

Osijek, 2025.

Josip Juraj Strossmayer University of Osijek
University of Dubrovnik
Ruđer Bošković Institute
University Postgraduate Interdisciplinary Doctoral Studies
Molecular Biosciences

Katarina Šunić Buljanić

**Metabolic, Biochemical, and Physiological Response of Winter Wheat
(*Triticum aestivum* L.) to Biotic Stress Caused by Infection with *Fusarium*
Species**

PhD Thesis

Osijek, 2025.

TEMELJNA DOKUMENTACIJSKA KARTICA

Sveučilište Josipa Jurja Strossmayera u Osijeku
Sveučilište u Dubrovniku
Institut Ruđer Bošković
Poslijediplomski interdisciplinarni sveučilišni
studij Molekularne bioznanosti

Doktorska disertacija

Znanstveno područje: Interdisciplinarno područje znanosti
Znanstvena polja: biologija, poljoprivreda

Metabolički, biokemijski i fiziološki odgovor ozime pšenice (*Triticum aestivum*) na biotički stres uzrokovan infekcijom vrstama roda *Fusarium*

Katarina Šunić Brčić

Disertacija je izrađena u: Odjelu za oplemenjivanje i genetsku strukturu strnih kultura Poljoprivrednog instituta Osijek (Hrvatska); Zavodu za biokemiju i molekularnu biologiju Odjela za biologiju Sveučilišta Josipa Jurja Strossmayera u Osijeku (Hrvatska); Odjelu za agrobiotehnologiju (IFA-Tulln) Instituta za analitiku i agrometabolomiku Sveučilišta za prirodne resurse i životne znanosti u Beču (BOKU) (Austrija); Odjelu za molekularnu genetiku Leibniz instituta za biljnu genetiku i istraživanje usjeva u Gaterslebenu (IGG Gatersleben) (Njemačka); Laboratoriju za molekularnu biologiju Zavoda za molekularnu biologiju Instituta Ruđer Bošković Zagreb (Hrvatska)

Mentor/i: dr. sc. Valentina Španić, znanstveni savjetnik
dr. sc. Rosemary Vuković, izvanredna profesorica

Kratki sažetak doktorske disertacije: Šest genotipova ozime pšenice (*Triticum aestivum*) koje su s dvije vrste roda *Fusarium* u poljskim i kontroliranim uvjetima kako bi se utvrdio utjecaj fuzarijske paleži klasa (FHB) na metabolički, biokemijski i fiziološki odgovor. Stres izazvan umjetnim inokulacijama utjecao je na razine mikotoksina, izazvao promjene u profilu sekundarnih metabolita, biomarkerima oksidativnog stresa i komponentama antioksidativnog sustava, kao i u relativnim razinama ekspresije gena kod svih proučavanih genotipova. Razina promjene ovisila je o razini otpornosti na FHB, pri čemu su umjereno osjetljivi i osjetljivi genotipovi pokazivali izraženije promjene mjerenih parametara. Ovo istraživanje pridonijeti boljem razumijevanju metaboličkih, biokemijskih i fizioloških mehanizama odgovora na FHB te poboljšanju programa oplemenjivanja na otpornost na FHB u ranim fazama selekcije.

Broj stranica: 156

Broj slika: 37

Broj tablica: 5

Broj literaturnih navoda: 307

Jezik izvornika: Engleski

Ključne riječi: ozima pšenica, biotički stres, fuzarijska palež klasa, obrambeni odgovor

Datum obrane:

Stručno povjerenstvo za obranu:

- 1.
- 2.
- 3.
4. (zamjena)

Disertacija je pohranjena u: Nacionalnoj i sveučilišnoj knjižnici Zagreb, Ul. Hrvatske bratske zajednice 4, Zagreb; Gradskoj i sveučilišnoj knjižnici Osijek, Europska avenija 24, Osijek; Sveučilištu Josipa Jurja Strossmayera u Osijeku, Trg sv. Trojstva 3, Osijek

BASIC DOCUMENTATION CARD

Josip Juraj Strossmayer University of Osijek
University of Dubrovnik
Ruđer Bošković Institute
University Postgraduate Interdisciplinary Doctoral Study of
Molecular biosciences

PhD thesis

Scientific Area: Interdisciplinary area of science
Scientific Fields: biology, agronomy

Metabolic, Biochemical, and Physiological Response of Winter Wheat (*Triticum aestivum* L.) to Biotic Stress Caused by Infection with *Fusarium* Species

Katarina Šunić Brčić

Thesis performed at: Department for Cereal Breeding and Genetics, Agricultural Institute Osijek (Croatia); Subdepartment for Biochemistry and Molecular Biology, Department of Biology, Josip Juraj Strossmayer University of Osijek (Croatia); Department of Agrobiotechnology (IFA-Tulln), Institute of Bioanalytics and Agro-Metabolomics, University of Natural Resources and Life Sciences Vienna (BOKU) (Austria); Department of Molecular Genetics, Leibniz Institute of Plant Genetics and Crop Plant Research (IPK Gatersleben) (Germany); Laboratory for Chemical Biology, Division for Molecular Biology, Ruđer Bošković Institute Zagreb (Croatia)

Supervisor/s: Valentina Španić, PhD, Scientific Adviser
Rosemary Vuković, PhD, Associate Professor

Short abstract: Six winter wheat (*Triticum aestivum* L.) genotypes were inoculated with two *Fusarium* species in the field and controlled conditions to determine the impact of Fusarium head blight (FHB) on metabolic, biochemical, and physiological responses. Stress induced by artificial inoculations affected mycotoxin levels, caused changes in polar metabolite profile, oxidative stress biomarkers and components of the antioxidant system, and relative gene expression levels in the studied genotypes. The level of change depended on the level of FHB resistance, with moderately susceptible and susceptible genotypes exhibiting more pronounced changes in measured parameters. This research contributes to a better understanding of metabolic, biochemical, and physiological mechanisms in response to FHB stress and to the improvement of breeding programmes for FHB resistance in the early stages of selection.

Number of pages: 156

Number of figures: 37

Number of tables: 3

Number of references: 307

Original in: English

Keywords: winter wheat, biotic stress, *Fusarium* head blight, defence response

Date of the thesis defense:

Reviewers:

- 1.
- 2.
- 3.
4. (substitute)

Thesis deposited in: National and University Library in Zagreb, Ul. Hrvatske bratske zajednice 4, Zagreb; City and University Library of Osijek, Europska avenija 24, Osijek; Josip Juraj Strossmayer University of Osijek, Trg sv. Trojstva 3, Osijek

Acknowledgments

Ocjena rada
u tisku

Table of Contents

1. Introduction.....	1
1.1. Wheat.....	2
1.1.1. Origin of wheat.....	2
1.1.2. Importance of wheat in the world.....	2
1.2. Biotic stress in plants.....	4
1.3. Fusarium head blight.....	5
1.3.1. Types of resistance to Fusarium head blight.....	8
1.3.2. <i>Fusarium</i> mycotoxins.....	9
1.4. Plant metabolism in response to biotic stress.....	12
1.5. Photosynthesis in response to pathogen attack.....	13
1.6. Plant antioxidative system under pathogen attack.....	14
1.7. Phytohormones and their role in response to pathogen attack.....	16
1.8. Breeding and sources of resistance to Fusarium head blight.....	18
1.9. New perspectives in breeding for Fusarium head blight resistance.....	18
1.10. Aim of the research.....	20
2. Material and methods.....	22
2.1. Plant material.....	23
2.2. Inoculum preparation.....	23
2.3. Field experiment.....	23
2.3.1. Determination of disease severity and type I resistance to Fusarium head blight.....	25
2.3.2. Mycotoxin analysis.....	26
2.3.3. Polar metabolite profiling.....	27
2.4. Experiment in controlled conditions.....	27
2.4.1. Determination of type II resistance to Fusarium head blight.....	28
2.4.2. Photosynthetic activity.....	30
2.4.2.1. Measurement and analysis of fast chlorophyll <i>a</i> fluorescence.....	30
2.4.2.2. Determination of photosynthetic pigments.....	30
2.4.3. Oxidative stress biomarkers.....	31
2.4.3.1. Determination of the lipid peroxidation level.....	31
2.4.3.2. Determination of hydrogen peroxide content.....	31
2.4.4. Antioxidative plant system.....	32
2.4.4.1. Extraction and determination of the total soluble proteins.....	32
2.4.4.2. Determination of the ascorbate peroxidase activity.....	32
2.4.4.3. Determination of the monodehydroascorbate reductase activity.....	33
2.4.4.4. Determination of the dehydroascorbate reductase activity.....	33
2.4.4.5. Determination of the glutathione reductase activity.....	33

2.4.4.6. Determination of the catalase activity.....	34
2.4.4.7. Determination of the glutathione S-transferase activity.....	34
2.4.4.8. Determination of the guaiacol peroxidase activity.....	34
2.4.4.9. Determination of the total and oxidised glutathione content.....	35
2.4.5. Abscisic acid and salicylic acid analysis.....	35
2.4.6. Molecular analysis.....	36
2.4.5.1. Total RNA isolation from wheat spikes.....	36
2.4.5.2. DNase treatment and cDNA synthesis.....	37
2.4.5.3. Quantitative PCR.....	37
2.5. Statistical analysis.....	38
3. Results.....	40
3.1. Field conditions.....	41
3.1.1. General and type I resistance to <i>Fusarium</i> head blight.....	41
3.1.2. Mycotoxins.....	42
3.1.2.1. Deoxynivalenol, deoxynivalenol-3-glucoside, 3-acetyldeoxynivalenol, and nivalenol content.....	42
3.1.2.2. Zearalenone content.....	45
3.1.2.3. Culmorin, 15-hydroxyculmorin, 15-hydroxyculmoron and 5-hydroxyculmorin content.....	45
3.1.2.4. Aurofusarin, butenolide, chrysogin, and fusarin C content.....	49
3.1.3. Polar metabolites content in naturally infected and inoculated wheat grains.....	51
3.2. Controlled condition (greenhouse).....	56
3.2.1. Type I resistance to <i>Fusarium</i> head blight.....	56
3.2.2. Photosynthetic efficiency.....	58
3.2.2.1. Chlorophyll <i>a</i> fluorescence.....	58
3.2.2.2. Photosynthetic pigments content.....	62
3.2.3. Oxidative status.....	65
3.2.3.1. Lipid peroxidation level.....	65
3.2.3.2. Hydrogen peroxide content.....	66
3.2.4. Antioxidative status.....	66
3.2.4.1. Ascorbate-glutathione cycle.....	66
3.2.4.1.1. Ascorbate peroxidase activity.....	66
3.2.4.1.2. Monodehydroascorbate reductase activity.....	67
3.2.4.1.3. Dehydroascorbate reductase activity.....	68
3.2.4.1.4. Glutathione reductase activity.....	68
3.2.4.1.5. Reduced and oxidised glutathione content.....	69
3.2.4.2. Catalase activity.....	70
3.2.4.3. Glutathione S-transferase activity.....	71

3.2.4.4. Guaiacol peroxidase activity.....	72
3.2.5. Absciscic acid and salicylic acid content.....	72
3.2.5. Genes relative expression levels.....	74
3.2.5.1. <i>NPR1</i> relative expression.....	74
3.2.5.2. <i>TGA2</i> relative expression.....	74
3.2.5.3. <i>PR1</i> relative expression.....	75
3.2.5.4. <i>PR3</i> relative expression.....	76
3.2.5.5. <i>PR5</i> relative expression.....	76
4. Discussion.....	78
5. Conclusions.....	102
6. References.....	106
7. Summary.....	141
8. Sažetak.....	145
9. Supplementary material.....	149
10. Curriculum vitae.....	151
11. Publication list.....	153

Abbreviations

•OH	Hydroxyl radical
15-ADON	15-acetyldeoxynivalenol
¹ O ₂	Singlet oxygen
3-ADON	3-acetyldeoxynivalenol
4-ANIV	4-acetylnivalenol
ABA	Absciscic acid
APX	Ascorbate peroxidase
AsA	Ascorbic acid
AUDPC	Area under disease progress curve
Car	Carotenoids
Car/Chl <i>a</i> +Chl <i>b</i>	Carotenoids to total chlorophyll ratio
CAT	Catalase
cDNA	Deoxyribonucleic acid complementary to messenger RNA
CDNB	1-chloro-2,4-dinitrobenzene
Chl	Chlorophyll
Chl <i>a</i>	Chlorophyll <i>a</i>
Chl <i>a</i> /Chl <i>b</i>	Chlorophyll <i>a</i> to chlorophyll <i>b</i> ratio
Chl <i>b</i>	Chlorophyll <i>b</i>
CUL	Culmospirin
D3G	Deoxynivalenol-3-glucoside
DHA	Dehydroascorbate
DHAPAR	Dehydroascorbate reductase
DNV	Deoxyribonucleic acid
ADON	Deoxynivalenol
dpi	Day post-inoculation
DTNB	5,5-dithiobis (2-nitrobenzoic acid)
EDTA	Ethylene diamine tetraacetic acid
ETI	Effector-triggered immunity
FHB	Fusarium head blight
GC-MS	Gas chromatography mass spectrometry
GPOD	Guaiacol peroxidase
GR	Glutathione reductase
GSH	Reduced glutathione
GSSG	Oxidised glutathione
GST	Glutathione S-transferase

H ₂ O ₂	Hydrogen peroxide
LC-MS/MS	Liquid chromatography tandem mass spectrometry
LOD	Limit of detection
MDA	Malondialdehyde
MDHA	Monodehydroascorbate
MDHAR	Monodehydroascorbate reductase
NADPH	Nicotinamide adenine dinucleotide phosphate
NIV	Nivalenol
NPR1	Non-expressor of pathogenesis related genes 1
O ₂ ^{•-}	Superoxide radical
OJIP	Fluorescence rise from O to P step
PAMPs	Pathogen-associated molecular patterns
PC	Principal component
PCA	Principal component analysis
PCR	Polymerase chain reaction
PI _{abs}	Performance index on absorption basis
PR	Pathogenesis related proteins
PTI	PAMP-triggered immunity
qPCR	Quantitative polymerase chain reaction
QTLs	Quantitative trait loci
RNA	Ribonucleic acid
ROS	Reactive oxygen species
RT	Reverse transcription
SA	Salicylic acid
SAR	Systemic acquired resistance
SO ₂	Superoxide dismutase
TBA	Thiobarbituric acid
TBARS	Thiobarbituric acid reactive substance
TCA	Trichloroacetic acid
TCF	Transcription factors belonging to the basic region leucine zipper family
TGSH	Total glutathione
TNB	5-thio-2-nitrobenzoic acid
TR ₀ /ABS	Maximum quantum yield of primary photochemistry
ZEN	Zearalenone

Ocjena rada
u tijeku

1. INTRODUCTION

1.1. Wheat

1.1.1. Origin of wheat

The domestication of wheat that began 8,000 to 10,000 years ago in the Fertile Crescent between the rivers Euphrates and Tigris marked a significant shift in humankind from hunter-gatherer to sedentary farmer (Curtis & Halford, 2014). Nowadays, cultivated wheat usually refers to two polyploid types: hexaploid bread common wheat, *Triticum aestivum* ($2n = 6x = 42$, BBAADD), and tetraploid durum wheat, *Triticum durum* var. *durum* ($2n = 4x = 28$, BBAA). Genomes (A, B, and D) of hexaploid bread wheat originate from three diploid wild progenitors: *Triticum urartu*, an unidentified relative of *Aegilops speltoides*, and *Ae. tauschii*, respectively (Haaft et al., 2020; Levy & Feldman, 2022). Hexaploid bread wheat is an annual and primarily self-fertilizing plant species which currently accounts for 95% of total wheat production worldwide (Peng et al., 2011; Tadesse et al., 2015). According to its growth habit, it is often classified as winter and spring wheat (Tadesse et al., 2015).

1.1.2. Importance of wheat in the world

Today, wheat is one of the world's most widely grown cereals after maize (Web source 1) and one of the most adapted crops growing in versatile habitats with a plethora of uses developed, such as all sorts of bread, pasta, biscuits, noodle, couscous, and beer (Gustafson et al., 2020; Curtis & Halford, 2014). World wheat production has been steadily rising. This is mostly due to higher wheat yields and more intensive wheat farming rather than land expansion (Reynolds & Loun, 2022). Plant breeding and the further development and application of fertilizers, insecticides, and herbicides had a significant impact on the productivity of wheat. According to the Food and Agriculture Organization of the United Nations (FAO), the world area under wheat cultivation in 2023 was over 220 million ha, resulting in a production of over 798 million t of wheat with a grain yield of 3,625 kg/ha (Figure 1). Asia constituted a significant portion of global wheat production, with China (17%) and India (13%) as the leading producers, while the Russian Federation ranked third, contributing 11% to global wheat production in 2023. In Croatia, wheat was grown in an area of more than 172,000 ha in 2023, resulting in a production of around 834,230 t (Web source 1).

The consumption of wheat is rising worldwide, including regions with climates unsuitable for its cultivation, and the growth of the population will exacerbate the need for wheat even more (Shewry & Hey, 2015). The global population is projected to rise by 2 billion, from the present 7.7 billion to 9.7 billion by 2050, with estimates ranging from 8.9 to 10.7 billion based on varying fertility rates. Assuming a steady annual per capita consumption, this indicates a potential yearly increase of 132 million t of wheat for food by 2050 (ranging from 106 to 224 million t based on the projected fertility) (Reynolds & Braun, 2022). Besides being essential to human civilization, wheat has also enhanced food security, both globally and regionally. It holds the greatest importance among cereals mostly due to its grains, which contain protein with unique physical and chemical properties (Khalid et al., 2023; Španić, 2023). It provides around 20% of daily human requirements for calories and proteins on a worldwide scale and serves as a fundamental food source for 40% of the population (Tadesse et al., 2015).

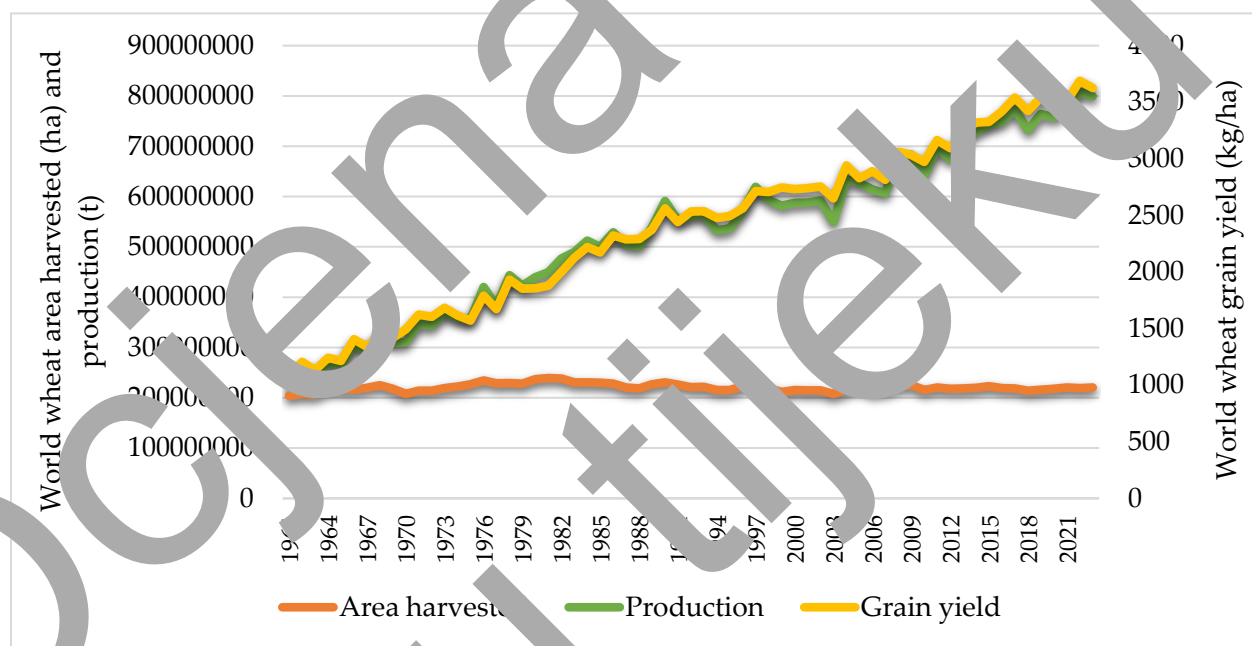


Figure 1. World wheat area harvested, production, and grain yield from 1961 until 2023 (Web source 1).

Besides providing significant daily requirements of energy in the form of carbohydrates and serving as an important source of proteins, wheat also provides significant amounts of dietary fibre, B vitamins, and other micronutrients such as lipids, minerals, and phytochemicals which contribute to a healthy diet (Shewry & Hey, 2015; Hazard et al., 2020; Khalid et al., 2023). However, these components may differ in quantity and content as a result of the effect of genotype and environment.

1.2. Wheat under biotic stress

Along with the increase in the population and the escalation of abiotic stresses due to climate change, biotic stresses significantly threaten wheat production. Climate change also heightens the risk of biotic stress by expanding larger pathogen populations, more frequent disease outbreaks, and enhanced spread of diseases to new areas. Biotic stress adversely affects wheat in growing regions around the world, resulting in annual yield losses of around 22% that are projected to escalate even more. Biotic stress is induced by various living organisms, including fungi, viruses, insects, nematodes, and weeds (Mao et al., 2023).

Among causal agents of biotic stress, pathogenic fungi represent one of the most significant challenges to wheat global production. To survive and cope with such pathogens, wheat has evolved a sophisticated immune system consisting of a passive and active line of defence. Passive defence comprises physical barriers such as cuticle waxes, lignin deposition on cell walls, and specialised trichomes, which prevent pathogens from entering plant cells or the recognition of antimicrobial molecules. Active defence includes two levels of pathogen recognition triggering defence responses: pathogen-associated molecular patterns (PAMP)-triggered immunity or PTI (first level, recognising PAMPs by pattern recognition receptors) and effector-triggered immunity (ETI (recognising pathogen specific effector or Avr proteins by plant resistance or R proteins) (Ali et al., 2018; Gimenez et al., 2013; Iqbal et al., 2011). The first reactions to a pathogen attack include disturbances of the cytosolic calcium concentration and the formation of reactive oxygen species (ROS). These initial responses lead to the activation of mitogen-activated protein kinases and defence hormones, as well as a variety of transcriptional, translational, and metabolic reprogramming. Thus, PTI and ETI lead to a comprehensive reprogramming of wheat gene expression via various receptor proteins, signal transduction cascades, kinases, ROS, hormones, and transcription factors, which protect against invading pathogens (Mehamizadeh & Prasad, 2013; Seybold et al., 2014; Aldon et al., 2018). PTI and ETI are both salicylic acid (SA) dependent and induce a systemic defence response termed systemic acquired resistance (SAR), a type of long-term resistance which results in the stimulation of resistance in plant parts distant from the site of infection (Iqbal et al., 2021; Movahedi et al., 2022).

1.3. Fusarium head blight

Fusarium head blight (FHB) is one of the most devastating mycotoxigenic preharvest fungal diseases globally, infecting cereals such as maize, barley, and wheat. The severe effect of this wheat disease is attributed to the absence of resistant genotypes, substantial grain yield loss, and deterioration of grain quality during epidemic years, as well as the health risks associated with wheat food or feed derived from grains contaminated with mycotoxins produced by the fungi (Dweba et al., 2017; Ma et al., 2020). The dominating species causing FHB fluctuate annually and geographically, based on temperature, rainfall, and crop rotations. Species *Fusarium graminearum* Schwabe (teleomorph *Gibberella zeae*) is the most common pathogen worldwide and was previously considered the only cosmopolitan species. Recent genetic investigations revealed that *F. graminearum* comprises at least 16 species, collectively referred to as the *F. graminearum* species complex (Xu et al., 2005; Boutigny et al., 2011; Sarver et al., 2011; Vaughan et al., 2016; Peršić et al., 2023). *F. graminearum* is a species that can typically be found in warm and hot climate zones with an average annual temperature of over 15 °C. Nevertheless, it is also prevalent in temperate climate regions during the wheat growing season, marked by elevated temperatures and high humidity (Spanic et al., 2010; Mallin et al., 2016; Hietaniemi et al., 2016; Mielniczuk & Skwaryło-Bednarz, 2020). *F. culmorum* (Wm. G. Sm.) Sacc., *F. avenaceum* (Fr.) Sacc., and *F. poae* (Peck) Wollenw. species often infect cereals in cooler regions (Jin et al., 2007; Popovski & Celar, 2013; Engelke et al., 2014). *F. culmorum* exhibits tolerance to fluctuating thermal conditions, although its detrimental impact on cereals is amplified at elevated temperatures. *F. avenaceum* usually occurs in regions with an average annual air temperature ranging from 5 to 15 °C and moderate to high precipitation between 500 and 1,000 mm annually or even above 1,000 mm. Although this species is characteristic for cooler regions, it exhibits considerable tolerance to variations in temperature and humidity. Recent years have witnessed an increased importance of FHB caused by *F. poae*, which while infecting cereal spikes, does not produce usual disease symptoms, but contaminates the grain with mycotoxins. Multiple publications assert that *F. poae* is capable of colonising spikes even under drier conditions (Xu et al., 2008; Mielniczuk & Skwaryło-Bednarz, 2020). Nevertheless, when environmental conditions are not optimal for the primary FHB causal agents, other species such as *F. sporotrichioides* Sherb., *F. crookwellense* L.W. Burgess, P.E. Nelson & Toussoun, *F. roseum* Link (synonym *F. cerealis* (Cooke) Sacc.), *F. equiseti* (Corda) Sacc., *F. tricinctum* (Corda) Sacc., *F. oxysporum* Schltdl., and *F. langsethiae* Torp & Nirenberg are likely to play

significant roles in pathogenesis (Yli-Mattila, 2011; Infantino et al., 2012; Yli-Mattila et al., 2013). Most of the *Fusarium* species can be classified as hemibiotrophs, where in the initial phases of the infection, the pathogen relies on a living host (biotrophic) but then shifts to colonising and killing host cells (necrotrophic) (Ma et al., 2013).

The life cycle of *Fusarium* species comprises a saprophytic and a pathogenic phase (Walter et al., 2010). Infected plant debris, on which the fungus overwinters as the saprophytic mycelia, serves as the primary source of inoculum for disease development. Although the saprophytic mycelia allow the production of both asexual (microconidia, macroconidia, and chlamydospores) and sexual (ascospores) spores, ascospores cause primary infection of wheat (Leplat et al., 2012; Dweba et al., 2017; Brauer et al., 2020). Warm and humid weather triggers the development and maturity of perithecia, and consequently, the production of ascospores simultaneously with the wheat flowering stage. The produced ascospores are then ejected from the mature perithecia and dispersed by wind or rain (Goswami & Kistler, 2004; Leplat et al., 2013).

Wheat is the most susceptible to disease during the flowering stage when the deposition of spores on or inside the spike tissue initiates the infection process. *Fusarium* hyphae then proliferate on the external surfaces of florets and glumes, facilitating the fungus's growth towards stomata and other susceptible spots within the inflorescence. Hyphae can also develop distinctive formations between the cuticle and cell wall on the surface of infected glumes. Such formations are believed to facilitate fungal spread and likely result in direct penetration of epidermal cells. After penetration, *Fusarium* hyphae are able to spread within the cell apoplast. The floret, the anthers, the stigma, and lodicules are most readily colonised, resulting in substantial cytological changes and, ultimately, cell death (Figure 2) (Goswami & Kistler, 2004; Traut, 2009; Walter et al., 2010). Alternative pathways for direct entry encompass stomata and near parenchyma, partially or fully exposed anthers, gaps between the lemma and palea during anther opening, and via the base of the wheat glumes, where the epidermis and parenchyma are thin-walled. The primary mechanism of fungal spread in wheat occurs from floret to floret inside a spikelet and from spikelet to spikelet via the vascular bundles in the rachis and rachilla.

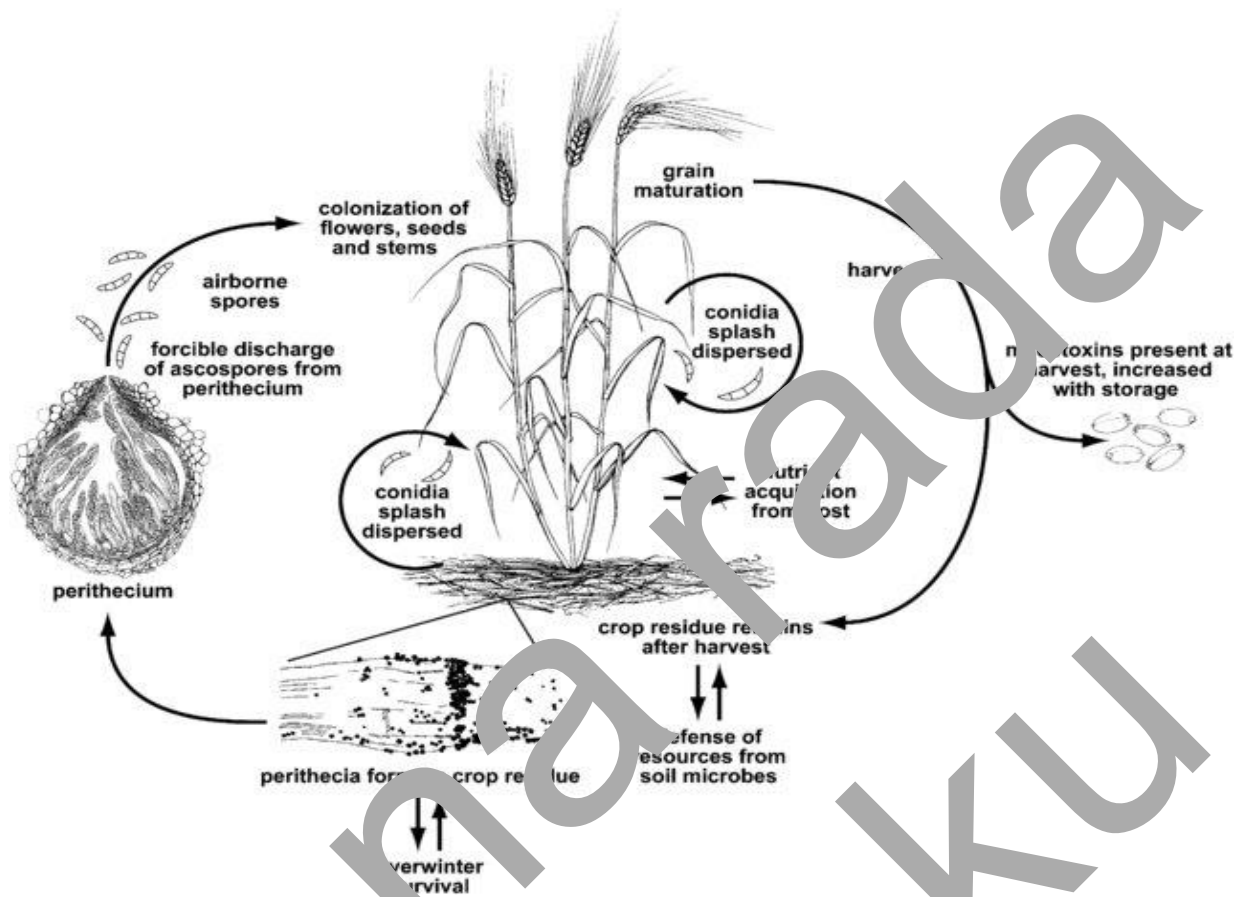


Figure 2. The life cycle of *Fusarium graminearum*, the causal agent of Fusarium head blight on wheat (Trail, 2009).

Symptoms of the disease on the infected spike are evident throughout the milk stage of the grain development. Spikes or isolated spikelets infected by *Fusarium* spp. exhibit a complete discoloration, appearing bleached and tall. Awns of the spike often become deformed, twisted and curved downward. Infected plant tissues undergo earlier senescence, exhibiting the characteristic coloration of mature spikes in comparison to the green, uninfected spikes. Pink sporodochia containing conidial spores, along with a mycelial layer, emerge on infected chaff in spikes following several days of infection under sustained high humidity. Atrophy of infected spikelets blocks grain filling, resulting in a decrease of grain quantity within the spike, while the grains maturing inside infected spikes are often small, grey, shrivelled, exhibiting a loose texture, frequently covered with sporodochia and mycelium (Pirgozliev et al., 2003; Goswami & Kistler, 2004; Golinski et al., 2010; Španić, 2016; Mielniczuk & Skwaryło-Bednarz, 2020).

1.3.1. Types of wheat resistance to *Fusarium* head blight

The resistance of wheat to FHB is complex and encompasses numerous resistance mechanisms (Martin et al., 2017). It includes passive resistance factors (defined by plant characteristics that indirectly reduce susceptibility, including morphological and developmental traits) and active resistance factors (defined by gene products that enhance plant resistance) (Buerstmayr et al., 2020). Morphological and developmental traits such as plant height, spikelet density, awn morphology, flowering date, degree of floret opening at the flowering stage, anther extrusion, and grain filling rate are all associated with passive mechanisms of FHB resistance (Bai et al., 2018; Buerstmayr et al., 2020). For instance, plant height is particularly important for FHB resistance. In field conditions, the pathogen survives on crop debris on the soil surface, serving as a reservoir of inoculum for the subsequent season. For effective infection, *Fusarium* spores need to reach the spikes. Thus, shorter plants are more susceptible to infection by rain-splash-dispersed conidia or ejected ascospores, while taller plants are more likely to evade infection (Jenkinson & Parry, 1994). In addition, microscopic analysis found enhanced hyphal growth on deteriorating tissues including retained anthers, pollen, and stigma, whereas colonisation occurred at a lower rate on the more resistant tissues of the lemma and palea (Kang & Buchenauer, 2000).

Active resistance mechanisms comprise five types of resistance (Martin et al., 2017; Mesterhazy, 2020; Spaniol & Sarcevic, 2022). Schroeder and Christensen (Schroeder & Christensen, 1963) first observed two types of resistance – type I and type II. Type I resistance is characterised by the host's ability to prevent pathogen penetration during the initial phase of infection. It is often assessed by applying a spore suspension to flowering spikes and quantifying disease incidence (the proportion of spikes exhibiting disease symptoms). Type II resistance relates to resistance to the spread of the pathogen inside a spike, and it is assessed by introducing conidia into an individual spike floret and determining the percentage of symptomatic spikelets (Bai & Shaner, 2004). Genotypes exhibiting high type I resistance show reduced final disease severity, even when numerous florets are infected. In contrast, susceptible genotypes with low type II resistance undergo complete bleaching of the spike despite initial infection of only a single spikelet (Bai et al., 2018). The precise evaluation of type I resistance is more challenging than that of type II resistance, which has been thoroughly examined and is frequently used in breeding programmes due to its stability and ease of evaluation (Wu et al., 2022). These two types of resistance were later extended to type III resistance or

resistance to mycotoxin accumulation, type IV resistance or resistance to kernel infection, and type V resistance or tolerance to the FHB (Mesterházy, 1995). Since type III resistance has a role in reducing disease spread, it is often considered a component of type II resistance. In addition, some authors proposed type III resistance to be classified into two categories – resistance to trichothecene accumulation through metabolic transformation and resistance via suppression of trichothecene biosynthesis (Foung et al., 2008). For the parameter of type IV resistance, researchers typically utilise damage:kernel rate (Wu et al., 2022). Tolerance to the FHB or type V resistance assesses the grain yield response to FHB infection.

1.3.2. *Fusarium* mycotoxins

Apart from the reduction of wheat grain yield and quality, each *Fusarium* species produces a distinct profile of secondary metabolites toxic to human and animal health. Consequently, the European Union Commission established legal limits and recommendations for several FHB mycotoxin concentrations in food and feed (European Commission, 2006a, 2006b, 2013; Spanic et al., 2020). Three types of mycotoxins - trichothecenes, fumonigins, and zearalenone, have been demonstrated to induce outbreaks of disease in both humans and animals.

Trichothecenes, sesquiterpene epoxides, are one of the most important and chemically diverse groups of *Fusarium* mycotoxins, which include more than 200 toxins (Escrivá et al., 2015; Ji et al., 2019). Based on the presence of a keto group on the C-8 position, *Fusarium* trichothecenes are divided into two groups: type A, which lacks a keto group, and type B, where a keto group is present (Casquero et al., 2016). Type A trichothecenes mainly comprise the highly toxic T-2 toxin and its deacetylated form HT-2 toxin, diacetoxyscirpenol, and neosolaniol (Ekwomadu et al., 2021). However, some of the most significant trichothecenes are type B trichothecenes - deoxynivalenol (DON) (Figure 3a), nivalenol (NIV) (Figure 3b) and their acetylated derivatives (Spanic et al., 2023). According to the profiles of trichothecene production, specific chemotypes of *Fusarium* spp. were determined (Pirgozliev et al., 2003; Mielniczuk & Skwaryło-Bednarz, 2020). In chemotype I are included strains that produce DON and/or its acetylated forms 3-acetyldeoxynivalenol (3-ADON) and 15-acetyldeoxynivalenol (15-ADON), while in chemotype II are included strains that produce NIV and/or 4-acetylnivalenol (4-ANIV). Within chemotype I, two separate chemotypes are distinguished based on the production of 3-ADON (chemotype IA) and 15-ADON (chemotype IB) (Gilbert & Haber, 2013;

Pasquali et al., 2016). According to Dweba et al. (Dweba et al., 2017), the data indicate that 15-DON is the predominant FHB chemotype worldwide. At the molecular level, trichothecenes exhibit inhibitory effects on the primary metabolism of eukaryotic cells, including the suppression of protein, DNA and RNA synthesis (Allassane-Klein et al., 2013). Diseases linked to these toxins in humans and animals encompass fever, nausea, vomiting, abortions, weight loss, skin irritation, internal organ haemorrhaging, haematological problems, immunosuppression, and neurological disturbances (Escrivá et al., 2015; Ekwomadu et al., 2021).

Zearalenone (ZEN) (Figure 3c), in conjunction with trichothecenes and type B trichothecenes, is regarded as the most significant representative of *Fusarium* mycotoxins concerning human and animal health consequences and related economic losses (Escrivá et al., 2015). ZEN is a 6-(10-hydroxy-6-oxo-trans-11-decenyl)- β -resorcylic acid lactone and is biosynthesized through a polyketide pathway. When present in the body of mammals, ZEN is metabolized to α -zearalenone, which has greater toxicity than ZEN and even low doses of this mycotoxin can affect the sex hormone cycle (Zhang et al., 2018). Due to the structural similarity with the estrogen hormones, ZEN and its metabolites are often termed as nonsteroidal mycoestrogens, a subgroup of naturally occurring estrogenic compounds. Hence, its main target is the reproductive system, where ZEN competitively binds to estrogen receptors. It has been shown that ZEN not only causes changes in the reproductive system, but it can also be genotoxic, immunotoxic, hepatotoxic, nephrotoxic, and an inducer of lipid peroxidation in both domestic and laboratory animals (Pisto et al., 2014). Although ZEN toxicity in humans has not been studied in detail, studies indicate that it has carcinogenic potential and that it can cause reproductive toxicity by acting as an endocrine disruptor (Rai et al., 2020; Han et al., 2022). Prolonged exposure to ZEN through dietary sources in pregnant women may lead to lower embryo survival, reduced fetal weight, and impaired lactation. ZEN is also considered to alter uterine tissue morphology and reduce progesterone and luteinizing hormone levels, while in men, ZEN decreases the number of sperm and their viability and obstructs spermatogenesis (Ropejko & Twarużek, 2021).

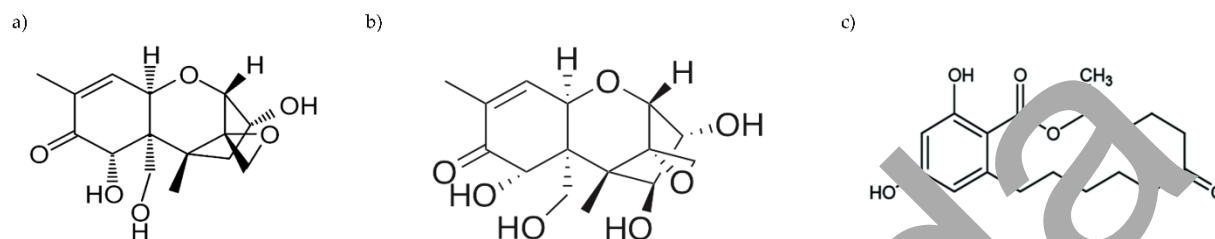


Figure 3. Molecular structures of a) deoxynivalenol (DON), b) nivalenol (NIV), and c) zearalenone (ZEN) (Escrivá et al., 2015).

Occasionally, clinical symptoms of diseases resulting from the consumption of mycotoxin-contaminated food and feed in humans and animals have been significantly more severe than expected based on the measured concentrations of well-known mycotoxins in the food and feed. This has resulted in the identification of “masked” mycotoxins or mycotoxin glucosides, named for their ability to evade detection by standard analytical techniques (Broekaert et al., 2015). Although the term “masked” mycotoxins initially referred to DON and ZEN glucosides, recent discoveries of other mycotoxin derivatives, such as N-deoxyfructosyl-fumonisin, have led to the suggestion of the name “modified” mycotoxins (Nakagawa et al., 2017). While *in vitro* research indicates that masked forms exhibit less toxicity on animal and human cells compared to free mycotoxins, *in vivo* studies reveal that masked forms possess considerable toxicity owing to their enzymatic conversion to the free form. Consequently, it is essential to consistently monitor the prevalence of *Fusarium* mycotoxins and their modified variants in food and feed products (Broekaert et al., 2015; Elvomashi et al., 2021).

Except for “masked” mycotoxins, there are also mycotoxins termed as minor or “emerging”, which refers to mycotoxins which are not routinely determined or legislatively regulated, but the evidence of their incidence is rapidly increasing (Woelflingseder et al., 2019). This category includes mycotoxins such as beauvericin, enniatins, fusaproliferin, moniliformin, and culmorin (CUL). Although CUL is often considered a fungal secondary metabolite, in recent times, it is also referred to as an “emerging” mycotoxin. It is a tricyclic sesquiterpene diol synthesised by many *Fusarium* species, including *F. culmorum*, *F. graminearum*, *F. venenatum*, and *F. cerealis* (syn. *crookwellense*) (Woelflingseder et al., 2019). Only a limited number of studies describing the toxicological relevance of CUL. However, it has been shown that this metabolite possesses antifungal and phytotoxic effect to wheat coleoptile tissue (Weber et al., 2018).

Furthermore, naturally contaminated grain samples are found to have elevated amounts of CUL, which are often positively associated with the levels of DON. Although CUL alone does not seem to impact insects or animals, its co-occurrence with DON may have a synergistic effect on toxicity. Recent results suggest that CUL may inhibit the activity of uridine diphosphate glucosyltransferases. These enzymes, found in most mammalian cells, facilitate the glucuronidation which is a major phase II conjugation pathway for xenobiotics. Consequently, inhibition of these enzymes suppresses glycosylation of DON into the less toxic DON-3-glucoside (D3G) (Wipfler et al., 2019). Other naturally occurring related compounds of CUL include 5-hydroxyculmorin, 7-hydroxyculmorin, and 15-hydroxyculmorin (Weber et al., 2018).

1.4. Plant metabolism in response to pathogen attack

Plants synthesise thousands of distinct metabolites that function to attract pollinators, repel herbivores, resist microbial infection, and provide protection against different kind of stress (Kessler & Kalske, 2015). Plant metabolism is categorised into two main categories: primary metabolism, which comprises molecules essential for the plant's growth, development, and reproduction, and specialised (secondary) metabolism, which includes compounds necessary for the plant to effectively manage abiotic and biotic stress factors. These categories are inherently interconnected, where metabolites from primary metabolism act as building blocks for secondary metabolism (Sulice & McKeown, 2015; Fang et al., 2019).

Metabolites exhibit several functions in plant-pathogen interactions, encompassing pathogen detection, signal transmission, enzyme control, intercellular signalling, and antimicrobial activity (Castro-Moretti et al., 2017). Phytopathogen infection induces modifications in secondary metabolism through the activation of defensive mechanisms, as well as modifications in primary metabolism that impact the plant's growth and development. Consequently, pathogen invasion results in reductions in crop yield, even in cases that do not result in disease or plant death (Berger et al., 2007). A substantial array of metabolites that may function in cereals to mitigate the effects of toxigenic fungi, specifically *Fusarium*, and diminish mycotoxin accumulation has been identified. These metabolites originate from primary and secondary plant metabolism and can be broadly categorised into six principal groups: fatty acids, amino acids and their derivatives, carbohydrates, amines and polyamines, terpenoids, and phenylpropanoids (Atanasova-Penichon et al., 2016). While the biochemical foundations of pathogenesis in plant-

pathogen interactions have been thoroughly examined, recent advancements in metabolomics enable the holistic monitoring of the plant's metabolome and metabolic regulation in response to stimuli, allowing for an integrated study rather than an analysis of isolated pathways (Aliferis et al., 2014). This suggests that in the future, metabolomics could open a new approach in examining plant-pathogen interactions during FHB infection and thus contribute to the discovery and development of a strategy for adapting wheat genotypes resistant to the FHB (Dong et al., 2023).

1.5. Photosynthesis in response to pathogen attack

Phytopathogen infection induces alterations in secondary metabolism through the activation of defence mechanisms, as well as modification in primary metabolism that impact plant growth and development. Although the regulation of defence responses has been thoroughly studied, the impact of pathogen infection on primary metabolism, such as photosynthesis, remains poorly understood (Berger et al., 2007). Photosynthesis is a process that occurs in diverse green organs including leaves, young stems, green fruits, and immature spikes, supplying the energy necessary for numerous processes in plants (Yang & Luo, 2021). The initiation of defence mechanisms and the pathogen's uptake of nutrients subsequently result in greater demand for assimilates inside the plant. However, pathogen infection frequently also results in the formation of chlorotic and necrotic regions on the surface of green organs, which lead to the reduction in chlorophyll (Chl) photosynthesis and photosynthetic assimilate production (Berger et al., 2007; Elneib & Killiny, 2024). Photosynthetic source organs, primarily the leaves, are plant organs that can carry out photosynthesis, whereas photosynthetic sink organs, including stems, roots, fruits, and grains, serve as store organs for the organic matter synthesised by photosynthesis. During various stages of growth and development, the photosynthetic sources and sinks may alter correspondingly (Paul & Foyer, 2001). The down-regulation of photosynthesis, coupled with an increased need for assimilates during plant-pathogen interactions, usually results in the conversion of source tissue into sink tissue (Berger et al., 2007).

In the beginning, plant defence mechanisms and photosynthesis were investigated separately. However, as the mechanisms of plant photosynthesis and immune defence have been clarified, it has been discovered that photosynthesis functions as a basis for signal transduction in plant immune defence, indicating an interconnection between these two processes (Pieterse et al., 2009; Yang & Luo, 2021). The impact of pathogen

infection on photosynthesis can be assessed by photosynthetic pigment analysis and by observing *in vivo* Chl *a* fluorescence. This non-invasive technique involves quantifying the fluorescence of Chl *a* in a dark-adapted plant tissue following exposure to saturating light pulses. Chl *a* fluorescence serves as a highly sensitive indicator of photosynthetic efficiency, as this approach has been reported to show the down-regulation of the effective photosystem II quantum yield in compatible interactions with both biotrophic and necrotrophic pathogens. As such, Chl *a* fluorescence can be used for early detection of pathogen infection when symptoms are not yet visible (Torgersen et al., 2007). Besides Chl, carotenoids (Car) also play a significant role in photosynthesis, photo-oxidative defence, and the synthesis of phytohormones such as abscisic acid (ABA) (Colasuonno et al., 2017).

1.6. Plant antioxidative system under pathogen attack

ROS such as superoxide radical ($O_2^{\cdot-}$), singlet oxygen (1O_2), hydroxyl radical ($\cdot OH$), and hydrogen peroxide (H_2O_2) are produced in different cell parts, including cytoplasm, mitochondria, chloroplasts, and peroxisomes, as natural by-products of aerobic metabolism. However, ROS production is also one of the earliest plant responses following pathogen recognition (Majedi et al., 2016; García-Caparrós et al., 2021). If not regulated, disrupted ROS homeostasis increases plant vulnerability to pathogens through lipid peroxidation, which initiates a chain reaction that intensifies oxidative stress by generating lipid radicals, leading to protein and DNA damage (Mittler et al., 2011; Taheri, 2018; García-Caparrós et al., 2021). Redox homeostasis in plants during stressful conditions is maintained by the plant antioxidative system, which involves both enzymatic and non-enzymatic antioxidants. The enzymes in various subcellular compartments that constitute the enzymatic antioxidant system include superoxide dismutase (SOD), catalase (CAT), ascorbate peroxidase (APX), monodehydroascorbate reductase (MDHAR), dehydroascorbate reductase (DHAR), glutathione reductase (GR), glutathione-S-transferase (GST), and guaiacol peroxidase (GPOD). The other half of the antioxidant system includes ascorbic acid (AsA), glutathione (γ -glutamyl-cysteinylglycine, GSH), α -tocopherol, Car, phenolics, flavonoids, and proline (Das & Roychoudhury, 2014). The involvement of the antioxidative system in defence against pathogens and ROS removal is considered an indicator of wheat genotype resistance (Spanic et al., 2017).

A key role in ROS scavenging by the antioxidant system is assigned to the ascorbate-glutathione (AsA–GSH) cycle, also called the Asada-Halliwell-Foyer cycle or the Foyer-

Halliwell-Asada pathway. The cycle consists of metabolites (AsA, GSH, and nicotinamide adenine dinucleotide phosphate (NADPH)) and enzymes (APX, MDHAR, DHAR, and GR) which regenerate reduced forms of AsA and GSH (Foyer & Kunert, 2024).

The initial stage of the cycle involves the reduction of H_2O_2 to H_2O by APX utilising AsA as the electron donor. Oxidised AsA or monodehydroascorbate (MDHA) may subsequently either undergo spontaneous disproportionation to AsA and dehydroascorbate (DHA) or be enzymatically reduced to AsA by enzyme MDHAR, utilising the reducing potential of NAD(P)H. DHA is converted to AsA by the enzyme DHAR, utilising reduced GSH as the reducing agent. The enzyme GR converts oxidised glutathione (GSSG) to GSH with NADPH as the reductant (Figure 4) (Foyer & Halliwell, 1976). In addition to its function in ROS scavenging, the AsA-GSH cycle also modulates the signalling capacity of AsA and GSH. As AsA and GSH, the principal redox buffers of plant cells, interact with various compounds, the alterations in their concentrations induced by ROS can be detected and transmitted to other redox-sensitive signalling pathways, such as those mediated by phytohormones like SA and ABA (Foyer & Noctor, 2011).

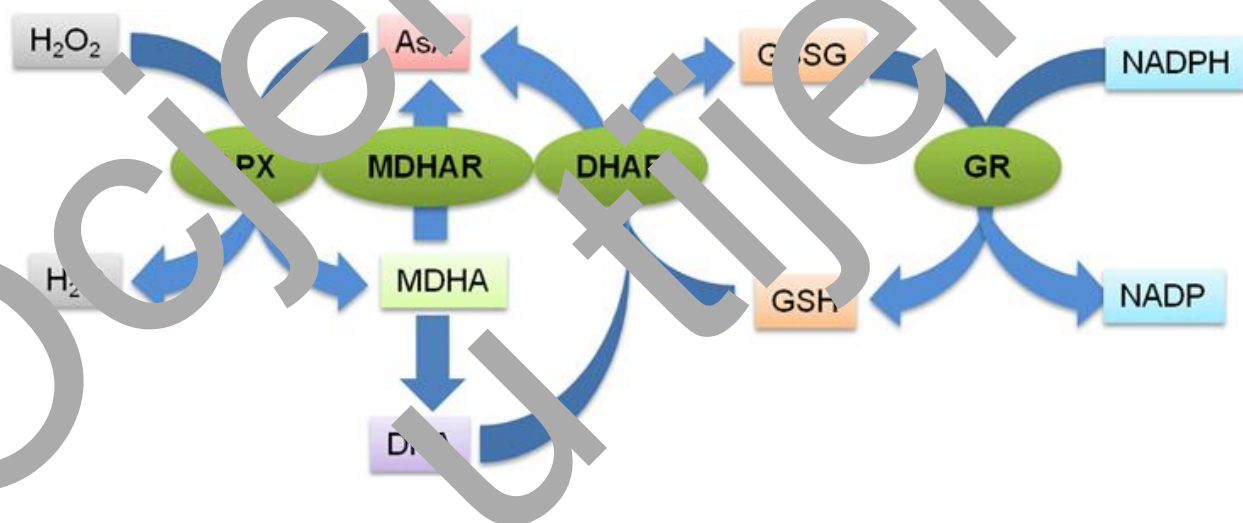


Figure 4. Schematic representation of the ascorbate-glutathione (AsA-GSH) pathway. H_2O_2 (hydrogen peroxide); H_2O (water); AsA (ascorbic acid); MDHA (monodehydroascorbate); DHA (dehydroascorbate); GSSG (oxidised glutathione); GSH (reduced glutathione); NADPH (reduced nicotinamide adenine dinucleotide phosphate); NADP (nicotinamide adenine dinucleotide phosphate); APX (ascorbate peroxidase); MDHAR (monodehydroascorbate reductase); DHAR (dehydroascorbate reductase); GR (glutathione reductase) (Pandey et al., 2015).

1.7. Phytohormones and their role in response to pathogen attack

Plants synthesise a diverse array of hormones, including auxins, gibberellins, ABA, SA, cytokinins, ethylene, jasmonic acid, brassinosteroids, and peptide hormones (Bari & Jones, 2009). Alterations in hormone concentrations or sensitivity, induced by interactions with biotic agents, initiate a series of hormone-signalling events that regulate adaptive responses in plants. The ultimate result of the activated defence response is significantly affected by the content and dynamics of combinations of produced hormones (Verhage et al., 2010).

ABA is a 15-carbon sesquiterpenoid containing two chiral centres. Consequently, one of these centres (at C-1') allows for the differentiation of two ABA forms: the natural (+)-ABA (cis-trans) and its unnatural stereoisomer (-)-ABA (trans-trans) (Kitahata & Asami, 2011). In higher plants, ABA is synthesised through an indirect carotenoid pathway (as it originates with the cleavage of β -carotene, the C40 carotenoid precursor), in contrast to a direct pathway that initiates with intermediates containing 15 or fewer carbon atoms (Chen et al., 2020). ABA detection initiates with the binding with pyrabactin-resistance 1/pyrabactin-resistance like/regulatory component of ABA protein receptors, commonly known as PYLs. The binding of ABA to these receptors inhibits the activity of protein phosphatase 2C, subsequently activating sucrose nonfermenting 1-related protein kinase 2. Activated through autophosphorylation or other protein kinases, sucrose nonfermenting 1-related protein kinase 2 then phosphorylates specific substrates (such as transcription factors and proteins), resulting in ABA-related physiological responses (Girdler et al., 2020). Although ABA is a well-known plant hormone which is essential for regulating stress tolerance, its function extends beyond abiotic stress responses to encompass other developmental processes, including seed dormancy, germination, and seedling growth (Vishwakarma et al., 2017). In addition to its recognised function in physiological processes and adaptation to abiotic stresses, ABA has recently also been regarded as a modulator of response to different diseases of plants, specifically in mediating FHB susceptibility in wheat (Gordon et al., 2016). While ABA can influence resistance in both positive and negative directions depending on the pathogen, the prevailing evidence suggests that ABA functions more as a susceptibility factor, particularly for fungal diseases (Mauch-Mani & Mauch, 2005; Asselbergh et al., 2008). Regardless of the considerable advancements in comprehending ABA signalling and

response at the molecular level, knowledge about cereals remains sparse (Gietler et al., 2020).

SA (2-hydroxybenzoic acid) is a member of a broad class of phenolic substances, characterised by an aromatic ring with a hydroxyl group or a functional derivative, synthesised by plants (Dempsey et al., 2011). Recent characterisation of the SA biosynthesis process identified two different pathways - the isochlorogenicate pathway and the phenylpropanoid pathway, both of which originate from chlorismate the end product of the shikimate pathway (Li et al., 2019). Besides participating in the enhancement of plant development, photosynthesis, flowering, and post-harvest longevity, SA is a phytohormone that significantly influences plant defence mechanisms. It is usually involved in activating defence responses against biotrophic and hemi-biotrophic infections, as well as in establishing SAR (Bari & Jones, 2009; Pokotylo et al., 2019). A major effect of SA in plant defence is the induction of pathogenesis-related (PR) genes expression, which encode proteins exhibiting antimicrobial properties. So far, PR proteins have been grouped into 17 families mainly based on their protein sequence similarities, enzymatic activities, and other biological features (Ali et al., 2018). The biochemical role of PR1 remains unidentified. However, a recent study indicated that PR1 possesses sterol-binding activity, which impedes pathogen proliferation by sequestering sterol from pathogens. In addition, other PR proteins show diverse functions, including β -1,3-glucanase (PR2), chitinases (PR3), a thaumatin-like protein (PR5), peroxidases (PR9), plant defensins (PR11), and thionins (PR13) (Ali et al., 2018; Ali et al., 2018). SA-mediated defence signalling requires nonexpression of pathogenesis-related genes 1 (NPR1), a redox-sensitive regulator and an SA receptor (Ulrich et al., 2023). Over 98% of SA-regulated genes exhibit expression that relies on NPR1. Before pathogen infection, NPR1 is located in the cytoplasm as oligomers formed through intermolecular disulfide bonds. Following pathogen stimulation or SA treatment, NPR1 experiences conformational alterations facilitating the translocation of NPR1 monomers into the nucleus. NPR1 then interacts with transcription factors TGA, which are in a basic leucine zipper form, and activates the transcription of PR genes (Withers & Dong, 2016; Qi et al., 2018; Arif et al., 2020; Peng et al., 2021). However, SA-mediated defence is not flawless. Numerous strategies exist through which plant pathogens escape this defence mechanism. The disruptive techniques employed by the pathogens can be classified into three primary strategies: (1) directly reducing SA accumulation by converting it to inactive derivatives (Li et al., 2017), (2) obstructing SA production by targeting specific pathways (Liu et al.,

2014), and (3) interfering with SA signalling (Qi et al., 2018). The insights acquired from these studies may be utilised to design effective approaches for managing plant diseases by inhibiting the impairment of SA-mediated plant defence mechanisms (Qi et al., 2018).

1.8. Breeding and sources of resistance to Fusarium head blight

The effective management of FHB cannot be accomplished with only one control technique, as each possesses certain limits. The utilisation of several control techniques, including cultural, biological, chemical, and host plant resistance, constitutes effective measures for managing FHB. Genetic control, through breeding for resistance, when combined with other aforementioned control measures, has the ability to serve as a sustainable solution for FHB management (Dwivedi et al., 2015; Zhu et al., 2019). However, the efficacy of breeding programmes targeting FHB-resistant genotypes is predominantly dependent upon several factors, including the accessibility of resistant germplasm, genetic diversity within breeding populations, and methodologies for accurately assessing the resistance levels of breeding lines to facilitate the efficient selection of improved individuals (Steiner et al., 2017).

Resistance to FHB is a quantitative inherited trait affected by environmental factors, exhibiting notable genotype × environment interactions (Andersen et al., 2007; Steiner et al., 2017). Despite substantial efforts to identify FHB resistance during the past decades and thousands of accessions evaluated, only a limited number of resistant accessions have been recognised, and sources of resistance for FHB enhancement in breeding programmes remain scarce. Some of them include Arina, Fundulea 201R, and Renan from Europe, Wanghui 1 and Sumai 3 from China, Froiana and Encruzilhada from Brazil, Chinkabouzu and Nobeokabouzu from Japan, and Ernie and Freedom from the United States (Shi et al., 2020). While several resistant accessions have been effectively utilised to enhance FHB resistance in global wheat-breeding programmes, the majority have proven ineffective due to their unfavourable agronomic characteristics or the challenges associated with integrating the resistance into elite lines (Shi et al., 2020).

1.9. New perspectives in breeding for Fusarium head blight resistance

Breeding for FHB resistance was long limited to phenotypic selection. However, the advancement of high-throughput marker systems facilitated the incorporation of genotypic data in the development of new wheat genotypes. Molecular breeding

techniques, including marker-assisted selection and the more sophisticated genomic selection, utilise associations between markers and traits to predict phenotypes and identify favourable genotypes, significantly enhancing the rate of genetic gain. In marker-assisted selection, molecular markers that indicate quantitative trait loci (QTLs) for improving FHB resistance are employed for indirect selection (Buerstmayr et al., 2020). Utilising QTLs from genetic sources to breed for FHB resistance is one of the most efficient strategies for managing this disease and mitigating toxin contamination in harvested grains (Wu et al., 2022). Hundreds of QTLs, including 50 unique QTLs, associated with FHB resistance have been found throughout all 21 wheat chromosomes, but only a few QTLs have been validated across research and successfully applied in breeding programmes worldwide (Buerstmayr et al., 2020; Steiner et al., 2017; Ren et al., 2019; Venske et al., 2019; Fabre et al., 2020; Shi et al., 2020). The most significant and well-validated resistance QTL was found in Chinese germplasm, *Fhb1*, initially discovered in Sumai 3, is the most accurate QTL for FHB resistance and is extensively utilised in breeding programmes (Su et al., 2019). In addition, derived from Sumai 3 are also *Fhb2* and *Qfhs.ifa-5A* (Španić, 2016). Additional resistant sources comprise the QTL *Fhb4* and *Fhb5* identified in Wangshuibai and *Qfhs.nau-2DL* discovered in the breeding line CJ9306. Furthermore, wild relatives of wheat have also provided multiple resistance genes/loci, including *Fhb3* from species *Leymus racemosus* (Qi et al., 2008), *Fhb6* from *Elymus tsukushensis* (Cannon et al., 2015), and *Fhb7* from *Thinopyrum elongatum* (Guo et al., 2015), all conferring Type II resistance (Wu et al., 2022). To enhance the utility of these mapped QTLs for plant breeding and to better understand FHB resistance in wheat and other small grain cereals, a thorough QTL meta-analysis has demonstrated efficacy. Several QTL meta-analyses have been conducted on FHB resistance in wheat (Liu et al., 2009; Löffler et al., 2009; Mao et al., 2010), with the most recent study identifying a total of 323 QTLs and generating 65 meta-QTLs which are regions statistically validated as unique (Venske et al., 2019). Candidate gene mining inside the meta-QTL 1 on chromosome 3B yielded 324 genes, where 10 of these genes were found responsive to FHB. Two of these genes encode a glycosyltransferase and cytochrome P450, proteins that have already been confirmed to contribute to FHB resistance. However, the remaining eight genes require more investigation (Venske et al., 2019). It is, therefore, imperative to identify additional FHB resistance QTLs, especially those exhibiting major effects and high stability across different environments, to increase resistance diversity for sustainable FHB management.

and to extend the selection of FHB-resistant germplasm for breeding programmes (Ren et al., 2019).

Genomic selection, in contrast to the marker-assisted selection, utilises all available marker data to calculate the genomic estimated breeding value, thereby capturing variation from typically undetectable minor-effect QTLs. Genomic selection is a completely predictive methodology designed to predict the phenotype of untested genotypes by utilising estimated marker effects, using existing knowledge of the phenotypic performance of previously genotyped lines known as the training population (Buerstmayr et al., 2020). As breeding for FHB resistance is mostly based on phenotypic data and FHB resistance is strongly influenced by the environment, accurate assessments of the actual genetic resistance of specific breeding lines are often imprecise. Therefore, utilising genomic estimated breeding values for selection rather than phenotypic data may enhance the breeder's capacity for the selection of individuals with FHB resistance (Arruda et al., 2019).

1.10. Aim of the research

Due to frequent exposure to a diverse array of pathogens, wheat plants have evolved complex mechanisms to control responses to these pathogens. Despite of numerous previous studies trying to decipher the mechanisms of resistance to FHB, the complexity of these mechanisms is still insufficiently investigated. Previous studies focused mainly on the investigation of separate plant systems while studying wheat response to FHB (e.g. antioxidant system). This study is a first comprehensive analysis investigating the metabolic, physiological, biochemical, and molecular response of different winter wheat genotypes to FHB stress in field and controlled environments. It focuses on the mycotoxins and polar metabolites in wheat grains, oxidative stress markers, enzymatic and nonenzymatic antioxidants, photosynthetic efficiency, stress hormone levels, and stress-responsive gene expression, shedding light on potential interactions between defence mechanisms during infection.

The basic hypothesis of the research is that mycotoxin levels vary in different winter wheat genotypes and under different environmental conditions, with higher levels in genotypes that are more susceptible to FHB and in environments that favour greater infection development. In addition, FHB will alter the polar metabolite profile of the genotypes studied, with metabolite synthesis being induced or suppressed depending on

the genotype's resistance or susceptibility. Furthermore, it is hypothesised that FHB will induce a genotype-specific antioxidant response in artificially infected plants, with FHB-susceptible genotypes showing more pronounced changes. In order to investigate the validity of the hypotheses, the following research objectives were set:

- to determine the impact of FHB on winter wheat genotypes (*Triticum aestivum* L.) that differ in the level of resistance to FHB
- to determine the impact of the disease on the synthesis of polar metabolites and mycotoxin levels in wheat grain
- to determine biochemical, physiological, and molecular responses of wheat spikes to FHB.

This research will enable the selection of genotypes with more effective defence mechanisms against FHB, which will contribute to developing genotypes tolerant to FHB in the wheat breeding program.

Ocjena rada
u tileku

2. MATERIAL AND METHODS

2.1. Plant material

Field experiment and experiment in controlled conditions (greenhouse) will be conducted on six winter wheat (*Triticum aestivum* L.) genotypes (Malka, Kraljica, Galloper, Tika Taka, El Nino, and Golubica) originating from the Agricultural Institute Osijek. All selected genotypes were characterised as early or very early winter wheat genotypes with varying levels of resistance to FHB based on the results obtained in the previous field experiments (Spanic et al., 2017).

2.2. Inoculum preparation

Fusarium species used in this experiment were *F. graminearum* (PIO 31), isolated from the winter wheat collected in the eastern part of Croatia, and *F. culmorum* (IFA 104), obtained from IFA-Tulln, Austria. The conidial inoculum of *Fusarium* spp. was produced by a mixture of wheat and oat grains (3:1 by volume). Grains were soaked in glass jars filled with distilled water overnight. The following day, excess water was decanted, and the grains were sterilized. To inoculate the mixture of grains with macroconidia, a piece of synthetic nutrient agar containing fungal mycelium of each species isolate was placed in the appropriate jar. The glass jars were left at room temperature exposed to diffused daylight and shaken daily for two weeks to ensure proper aeration and drying. Macroconidia were then washed off the colonized grains with sterilised water, and the suspension was diluted while final conidial concentration of both fungi were determined using a hemocytometer (Bürker-Türk, Leucht Assistent, Sondheim vor der Rhön, Germany) and were set to 1×10^5 mL⁻¹ for the inoculation in the field experiment, and 5×10^4 mL⁻¹ for the inoculation in controlled conditions.

2.3. Field experiment

The field experiment was conducted in the growing season 2019/2020 at Osijek (45° 32' N, 18° 44' E) and Tovarnik (45° 10' N, 19° 09' E), Croatia. The soil types in these two regions are the major soil types used for crop production in continental Croatia, eutric cambisol and black soil chernozem, respectively. According to data from the Croatian meteorological and hydrological service, the precipitation during the growing season (from October 2019 until July 2020) was 408.6 mm in Osijek and 448.3 mm in Tovarnik, and the average temperature was 11.1 °C in Osijek and 11.7 °C in Tovarnik (Figure 5). The amount of precipitation during May, at the flowering stage (Zadoks scale 65) (Zadoks

et al., 1974), when the plants are the most vulnerable to FHB, was 53.3 mm in Osijek and 58.8 mm in Tovarnik, while the average temperature was 15.3 °C in Osijek and 15.6 °C in Tovarnik. The seeds of six winter wheat genotypes were sown with a plot sowing machine (Hege 80, Wintersteiger) in October 2019 in 7.56 m² plots at the experimental field of the Agricultural Institute Osijek at Osijek and at the experimental field of Agro-Tovarnik at Tovarnik. The seed density was 330 seed m⁻² for all wheat genotypes. The field experiment was set up in a randomized complete block design, where two replicates were subjected to artificial *Fusarium* treatment and two replicates were subjected to natural infection treatment. *Fusarium* treatment was performed when 50% of the plants inside each plot were at the flowering stage, with 100 mL of prepared inoculum sprayed on an area of 1 m². One treatment was grown according to standard agronomical practice with no usage of fungicide and without misting treatment, while another treatment was subjected to two inoculation events, two days apart, using a tractor-back (Osijek) and hand sprayer (Tovarnik). To provide high humidity necessary for the development of the infection, misting was provided by water spraying with sprinklers on several occasions after inoculations. Except for fungicide application, which was excluded in these experiments, the agro-technical practices utilized were usual for commercial wheat cultivation in Croatia. The seed was treated with Vitavax 200 F (carboxin) at a rate of 200 g Vitavax per 100 kg of seeds in order to control seed-borne diseases. Weed control was conducted with a herbicide at the wheat tillering stage (Zadoks scale 31) (Zadoks et al., 1984). Insecticides were sprayed in the spring of the growing season. Fertilization was in proportions N:P:K 130:100:120 kg ha⁻¹. In July 2020, experimental plots were harvested with a Wintersteiger reel plot combine-harvester, and grains were stored until further analysis.

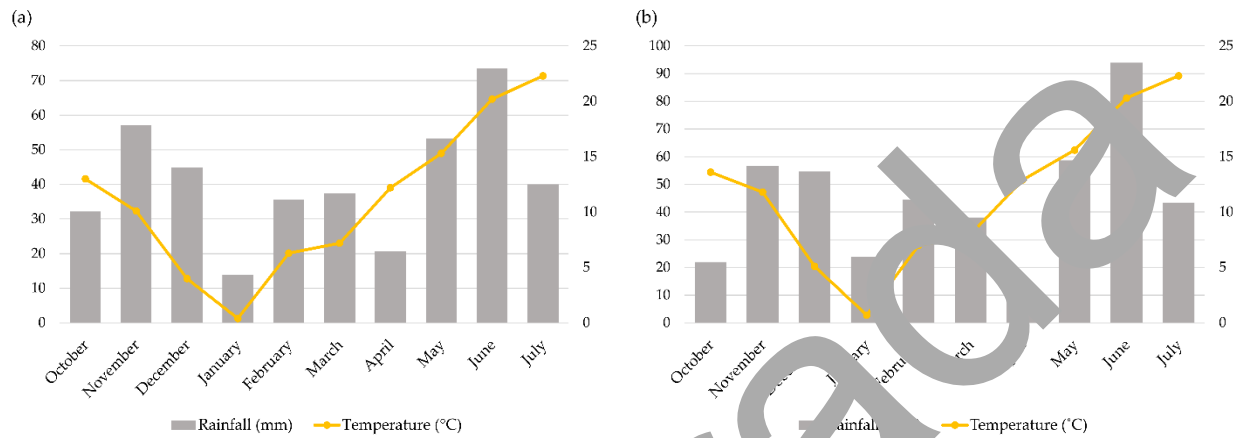


Figure 5. Climate diagrams for the growing season 2019/2020 for (a) Osijek and (b) Tovarnik.

2.3.1. Determination of disease severity and type I resistance to Fusarium head blight

General resistance (disease severity) represented a percentage of diseased spikelets in the plot and was determined by assessing the whole plot area, which consisted of 4,400–4,600 plants. Type I resistance (resistance to initial infection) indicated a percentage of diseased spikes per plot and was determined following an evaluation of a random sample of 30 spikes. Both general and type I resistance were firstly evaluated on 10th day post-inoculations (dpi), followed by the next four evaluations at four-day intervals (on the 14th, 18th, 22nd, and 26th dpi) according to a linear scale (0–100%) after which the area under the disease progress curve (AUDPC) was calculated according to the following formula:

$$AUDPC = \sum_{i=1}^n \left\{ \left[\frac{Y_i + Y_{i-1}}{2} \right] * (X_i - X_{i-1}) \right\},$$

where Y_i is the percentage of visibly infected spikelets ($Y_i/100$) at the i^{th} observation, X_i is the day of the i^{th} observation, and n is the total number of observations.

2.3.2. Mycotoxin analysis

Determination of mycotoxins was performed by liquid chromatography tandem mass spectrometry (LC-MS/MS) (Sulyok et al., 2020). Two replicates from naturally infected (control) and *Fusarium* inoculated treatment were pooled together, resulting in one measurement for naturally infected and one measurement for *Fusarium* inoculated treatment. Due to the method accuracy and reliability, one measurement was found to be sufficient in this kind of experiment. Previously grounded by mill IK A M20 (Staufen, Germany), 5 g of wheat grains were extracted using 20 mL extraction solvent (acetonitrile:water:acetic acid = 79:20:1, *v/v/v*) on a rotary shaker (GFL 3017, GFL; Burgwedel, Germany) for 90 min at room temperature in a horizontal position. After extraction, 0.5 mL of the extract was diluted with 0.5 mL of dilution solvent composed of acetonitrile:water:acetic acid = 20:79:1 (*v/v/v*) in vial. Finally, 5 μ L was injected into an LC-MS/MS system, and the screening of target fungal metabolites was performed with a QTrap 5500 LC-MS/MS System (Applied Biosystems, Foster City, CA, USA) equipped with a TurboIon Spray electrospray ionization source and a 1290 Series HPLC system (Agilent, Waldbronn, Germany).

Chromatographic separation was performed at 25 °C on a Gemini 18-column, 150 \times 4.6 mm i.d., 5 μ m particle size, equipped with a C18 4 \times 3 mm i.d. security guard cartridge (all from Phenomenex, Torrance, CA, USA). The eluents used were composed of methanol:water:acetic acid = 10:89:1 (*v/v/v*) as eluent A, and methanol:water:acetic acid = 97:2:1 (*v/v/v*) as eluent B. Confirmation of positive analyte identification was obtained by the acquisition of two multiple reaction monitorings per analyte (with the exception of moniliformin and 2-nitropropionic acid that exhibit only one fragment ion), which yielded 4.0 identification points according to commission decision (European Parliament and the Council of the European Union, 2002). In addition, the liquid chromatography retention time and the intensity ratio of the two multiple reaction monitorings transitions agreed with the related values of an authentic standard within 0.03 min and 30% relative deviation, respectively. Quantification was performed via external calibration using serial dilutions of a multi-analyte stock solution. Results were corrected for apparent recoveries obtained for wheat (Sulyok et al., 2020). The accuracy of the method is verified on a continuous basis by regular participation in proficiency testing scheme organized by BIPEA (Gennevilliers, France).

2.3.3. Polar metabolite profiling

Determination of polar metabolites was performed by gas chromatography mass spectrometry (GC-MS). Prior to extraction for metabolic analyses, the grains were flash frozen in liquid nitrogen and ground in 10 mL plastic tubes together with a grinding ball for 2 min per sample in the automatic Labman's cryogenic grinding system (Labman, Middlesbrough, UK). Polar metabolites were extracted from 15 mg of deep-frozen homogenized plant material using the polar metabolite extraction protocol (Lisec et al., 2006; Erban et al., 2007; Riewe et al., 2012, 2016). Extraction proceeded by adding 1 mL chilled extraction buffer (methanol:chloroform:water = 2.5:1, v/v) containing 1 μ L of a 2 mg mL⁻¹ stock solution of ¹³C-sorbitol, and D4-Aminine to the flash frozen and pulverized tissue. Following 15 min incubation at 4 °C, 0.4 mL of water was added and the extraction was split into three batches and aliquots of 50 μ L of polar phase were sampled. The dried extracts were immediately derivatised directly prior to injection (Erban et al., 2007) using a Gerstel MPS2-XI autosampler (Gerstel, Mühlheim/Ruhr, Germany) and analysed in split mode (1:3) using a LECO Pegasus HT time-of-flight mass spectrometer (LECO, St. Joseph, MI, USA) connected to an Agilent 7890 gas chromatograph (Agilent, Santa Clara, CA, USA).

Sample identification of known and unknown features was performed by the LECO ChromaTOF software package in conjunction with the Polar Metabolome Database. Peak intensities were determined using the R package *targetsearch* (Cuadros-Inostroza et al., 2009) within the R software version 4.1.1 (R Core Team, 2021) and normalized regarding sample weight, internal standards and measuring day/ detector response. Metabolites showing >5% missing values among the samples were excluded from the analysis.

2.4. Experiment in controlled conditions

Seeds of each winter wheat genotype were first sown in seedlings' trays and placed at room temperature to germinate. Trays with five-day-old winter wheat seedlings were moved in a plant growth chamber for six weeks to undergo a period of vernalization (12/12 h light/dark photoperiod, 4/3 °C day/night temperature, with light intensity reduced by 60%, and 60% relative humidity). Plants were then transferred in 2.5 L pots filled with soil (pH: 5.5–7.0, organic matter: 70.0–85.0%, N (1/2 vol.): 100–200 mg L⁻¹, P₂O₅ (1/2 vol.): 100–150 mg L⁻¹, K₂O (1/2 vol.): 200–400 mg L⁻¹) and placed in a greenhouse (Gis Impro d.o.o., Vrbovec, Croatia). During the tillering stage (Zadoks scale 21) (Zadoks et

al., 1974), the conditions maintained in the greenhouse were 10/14 h light/dark photoperiod, 10–14/8–12 °C day/night temperature, with the maximum light intensity of 250 $\mu\text{mol m}^{-2} \text{s}^{-1}$. With the start of the stem elongation stage (Zadoks scale 12) (Zadoks et al., 1974), conditions were set up to be 12/12 h light/dark photoperiod and 10–13/11–14 °C day/night temperature, while before flowering stage (Zadoks scale 51) (Zadoks et al., 1974) and until the end of experiment conditions were set up to be 14/10 h light/dark photoperiod, 21–24/17–20 °C day/night temperature with the maximum light intensity of 750 $\mu\text{mol m}^{-2} \text{s}^{-1}$ (Figure 6). During the experiment, plants were irrigated with water as necessary, usually twice weekly. Nitrogen fertilization was carried out at the two-leaf development stage (Zadoks scale 12) (Zadoks et al., 1974) using calcium ammonium nitrate (27% nitrogen) and one protection against pests with the insecticide Vantex (gamma-cyhalothrin 60 g L⁻¹) (Zadoks scale 31) (Zadoks et al., 1974).

When the anthers started to extrude and the flowering stage appeared (Zadoks scale 61) (Zadoks et al., 1974), plants were inoculated with a mixture of *F. graminearum* and *F. culmorum* inoculum. The 20 μL of prepared inoculum mixture was injected with an automatic pipette (Eppendorf, Wien, Austria) in the middle of two spikelets of the spike of each plant. Plants were subjected to two inoculation events, 10 days apart. To provoke infection, watering treatment started one hour after each inoculation and lasted for the next 36 h when foggers sprayed the water every hour for a period of 2 min. Each treatment consisted of six replicates set up in a randomized complete block design, where each replicate contained four plants/pot. Untreated plants were used as controls. Ten days after inoculation, spike tissue for determination of photosynthetic pigments, lipid peroxidation level, the content of H₂O₂, GSH and GSSG, activities of the enzymes CAT, SOD, GP, and activities of the enzymes of the Ascorbate-GSH cycle (APX, MDHAR, DHAR and GR) and molecular analysis was sampled, frozen in liquid nitrogen, and stored at -80 °C prior to further analysis. For the analysis of stress hormones, ABA and SA, sampled wheat spikes were frozen in liquid nitrogen and lyophilized.

2.4.1. Determination of type II resistance to Fusarium head blight

Type II resistance to FHB (resistance to disease spread within the spike) was evaluated by counting the number of infected spikelets in the inoculated spike of one plant per pot on the 10th dpi.



Figure 6. Experiment in controlled conditions – (a) vernalisation in the plant growth chamber for six weeks, (b) plants in the tillering stage, (c) appearance of the first node and beginning of the stem elongation stage, (d) emergence of the spike, and (e) plants in the flowering stage (author: Katarina Šunić Budimir).

2.4.2. Photosynthetic activity

2.4.2.1. Measurement and analysis of fast chlorophyll *a* fluorescence

Chl *a* fluorescence measurements on spikes of inoculated and control wheat were performed at four measurement points: 24 h after inoculations, 48 h after inoculations, 168 h after inoculations, and 240 h after inoculations. The OJIP fluorescence transients were measured with a Handy-PEA fluorimeter (Plant Efficiency Analyzer, Hansatech Instruments Ltd., King's Lynn, Norfolk, UK). For each of the two genotypes, six plants from the controlled treatment and six plants from the FHB inoculated treatment were analysed by performing measurements on spikes. Before measurement, wheat spikes were fully dark-adapted for 30 min using a light weight 10 cm² clips shutter plate. The Chl *a* fluorescence was induced with a saturated red-light pulse (3,200 $\mu\text{mol m}^{-2} \text{s}^{-1}$, peak at 650 nm). Fluorescence intensity at 20 μs (F_0), fluorescence intensity at 300 μs (F_{300}), fluorescence intensity at 2 ms (F_i), fluorescence intensity at 30 ms (F_j), maximal fluorescence intensity (F_m) and time needed to reach F_m (t_{max}) were used by OJIP test to calculate biophysical parameters that quantify the stepwise energy flow through photosystem II. Parameters calculated and included in this study were: the maximum quantum yield of primary photochemistry (TR_0/ABS) and performance index on an absorption basis (PIabs) (Strasser et al., 2004; Yusuf et al., 2010).

2.4.2.2. Determination of photosynthetic pigments

For spectrophotometric determination of the photosynthetic pigments, previously frozen wheat spike tissues was ground in 10 mL of glass steel jar containing a grinding ball for 30 min at 30 Hz using a TissueLyser (Qiagen Retsch GmbH, Hannover, Germany). Fresh wheat spike tissue powder was homogenized in absolute acetone, followed by extraction for 15 min at 4 °C and centrifugation for 15 min at 16,000 $\times g$ and 4 °C. The supernatant was decanted into plastic tubes, and the extraction procedure with cold acetone was repeated three more times until the precipitate became colourless. The re-extracted supernatants were collected in the same test tube, and their volume was measured with a beaker. The extracts were then diluted to a final volume of 10 mL, and then transferred to a glass cuvette, in which the absorbances of the extracts were measured spectrophotometrically at 470 nm, 645 nm, and 662 nm (Lichtenthaler, 1987). The concentration of pigments was expressed in mg of Chl, i.e. Car per g of fresh weight ($\text{mg} \times \text{g}^{-1} \text{FW}$).

2.4.3. Oxidative stress biomarkers

2.4.3.1. Determination of the lipid peroxidation level

The level of lipid peroxidation in the wheat spikes was determined by a spectrophotometric method that measures thiobarbituric acid reactive substances (TBARS), mainly malondialdehyde (MDA) (Verma & Dubey, 2003). About 0.2 g of tissue, previously grounded in 10 mL stainless steel jars containing a grinding ball for 1 min at 30 Hz using a TissueLyser (Qiagen Retsch GmbH, Hanover, Germany), was homogenized with 1 mL of 0.1% (*w/v*) trichloroacetic acid (TCA), and the extraction was carried out for 15 min on ice. After extraction, the homogenates were centrifuged for 15 min at $16,000 \times g$ and 4°C . The resulting supernatant (0.5 mL) was mixed with 1 mL of 0.5% thiobarbituric acid (TBA) in 20% TCA. A blank sample was prepared in the same way, where 0.5 mL of 0.1% TCA was added instead of the sample. The reaction mixture was then incubated for 30 min in a water bath at 95°C , during which the reaction of MDA with TBA was accompanied by a change in colour to red. The reaction was stopped by cooling the reaction mixture on ice, after which the mixture was centrifuged for 5 min at $16,000 \times g$ and 4°C . The amount of TBARS was determined spectrophotometrically by measuring absorbance at 520 nm and 600 nm. Absorbance at 600 nm was subtracted from absorbance at 520 nm to correct for non-specific reaction. The amount of TBARS, as a product of lipid peroxidation, was calculated based on the molar extinction coefficient ($\epsilon=155 \text{ mM}^{-1} \times \text{cm}^{-1}$) and expressed in nmol per g of fresh weight ($\text{nmol} \times \text{g}^{-1} \text{FW}$).

2.4.3.2. Determination of hydrogen peroxide content

H_2O_2 content was estimated according to the method described by (Junglee et al., 2014). For determination of the amount of H_2O_2 in wheat spikes, 0.2 g of wheat tissue was crushed in 10 mL stainless steel jars containing a grinding ball for 1 min at 30 Hz using a TissueLyser (Qiagen Retsch GmbH, Hanover, Germany). The tissue was homogenised by adding 1 mL of 0.1% (*w/v*) TCA, and the extraction was carried out for 15 min on ice. After extraction, the homogenates were centrifuged for 15 min at $16,000 \times g$ and 4°C , and the resulting supernatant was decanted and protected from the light. The method is modified for the microplate assay, and the measurements were performed using Greiner UV Star 96-well plates on a Spark multimode microplate reader with SparkControl software (Tecan, Männedorf, Switzerland). The reaction mixture consisted of 0.1 mL of extract, 2 mM potassium phosphate buffer (pH 7.0), and 0.4 M potassium iodide in a final

volume of 0.25 mL. After incubation for 30 min at 25 °C, the absorbance was recorded at 390 nm at 25 °C. The content of H₂O₂ was determined using a standard curve obtained with known amounts of H₂O₂, and the results were expressed in nmol × g of fresh weight (nmol × g⁻¹ FW).

2.4.4. Antioxidative plant system

2.4.4.1. Extraction and determination of the total soluble proteins

The wheat spike tissue powder obtained by grinding was homogenized with a cold 100 mM phosphate buffer (pH 7.0) containing 1 mM ethylenediaminetetraacetic acid (EDTA). Homogenized samples were then incubated for 5 min on ice and centrifuged for 15 min at 19,000 × g, and 4 °C. Aliquots of obtained protein extracts were stored at -80 °C until further analysis. Protein concentration in the enzyme extracts was determined using bovine serum albumin as a protein standard (Bradford, 1976), adapted for measurement in microtiter plates. The method is based on the shift of the absorption maximum from 465 nm to 595 nm, which occurs when the dye Coomassie brilliant blue from the Bradford reagent binds to proteins. The reaction mixture, which consisted of 5 µL of diluted protein extract and 0.25 mL of commercial Bradford reagent (Sigma-Aldrich, Steinheim, Germany), was incubated for 5 min at room temperature. The intensity of the resulting blue coloration was measured at a wavelength of 595 nm on a Spark multimode microtiter plate reader with SparkControl software (Tecan, Männedorf, Switzerland). Bovine serum albumin was used as a standard in the concentration range of 0.125 - 1.4 mg mL⁻¹, and the protein concentration was calculated from the standard curve and expressed in mg per g of fresh weight (mg × g⁻¹ FW). The enzymes' activities were measured using Spark multimode microplate reader with SparkControl software (Tecan, Männedorf, Switzerland).

2.4.4.2. Determination of the ascorbate peroxidase activity

APX (EC 1.11.1.11) activity was determined according to the method described by Nakano and Asada (Nakano & Asada, 1981) and adjusted for a microplate assay. The reaction mixture (0.205 mL) consisted of 0.6 mM AsA, 5 mM H₂O₂, and 10 × diluted protein extract in 50 mM potassium phosphate buffer (pH 7.0). After 3 min of incubation at room temperature, the decrease in absorbance was measured at 290 nm for 5 min every

15 s. The APX activity was calculated using a molar extinction coefficient ($\epsilon=2.8 \text{ mM cm}^{-1}$) and expressed in units of APX activity per g of protein ($\text{U g}^{-1} \text{ protein}$).

2.4.4.3. Determination of the monodehydroascorbate reductase activity

MDHAR (EC 1.6.5.4) activity was determined according to a method described by Hossain et al. (Hossain et al., 1984) and adjusted for a microplate assay. The reaction mixture consisted of 50 mM Tris-HCl buffer (pH 7.8), 0.45 mM NADH, 2.25 mM AsA, and diluted protein extract in a final volume of 0.2 mL. After equilibration at room temperature, the reaction was started by adding ascorbate oxidase in a final concentration of 0.14 U mL^{-1} . The decrease in absorbance was monitored at 340 nm for 3 min. MDHAR activity was calculated using the molar extinction coefficient ($\epsilon=3.7 \text{ mM cm}^{-1}$) and expressed in units of MDHAR activity per g of protein ($\text{U g}^{-1} \text{ protein}$).

2.4.4.4. Determination of the dehydroascorbate reductase activity

DHAR (EC 1.8.5.1) activity was determined by a method based on monitoring the GSH-dependent reduction of DHAR described by Ma and Cheng (Yang M. & Cheng, 2004) and adjusted for a microplate assay according to Murshed et al. (Murshed et al., 2008). The reaction mixture consisted of 50 mM HEPES buffer (pH 7.0), 0.05 mM EDTA, 2.25 mM GSH and 0.2 mM DHAR (0.2 mM). The increase in absorbance was recorded at 265 nm for 3 min. DHAR activity was calculated using the molar extinction coefficient ($\epsilon=8.33 \text{ mM cm}^{-1}$) and expressed in units of DHAR activity per g of protein ($\text{U g}^{-1} \text{ protein}$).

2.4.4.5. Determination of the glutathione reductase activity

GR (EC 1.6.1.2) activity was measured according to a method by Racker et al. (Racker, 1959) and adjusted for microplate assay by Murshed et al. (Murshed et al., 2008). The reaction mixture consisted of 50 mM HEPES buffer (pH 8.0), 0.45 mM EDTA, 0.23 mM NADPH, and protein extract in a final volume of 0.2 mL. After 10 min of equilibration at room temperature, the reaction was started by adding GSSG in a final concentration of 0.5 mM. The decrease in absorbance was monitored at 340 nm for 5 min every 15 s. GR activity was calculated using the molar extinction coefficient for NADPH ($\epsilon=3.7 \text{ mM cm}^{-1}$) and expressed in units of GR activity per g of protein ($\text{U g}^{-1} \text{ protein}$).

2.4.4.6. Determination of the catalase activity

CAT (EC 1.11.1.6) activity was estimated according to the method described by Aebi (Aebi, 1984) using H_2O_2 as a substrate, and adjusted for a microplate assay. The reaction mixture consisted of 0.036% H_2O_2 in 50 mM potassium phosphate buffer (pH 7.0) and the reaction started with the addition of 50 μL of diluted protein extract. For measurement purposes, the wheat spike protein extract was diluted 4 \times . The decrease in absorbance due to the oxidation of H_2O_2 was measured at 240 nm for 3 min every 15 s. CAT activity was calculated using the molar extinction coefficient ($\epsilon=0.036 \text{ mM}^{-1} \text{ cm}^{-1}$) and expressed in units of CAT activity per g of protein ($\text{U g}^{-1} \text{ protein}$).

2.4.4.7. Determination of the glutathione S-transferase activity

GST (EC 2.5.1.13) activity was determined by the method of Habig et al. (Habig et al., 1974), which is based on the formation of glutathione-2,4-dinitrobenzene due to the conjugation of 1-chloro-2,4-dinitrobenzene (CDNB) with GSH. The method is adjusted for a microplate assay. The reaction mixture consisted of 1mM GSH, 2 mM CDNB, 1 mM EDTA, and 5 μL of undiluted protein extract in 100 mM phosphate buffer (pH 7.5) in a final volume of 0.2 mL. After incubation for 2 min at room temperature, the increase in absorbance was monitored at 240 nm for 3 min every 15 s. GST activity was calculated using a molar extinction coefficient of glutathione-1-chloro-2,4-dinitrobenzene conjugate ($\epsilon=5.7 \text{ mM}^{-1} \text{ cm}^{-1}$) and expressed in units of GST activity per g of protein ($\text{U g}^{-1} \text{ protein}$).

2.4.4.8. Determination of the guaiacol peroxidase activity

GPOD (EC 1.11.1.7) activity was determined by the method described by Siegel and Galston (Siegel & Galston, 1967), adjusted for microplate assay. The method is based on the oxidation of guaiacol to tetraguaiacol due to the presence of H_2O_2 . The reaction mixture consisted of 18 mM guaiacol and 5 mM H_2O_2 in 50 mM phosphate buffer (pH 7.0) in the final volume of 0.2 mL. The reaction was started by adding the 20 \times diluted sample, and the increase in absorbance was monitored at 470 nm for 3 min every 15 s. GPOD activity was calculated using the molar extinction coefficient ($\epsilon=15.83 \text{ mM}^{-1} \text{ cm}^{-1}$) and expressed in units of GPOD activity per g of protein ($\text{U g}^{-1} \text{ protein}$).

2.4.4.9. Determination of the reduced and oxidized glutathione content

GSH and GSSG contents were determined using a kinetic method based on a continuous reduction of 5,5-dithiobis (2-nitrobenzoic acid) (DTNB) to 5-thio-2-nitrobenzoic acid (TNB) by GSH, where GR and NADPH reduce the GSSG (Griffin, 1980), modified for the microplate assay. For total GSH (tGSH) and GSSG content determination, the frozen wheat spike tissue powder was homogenized with 5% 5-sulfosalicylic acid solution (1:10 *w/v*) and centrifuged for 15 min at $16,000 \times g$ and 4°C . The reaction mixture for tGSH measurement consisted of 10 μL of resulting supernatant, 0.03 mg mL^{-1} DTNB, 0.11 U mL^{-1} GR, 1 mM EDTA, and 100 mM phosphate buffer ($\text{pH } 7.0$) in a final volume of 0.21 mL. Following a 5-min equilibration period, NADPH in a final concentration of 0.04 mg mL^{-1} was added to initiate a reaction. The formation of TNB was continuously recorded at 412 nm for 5 min at 25°C . The amount of tGSH was determined by a standard curve of GSH. For GSSG determination, 2% of vinylpyridine and 5% of triethanolamine were added to an aliquot of deprotonized supernatant, and the reaction mixture was incubated for 1 h at room temperature. The measurements were performed the same way as for the tGSH. The content of GSSG was determined using a standard curve of GSSG, and the results were expressed as nmol per g of fresh weight ($\text{nmol g}^{-1}\text{FW}$). From the difference between tGSH and GSSG, the GSH content was obtained and expressed as nmol per g of fresh weight ($\text{nmol g}^{-1}\text{FW}$).

2.4.6. Abscisic acid and salicylic acid analysis

Determination of stress hormones ABA and SA was performed by LC-MS/MS. After plant tissue sampling, the samples were frozen in liquid nitrogen and lyophilized. Lyophilized wheat spike tissue was ground using a TissueLyser (Qiagen Retsch GmbH, Hannover, Germany) for 1 min and a frequency of 30 Hz. An aliquot of the powdered sample (30 mg) was extracted in 1 mL of extraction solution (10% methanol and 1% acetic acid) containing a mixture of internal isotope labelled standards SA- d_6 (Sigma-Aldrich) and (+)-cis, trans-ABA- d_6 (Trc) (final concentration 38.5 ng mL^{-1}). After vortexing, the samples were placed in a Mixer Mill (Roche) for 2 min at a 30 Hz frequency, after which they were homogenized for 1 h at 4°C . The samples were then centrifuged for 10 min and 13,000 rpm, and 100 μL of the resulting supernatant was used for analysis. LC-MS/MS screening of target stress hormones was carried out using an Agilent Technologies 1200 series HPLC system equipped with a 6420 triple quadrupole mass spectrometer with electrospray ionization (Agilent Technologies Inc., Palo Alto, CA,

USA). Chromatographic separation was performed on the Zorbax XDP C18 column (75 × 4.6 mm, 3.5 µm particle size) (Agilent Technologies Inc., Palo Alto, CA, USA). Solvents for the analysis were 0.1% formic acid in water (solvent A) and methanol (solvent B). The electrospray ionization source was operated in negative mode, and samples were detected in the multiple reaction monitorings modes. All data acquisition and processing was performed using Agilent MassHunter software (Agilent Technologies, Santa Clara, CA, USA). ABA and SA concentrations were calculated and expressed as ng per mg of dry weight (ng mg⁻¹ DW) (Duvnjak et al., 2023).

2.4.5. Molecular analysis

2.4.5.1. Total RNA isolation from wheat spike

Total RNA was isolated using the NucleoZOL reagent (Macherey-Nagel), following the manufacturer's instructions. For RNA isolation, frozen wheat spike tissue was crushed in 10 mL stainless steel jars containing a grinding ball for 1 min at 30 Hz using a TissueLyser (Qiagen Retsch GmbH, Hannover, Germany), and about 50 mg of tissue powder was homogenised with 0.5 mL of NucleoZOL reagent. For the purpose of deposition of cell debris, 2 mL of Milli-Q water was added to the homogenised mixture and vortexed. After 15 min incubation at room temperature, the homogenate was centrifuged for 5 min at 12,000 × g and 4 °C, and 0.5 mL of the resulting supernatant was separated into a new microtube. For the RNA precipitation, 0.5 mL of isopropanol was added to the supernatant. The contents of the microtube were mixed several times by inversion, incubated for 10 min at room temperature and centrifuged for 10 min at 12,000 × g and 4 °C. The supernatant was decanted, and the white RNA precipitate was washed with 0.5 mL of 75% ethanol. The contents were centrifuged again for 3 min at 8,000 × g, the ethanol was decanted, and the same procedure was repeated one more time. The wheat spike RNA precipitate was resuspended in 50 µL of RNase-free water and stored at -20 °C until further analysis.

RNA concentration was measured at a wavelength of 260 nm using a NanoPhotometer N80-Touch instrument (Implen, Munich, Germany). The ratios A260/A280 and A260/A230, indicators of the purity of the obtained RNA, were also measured. The ratio A260/A280 is an indicator of contamination with proteins, and A260/A230 of contamination with phenols and other compounds.

2.4.5.2. DNase treatment and cDNA synthesis

Before the reverse transcription (RT) of RNA into complementary DNA (cDNA), the RNA was treated with rDNase (Macherey-Nagel) to remove possible genomic DNA contamination. For DNA digestion, 5.5 μ L of rDNase-buffer premix (1/ μ L, v/v), was added to the 50 μ L of RNA solution and incubated for 10 min at 37 °C. RNA was subsequently repurified by ethanol precipitation: 5.5 μ L of 3 M sodium acetate (pH 4.2) and 138 μ L of 100% ethanol were added to the RNA solution. After 2 h of incubation at -20 °C, samples were centrifuged for 10 min at maximum speed. The RNA pellet was washed with 70% ethanol and centrifuged for 3 min at 8,000 \times g. The supernatant was decanted, and the procedure was repeated one more time. The RNA pellet was then dried and resuspended in 40 μ L of RNase-free water.

The cDNA was synthesised using commercial reagents for RT and quantitative polymerase chain reaction (qPCR) GoTaq[®] 2-Step RT-qPCR (Promega) according to the manufacturer's instructions. RNA obtained after DNA digestion was denatured together with 1 μ L oligo d(T) primer for 5 min at 70 °C. The mixture was then cooled for 5 minutes at 4 °C and cDNA was synthesized in a final volume of 20 μ L by combining the denatured premix with the reaction mixture consisting of 1 \times GoScript buffer, 1 mM MgCl₂, 0.5 mM nucleotide mix, 50 U of ribonuclease inhibitor (Recombinant RNasin), and 1U of reverse transcriptase. The cDNA synthesis was performed under the following conditions: primer annealing at 25 °C for 5 min, extension at 42 °C for 1 h and enzyme inactivation at 70 °C for 5 min. All incubation steps were performed on the MiniAmp Plus Thermal PCR Cycler (Applied Biosystems, Waltham, MA, USA).

2.4.5.3. Quantitative PCR

Following cDNA synthesis, qPCR using dye-based detection was performed to analyse transcript levels of five genes (*NPR1*, *TG2*, *PR1*, *PR3*, *PR5*) with *actin* as a reference gene. The specific oligonucleotide primers were designed based on sequences in the GeneBank database using Primer3 software. Some primers were designed to span the exon-exon junction containing an intron to differentiate between RNA versus genomic DNA amplification, thus confirming the absence of DNA contamination. A qPCR reaction was performed using the GoTaq[®] 2-Step RT-qPCR System (Promega), according to the manufacturer's recommendation. The obtained cDNA was diluted 5 \times for quantification purposes. The qPCR reaction mixture consisted of 5 μ L diluted cDNA, 1 \times commercial

qPCR mix (GoTaq qPCR Master Mix), 200 nM of each specific primer, 0.25 μ L CXR reference dye, and water to a final volume of 25 μ L. The commercial mixture for qPCR (GoTaq qPCR Master Mix) contains hot-start DNA polymerase, a mixture of dNTPs, Mg^{2+} ions, and fluorescent dye SYBR Green I, which binds to double-stranded DNA and fluoresces. qPCR analysis was performed on StepOnePlus™ Real-time PCR System with StepOnePlus™ Software v2.3 (Applied Biosystems, Waltham, MA, USA). The qPCR amplification was performed under the following conditions: GoTaq Hot Start Polymerase activation at 95 °C for 2 min, followed by 40 cycles consisting of denaturation at 95 °C for 15 s, primer annealing, and extension at 60 °C for 1 min. The specificity of the qPCR reaction was confirmed by melting curve analysis. Relative gene expression was quantified using a relative standard curve based on five points, corresponding to a three-fold dilution series from pooled cDNA, and normalized to a reference gene *actin*.

2.5. Statistical analysis

To estimate disease progress, the AUPPC was used to combine multiple observations from five data points (different dates) into a single value. Statistical analysis of the normalized, outlier-corrected pool metabolites data was performed using the Statistica software version 12.0 (Statsoft Inc., Tulsa, OK, USA). Metabolomics data were analysed using univariate (Mann-Whitney U test) analysis to prove if there were any significant differences between the two treatments (control, i.e., naturally infected, and artificially infected, i.e., inoculated). Further data processing and multivariate analysis, including Spearman correlation r values were determined using MetaboAnalyst version 6.0. Principal component analysis (PCA), was performed using *ggplot2* (Wickham & Sievert, 2009), *ggpubr* (Kassambara, 2020), *ggrepel* (Sewakowski, 2021), *FactoMineR* (Lê et al., 2008), and *factoextra* (Kassambara & Mundt, 2020) packages within R software version 4.1. (R Core Team, 2021). The data for determination of lipid peroxidation level, content of H_2O_2 , GSH and GSSG, activities of the antioxidant enzymes, photosynthetic pigments, and parameters of photosynthesis efficiency were presented as mean of six (or three for relative gene expression and four for ABA and SA content analysis) independent biological replicates \pm standard deviations. Determination of differences among treatments within each variety separately or among treatments of the same measurement point within each variety separately (for TR_0 /ABS and PI_{abs}) was performed using two sample t-test ($p < 0.05$). Determination of differences among measurement points for TR_0 /ABS and PI_{abs} within each treatment separately was done using one-way analysis of

variance (ANOVA), followed by Fisher LSD post hoc test ($p < 0.05$). Data analysis was performed within the R software version 4.1.1 (R Core Team, 2021) and Statistica software version 12.0 (Statsoft Inc., Tulsa, OK, USA).

Ocjena rada
u tileku

Ocjena rada
u tijeku

3. RESULTS

3.1. Field conditions

3.1.1. General and type I resistance to Fusarium head blight

Symptoms of FHB exhibited variability across locations. At both experimental locations, the highest AUDPC was recorded in the El Nino, Golubica, and Tika Tara genotypes. The highest general and type I resistance was observed at genotype Galloper at both locations, Osijek and Tovarnik. The lower AUDPC for initial infection, indicating higher type I resistance, was observed in genotypes Vulkan and Kraljica at Tovarnik. The highest AUDPC for Type I resistance was observed for genotype El Nino (AUDPC 421) at Tovarnik, followed by genotype Golubica at Osijek (AUDPC 22.2) (Table 1).

Table 1. Area under the disease progress curve (AUDPC) for general resistance and type I resistance (resistance to initial infection) to Fusarium head blight (FHB) at locations Osijek and Tovarnik and their standard deviations (SD). A higher AUDPC value means lower FHB resistance.

Genotype	AUDPC general resistance Osijek \pm SD	AUDPC general resistance Tovarnik \pm SD	AUDPC type I resistance Osijek \pm SD	AUDPC type I resistance Tovarnik \pm SD
El Nino	137.7 \pm 16.75	212.5 \pm 142.5	44 \pm 1	421 \pm 212.5
Galloper	1.3 \pm 0	17.5 \pm 9.5	35 \pm 16.63	87.4 \pm 25.85
Tika Tara	7 \pm 1.35	69.8 \pm 7.25	215.3 \pm 74.5	137.6 \pm 41.95
Vulkan	35.8 \pm 6.25	33.8 \pm 5.25	12.9 \pm 11.35	50.6 \pm 4.1
Kraljica	71.5 \pm 23.5	18.3 \pm 7.5	216.7 \pm 80.5	80.1 \pm 10.4
Golubica	10.3 \pm 22.75	93 \pm 7	22.3 \pm 9.2	111.3 \pm 8.3

3.1.2. Mycotoxins

3.1.2.1. Deoxynivalenol, deoxynivalenol-3-glucoside, 3-acetyldeoxynivalenol, and nivalenol content

The concentrations of DON, D3G, and 3ADON were higher in *Fusarium* infected grains compared to corresponding naturally infected (control) grains across all tested winter wheat genotypes. At both experimental locations, Osijek and Tovarnik, DON was one of the most prevalent mycotoxins produced in artificial and inoculated treatments. In addition, D3G and 3ADON were also detected in the grains of all winter wheat genotypes infected with FHB at both locations. The highest DON concentration at experimental location Osijek was recorded in the genotype Golubica (26,800 $\mu\text{g kg}^{-1}$), followed by 18,300 $\mu\text{g kg}^{-1}$ in the genotype El Nino, 17,700 $\mu\text{g kg}^{-1}$ in Tika Taka, 6,740 $\mu\text{g kg}^{-1}$ in Vulkan, and 6,370 $\mu\text{g kg}^{-1}$ in Kraljica. The lowest DON concentration of 5,410 $\mu\text{g kg}^{-1}$ was recorded in the genotype Galloper (Figure 7a). At the experimental location Tovarnik, the highest concentration was also recorded in the infected grains of the genotype Golubica (25,500 $\mu\text{g kg}^{-1}$). The second highest concentration was recorded in the genotype El Nino (21,100 $\mu\text{g kg}^{-1}$), followed by genotypes Tika Taka (21,000 $\mu\text{g kg}^{-1}$), Kraljica (19,800 $\mu\text{g kg}^{-1}$), and Galloper (13,400 $\mu\text{g kg}^{-1}$), while the lowest recorded concentration of DON was 13,200 $\mu\text{g kg}^{-1}$ in the infected grains of the genotype Vulkan (Figure 7b). In the naturally infected sample at the experimental location Osijek, DON was found only in the grains of the genotype Tika Taka at the concentration of 12 $\mu\text{g kg}^{-1}$. At the experimental location Tovarnik, DON was found in the naturally infected grains of all genotypes tested. The highest concentration was 62 $\mu\text{g kg}^{-1}$ in the genotype El Nino, followed by 141 $\mu\text{g kg}^{-1}$ (Golubica), 129 $\mu\text{g kg}^{-1}$ (Vulkan), 104 $\mu\text{g kg}^{-1}$ (Tika Taka), 44 $\mu\text{g kg}^{-1}$ (Galloper), while the lowest concentration was 1 $\mu\text{g kg}^{-1}$ in the genotype Kraljica.

D3G and 3ADON concentrations were lower than those of DON at both experimental locations. The highest concentration recorded of D3G at the experimental location Osijek was in the genotype Golubica (770 $\mu\text{g kg}^{-1}$), followed by genotypes El Nino (445 $\mu\text{g kg}^{-1}$), Tika Taka (410 $\mu\text{g kg}^{-1}$), Vulkan (339 $\mu\text{g kg}^{-1}$), Kraljica (286 $\mu\text{g kg}^{-1}$), while the lowest D3G concentration recorded was in the genotype Galloper (219 $\mu\text{g kg}^{-1}$) (Figure 7c). At the experimental location Tovarnik, the genotype with the highest concentration of D3G in infected grains was Tika Taka (731 $\mu\text{g kg}^{-1}$). Other concentrations found were 729 $\mu\text{g kg}^{-1}$ in the genotype El Nino, 663 $\mu\text{g kg}^{-1}$ in Golubica, 541 $\mu\text{g kg}^{-1}$ in Kraljica, 476 $\mu\text{g kg}^{-1}$ in Vulkan, while the lowest concentration was 326 $\mu\text{g kg}^{-1}$ in the genotype Galloper. At

experimental location Osijek, D3G was recorded only in the grains of the naturally infected genotype Tika Taka in the concentration of $6 \mu\text{g kg}^{-1}$, while at the experimental location Tovarnik D3G was found in the genotypes El Nino ($61 \mu\text{g kg}^{-1}$), Golubica ($15 \mu\text{g kg}^{-1}$), and Tika Taka ($6 \mu\text{g kg}^{-1}$) (Figure 7d).

At the experimental location Osijek 3ADON was recorded in the concentration of $1,154 \mu\text{g kg}^{-1}$ (Tika Taka), $957 \mu\text{g kg}^{-1}$ (El Nino), $877 \mu\text{g kg}^{-1}$ (Golubica), $283 \mu\text{g kg}^{-1}$ (Vulkan), $267 \mu\text{g kg}^{-1}$ (Kraljica), and $212 \mu\text{g kg}^{-1}$ (Galopper) (Figure 7e). At the experimental location Tovarnik the highest concentration of 3ADON was recorded in the genotype El Nino ($1,716 \mu\text{g kg}^{-1}$), followed by genotypes Golubica ($1,441 \mu\text{g kg}^{-1}$), Tika Taka ($1,254 \mu\text{g kg}^{-1}$), Kraljica ($1,122 \mu\text{g kg}^{-1}$), Galopper ($769 \mu\text{g kg}^{-1}$), and Vulkan ($672 \mu\text{g kg}^{-1}$) (Figure 7f). In the naturally infected grains of the studied genotypes at the experimental location Osijek 3ADON was not found, while at the experimental location Tovarnik 3ADON was found only in the genotype El Nino at the concentration of $44 \mu\text{g kg}^{-1}$.

At experimental location Osijek, NIV was only detected in artificially inoculated grains of the genotypes El Nino, Tika Taka, and Golubica, with concentrations of $21 \mu\text{g kg}^{-1}$, $31 \mu\text{g kg}^{-1}$, and $37 \mu\text{g kg}^{-1}$, respectively (Figure 7g). At experimental location Tovarnik, NIV was detected in artificially infected grains of all studied genotypes, with the highest concentration recorded in the genotype Golubica ($105 \mu\text{g kg}^{-1}$), followed by genotypes El Nino ($36 \mu\text{g kg}^{-1}$), Tika Taka ($35 \mu\text{g kg}^{-1}$), Kraljica ($34 \mu\text{g kg}^{-1}$), Vulkan ($1 \mu\text{g kg}^{-1}$), and Galopper ($24 \mu\text{g kg}^{-1}$) (Figure 7h). In the naturally infected grains of the studied genotypes at the experimental location Osijek NIV was not found, while at the experimental location Tovarnik it was found only in Golubica at the concentration of $70 (\mu\text{g kg}^{-1})$.

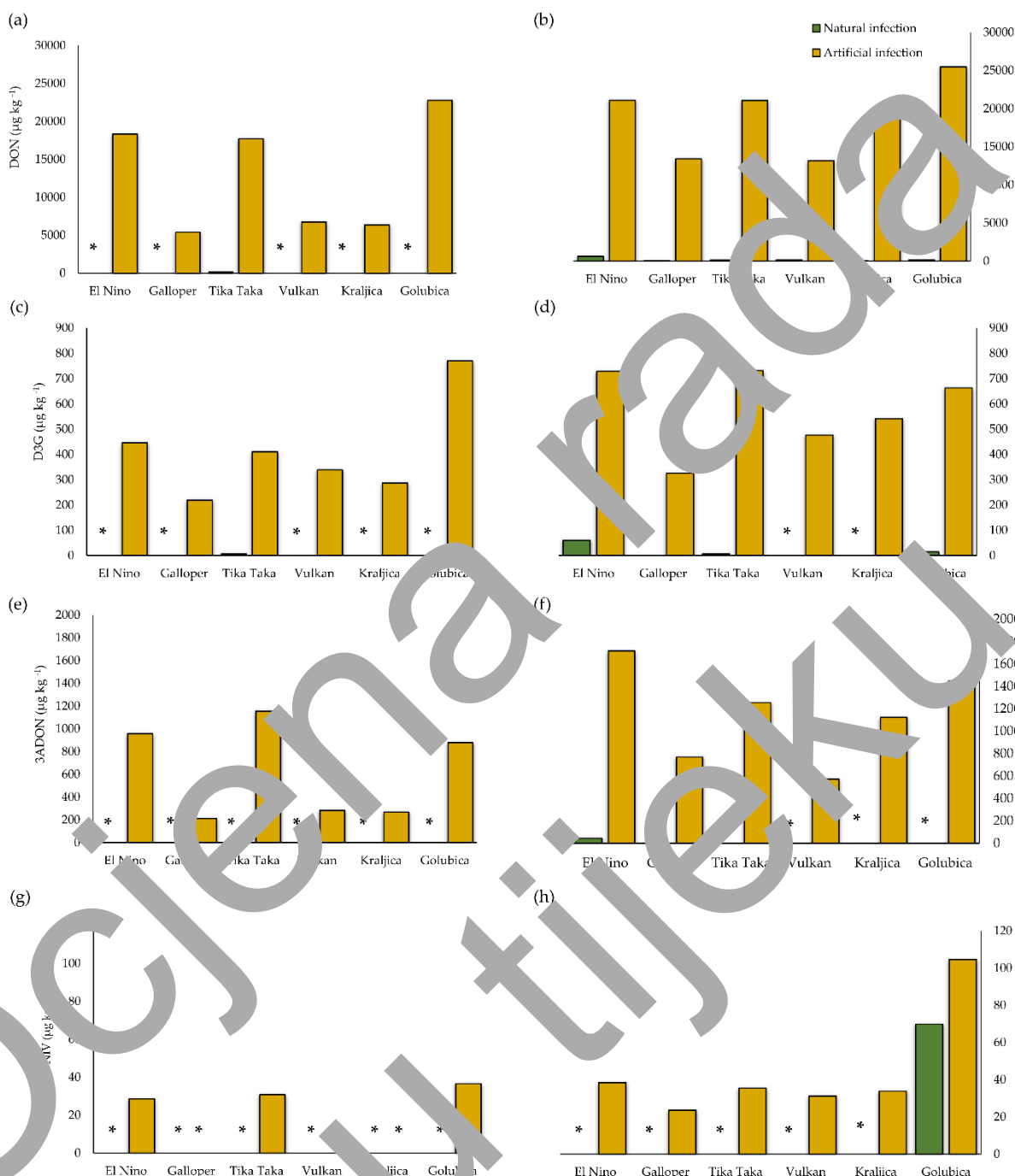


Figure 7. Concentrations of deoxynivalenol (DON) (a,b), deoxynivalenol-3-glucoside (D3G) (c,d), 3-acetyldeoxynivalenol (3ADON) (e,f), and nivalenol (NIV) (g,h) in artificially inoculated and naturally infected samples at Osijek (a,c,e,g) and Tovarnik (b,d,f,h). The asterisk (*) indicates that measured values are below LOD (limit of detection) values.

3.1.2.2. Zearalenone content

All artificially inoculated grains of six studied genotypes from both experimental locations were contaminated with ZEN. At Osijek, ZEN levels in artificially infected samples were $45 \mu\text{g kg}^{-1}$ in Kraljica, $16 \mu\text{g kg}^{-1}$ in Tika Taka, $12 \mu\text{g kg}^{-1}$ in Vulkan, $9 \mu\text{g kg}^{-1}$ in El Nino, $9 \mu\text{g kg}^{-1}$ in Golubica, and $1 \mu\text{g kg}^{-1}$ in Galloper (Figure 8c). At Tovarnik, recorded ZEN concentrations were $51 \mu\text{g kg}^{-1}$ in El Nino, $51 \mu\text{g kg}^{-1}$ in Tika Taka, $27 \mu\text{g kg}^{-1}$ in Kraljica, $18 \mu\text{g kg}^{-1}$ in Golubica, $11 \mu\text{g kg}^{-1}$ in Vulkan, and $5 \mu\text{g kg}^{-1}$ in Galloper (Figure 8d). In naturally infected grains, ZEN was not found at the experimental location Osijek. However, it was recorded at Tovarnik at a concentration of $1 \mu\text{g kg}^{-1}$ in the genotype El Nino.

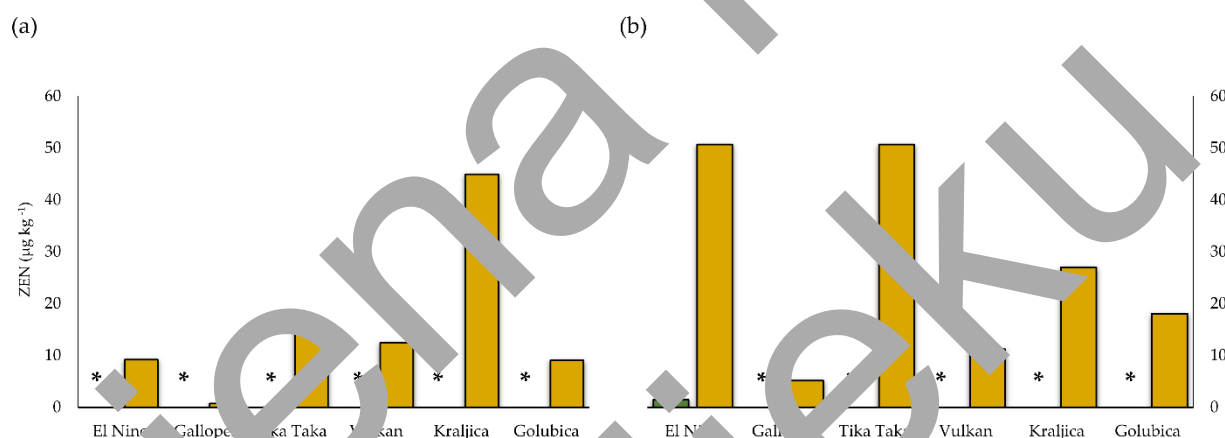


Figure 5. Concentrations of zearalenone (ZEN) (a, b) in artificially inoculated and naturally infected samples at Osijek (a) and Tovarnik (b). The asterisk (*) indicates that measured values are below LOD (limit of detection) value.

3.1.2.3. Culmorin, 15-hydroxyculmorin, 15-hydroxyculmoron and 5-hydroxyculmorin content

El Nino, Tika Taka, and Golubica accumulated CUL and its derivatives at higher levels than other genotypes. The highest amount of CUL at the experimental location Osijek was recorded in artificially inoculated grains of the genotype Golubica ($29,100 \mu\text{g kg}^{-1}$). The concentrations in other genotypes were $13,100 \mu\text{g kg}^{-1}$ in Vulkan, $12,971 \mu\text{g kg}^{-1}$ in Tika Taka, $11,417 \mu\text{g kg}^{-1}$ in El Nino, $8,482 \mu\text{g kg}^{-1}$ in Galloper, and $7,814 \mu\text{g kg}^{-1}$ in Kraljica. In naturally infected samples at Osijek, CUL was only recorded in the grains of the genotype Tika Taka at a concentration of $220 \mu\text{g kg}^{-1}$ (Figure 9a). At Tovarnik, CUL

contents in both naturally and artificially infected samples were recorded. In naturally infected grains of the genotype El Nino was recorded the highest concentration of CUL ($1,047 \mu\text{g kg}^{-1}$), followed by genotypes Vulkan ($115 \mu\text{g kg}^{-1}$), Golubica ($105 \mu\text{g kg}^{-1}$), and Galloper ($100 \mu\text{g kg}^{-1}$). The lowest concentration had genotype Tika Taka ($62 \mu\text{g kg}^{-1}$), while in genotype Kraljica it was not recorded. Concentrations in artificially infected grains were $14,260 \mu\text{g kg}^{-1}$ in Golubica, $13,483 \mu\text{g kg}^{-1}$ in Tika Taka, $11,860 \mu\text{g kg}^{-1}$ in El Nino, $11,425 \mu\text{g kg}^{-1}$ in Vulkan, $11,169 \mu\text{g kg}^{-1}$ in Kraljica, and $6,101 \mu\text{g kg}^{-1}$ in Galloper (Figure 9b).

The concentrations of CUL derivatives were also higher in artificially infected than in naturally infected samples at both locations. In artificially inoculated samples at Osijek, the highest concentration of 15-hydroxyculmorin was recorded in the genotype Golubica ($28,761 \mu\text{g kg}^{-1}$), followed by genotypes El Nino ($24,333 \mu\text{g kg}^{-1}$), Tika Taka ($24,808 \mu\text{g kg}^{-1}$), Kraljica ($11,843 \mu\text{g kg}^{-1}$), Vulkan ($10,463 \mu\text{g kg}^{-1}$), while the lowest concentration was recorded in the genotype Galloper ($8,325 \mu\text{g kg}^{-1}$) (Figure 9c). In naturally infected grains, it was found only in the grains of the genotype Tika Taka ($89 \mu\text{g kg}^{-1}$). At Tovarnik, recorded concentrations of 15-hydroxyculmorin were as follows: $29,375 \mu\text{g kg}^{-1}$ (Golubica), $24,094 \mu\text{g kg}^{-1}$ (El Nino), $22,878 \mu\text{g kg}^{-1}$ (Kraljica), $22,181 \mu\text{g kg}^{-1}$ (Tika Taka), $18,541 \mu\text{g kg}^{-1}$ (Galloper), and $15,647 \mu\text{g kg}^{-1}$ (Vulkan). It was also found in naturally infected grains of all studied genotypes. The highest concentration had genotype El Nino ($1,227 \mu\text{g kg}^{-1}$), followed by genotypes Golubica ($105 \mu\text{g kg}^{-1}$), Tika Taka ($73 \mu\text{g kg}^{-1}$), Galloper ($63 \mu\text{g kg}^{-1}$), Vulkan ($\mu\text{g kg}^{-1}$), and Kraljica ($\mu\text{g kg}^{-1}$) (Figure 9d).

The highest concentration of 15-hydroxyculmorin at the experimental location Osijek was recorded in the genotype Golubica ($4,611 \mu\text{g kg}^{-1}$), followed by genotypes Tika Taka ($4,329 \mu\text{g kg}^{-1}$), El Nino ($4,035 \mu\text{g kg}^{-1}$), Kraljica ($3,306 \mu\text{g kg}^{-1}$), Vulkan ($1,034 \mu\text{g kg}^{-1}$). The lowest concentration had genotype Galloper ($570 \mu\text{g kg}^{-1}$). In naturally infected grains of tested genotypes this metabolite was not recorded (Figure 9e). At the experimental location Tovarnik, same as at the experimental location Osijek, the highest concentration was also recorded in the genotype Golubica ($2,990 \mu\text{g kg}^{-1}$). The rest of the genotypes had the concentrations as follows: El Nino ($2,652 \mu\text{g kg}^{-1}$), Kraljica ($2,423 \mu\text{g kg}^{-1}$), Tika Taka ($1,983 \mu\text{g kg}^{-1}$), Galloper ($1,555 \mu\text{g kg}^{-1}$), and Vulkan ($1,198 \mu\text{g kg}^{-1}$). In naturally infected samples, it was recorded only in the genotype El Nino ($81 \mu\text{g kg}^{-1}$) (Figure 9f).

At the experimental location Osijek, the highest 5-hydroxyculmorin levels recorded were found in the genotypes Golubica ($24,352 \mu\text{g kg}^{-1}$), El Nino ($21,840 \mu\text{g kg}^{-1}$), and Tika Taka ($21,792 \mu\text{g kg}^{-1}$). Genotypes Kraljica, Vulkan, and Galloper had concentrations of $8,352 \mu\text{g kg}^{-1}$, $7,715 \mu\text{g kg}^{-1}$, and $5,074 \mu\text{g kg}^{-1}$, respectively. In naturally infected grain, it was not found (Figure 9g). Concentrations of 5-hydroxyculmorin at the experimental location Tovarnik were elevated in all artificially infected samples. The concentrations recorded were $30,008 \mu\text{g kg}^{-1}$ (El Nino), $28,792 \mu\text{g kg}^{-1}$ (Golubica), $22,048 \mu\text{g kg}^{-1}$ (Tika Taka), $21,520 \mu\text{g kg}^{-1}$ (Kraljica), $18,280 \mu\text{g kg}^{-1}$ (Galloper), and $14,016 \mu\text{g kg}^{-1}$ (Vulkan). In naturally infected samples, it was found only in genotypes El Nino ($307 \mu\text{g kg}^{-1}$), Vulkan ($226 \mu\text{g kg}^{-1}$), and Golubica ($138 \mu\text{g kg}^{-1}$) (Figure 9h).

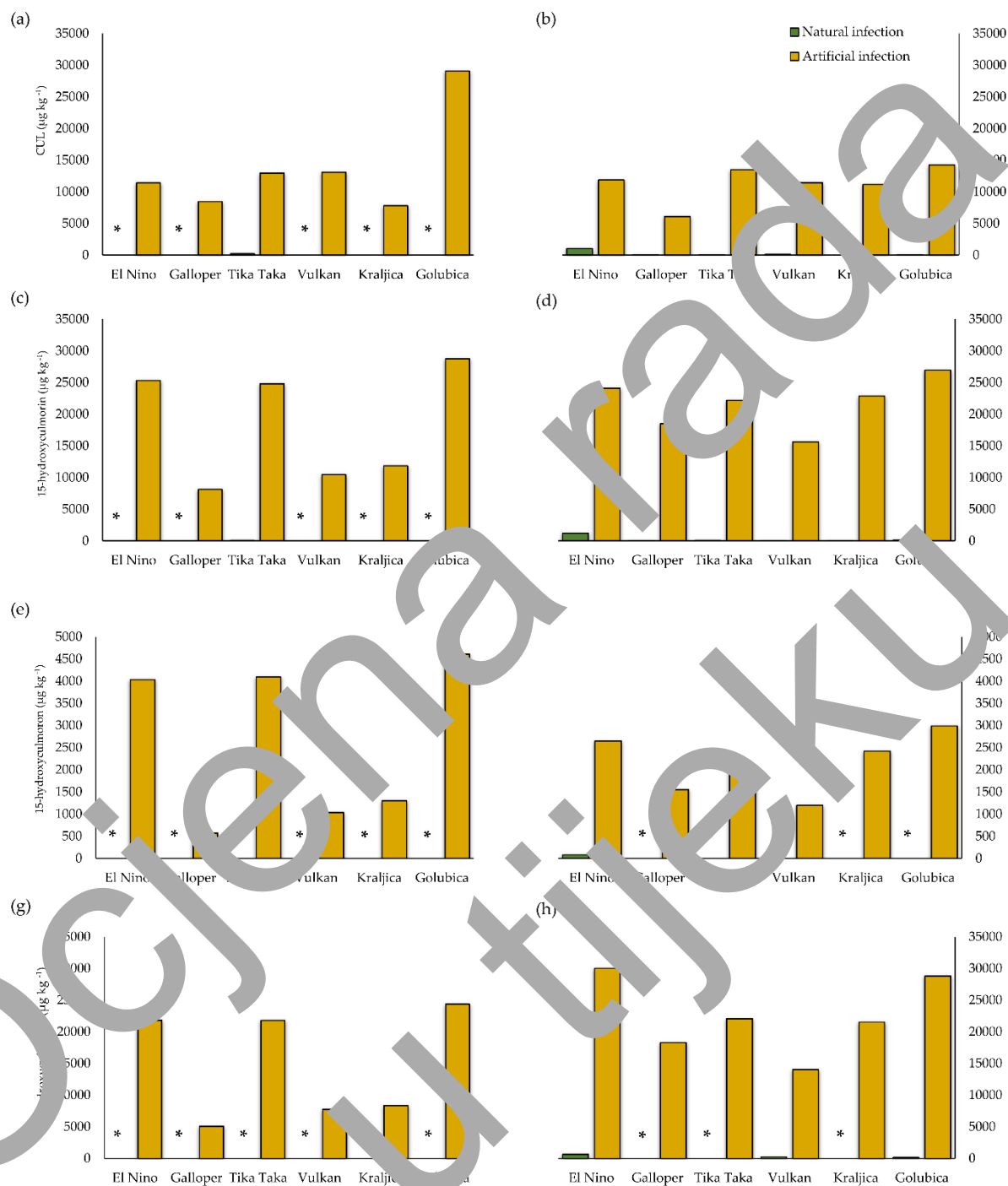


Figure 9. Concentrations of culmorin (CUL) (a,b), 15-hydroxyculmorin (c,d), 15-hydroxyculmoron (e,f), and 5-hydroxyculmorin (g,h) in artificially inoculated and naturally infected samples at Osijek (a,c,e,g) and Tovarnik (b,d,f,h). The asterisk (*) indicates that measured values are below LOD (limit of detection) values.

3.1.2.4. Aurofusarin, butenolide, chrysogin, and fusarin C content

At Osijek, aurofusarin levels were 12,511 $\mu\text{g kg}^{-1}$ (Tika Taka), 9,744 $\mu\text{g kg}^{-1}$ (El Nino), 5,610 $\mu\text{g kg}^{-1}$ (Golubica), 3,547 $\mu\text{g kg}^{-1}$ (Kraljica), 1,980 $\mu\text{g kg}^{-1}$ (Vulkan), and 1,356 $\mu\text{g kg}^{-1}$ (Galloper). In naturally infected samples, it was not found (Figure 10a). At Tovarnik, the highest levels of aurofusarin in artificially infected samples compared to Osijek with the highest concentration being 67,600 $\mu\text{g kg}^{-1}$ in the genotype El Nino, followed by genotypes Tika Taka (32,978 $\mu\text{g kg}^{-1}$), Golubica (21,233 $\mu\text{g kg}^{-1}$), Kraljica (14,922 $\mu\text{g kg}^{-1}$), Vulkan (12,867 $\mu\text{g kg}^{-1}$), and Galloper (11,356 $\mu\text{g kg}^{-1}$). In naturally infected samples, it was recorded only in genotype El Nino (739 $\mu\text{g kg}^{-1}$) (Figure 10b).

The highest concentration of butenolide was recorded in genotype Golubica (1,120 $\mu\text{g kg}^{-1}$), followed by Vulkan (723 $\mu\text{g kg}^{-1}$), El Nino (399 $\mu\text{g kg}^{-1}$), Kraljica (218 $\mu\text{g kg}^{-1}$), Galloper (183 $\mu\text{g kg}^{-1}$), and Tika Taka (167 $\mu\text{g kg}^{-1}$). It was not recorded in naturally infected grains of the tested genotypes (Figure 10c). At Tovarnik, the highest concentration of butenolide had genotype Vulkan (654 $\mu\text{g kg}^{-1}$). The rest of the genotypes had concentrations of 500 $\mu\text{g kg}^{-1}$ (Golubica), 472 $\mu\text{g kg}^{-1}$ (El Nino), 334 $\mu\text{g kg}^{-1}$ (Tika Taka), 294 $\mu\text{g kg}^{-1}$ (Kraljica), and 188 $\mu\text{g kg}^{-1}$ (Galloper). Like the naturally infected samples at Osijek, it was also not recorded at Tovarnik (Figure 10d).

Chrysogin levels at Osijek were 1,323 $\mu\text{g kg}^{-1}$ (El Nino), 1,107 $\mu\text{g kg}^{-1}$ (Tika Taka), 891 $\mu\text{g kg}^{-1}$ (Golubica), 500 $\mu\text{g kg}^{-1}$ (Kraljica), 386 $\mu\text{g kg}^{-1}$ (Vulkan), and 256 $\mu\text{g kg}^{-1}$ (Galloper). It was not found in the naturally infected samples (Figure 10e). At Tovarnik, the highest concentration had genotype El Nino (1,774 $\mu\text{g kg}^{-1}$), followed by Kraljica (822 $\mu\text{g kg}^{-1}$), Tika Taka (820 $\mu\text{g kg}^{-1}$), Golubica (725 $\mu\text{g kg}^{-1}$), Vulkan (600 $\mu\text{g kg}^{-1}$), and Galloper (528 $\mu\text{g kg}^{-1}$). In naturally infected samples, the highest concentration was recorded in the genotype El Nino (40 $\mu\text{g kg}^{-1}$), while the rest of the genotypes had negligible concentrations (Figure 10f).

Fusarin C levels at Osijek were 2,556 $\mu\text{g kg}^{-1}$ (El Nino), 2,390 $\mu\text{g kg}^{-1}$ (Tika Taka), 2,051 $\mu\text{g kg}^{-1}$ (Golubica), 997 $\mu\text{g kg}^{-1}$ (Galloper), 744 $\mu\text{g kg}^{-1}$ (Kraljica), and 665 $\mu\text{g kg}^{-1}$ (Vulkan) (Figure 10g). At Tovarnik, the highest concentration had genotype El Nino (6,715 $\mu\text{g kg}^{-1}$), followed by genotypes Golubica (4,582 $\mu\text{g kg}^{-1}$), Tika Taka (4,029 $\mu\text{g kg}^{-1}$), Kraljica (3,878 $\mu\text{g kg}^{-1}$), Galloper (3,461 $\mu\text{g kg}^{-1}$), and Vulkan (2,611 $\mu\text{g kg}^{-1}$) (Figure 10h). It was not found in naturally infected samples at both experimental locations.

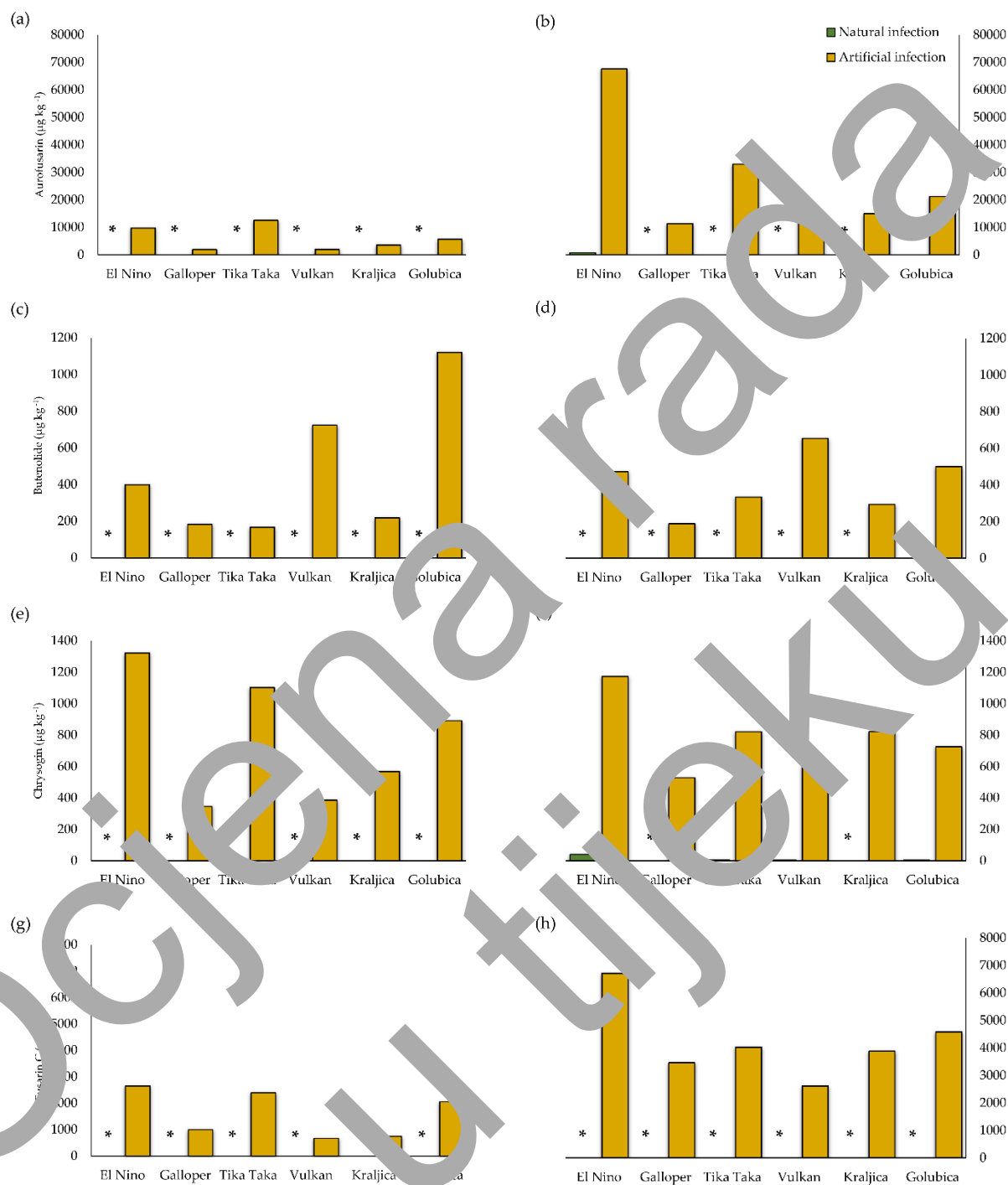


Figure 10. Concentrations of aurofusarin (a,b), butenolide (c,d), chrysogin (e,f), and fusarin C (g,h) in artificially inoculated and naturally infected samples at Osijek (a,c,e,g) and Tovarnik (b,d,f,h). The asterisk (*) indicates that measured values are below LOD (limit of detection) values.

3.1.3. Polar metabolites content in naturally infected and inoculated wheat grains

This study identified 275 polar metabolites in the naturally infected (control) and artificially inoculated grains of six winter wheat genotypes at two experimental locations (Osijek and Tovarnik). Results of the Mann-Whitney U test (p -value < 0.05 ; $n = 48$) revealed polar metabolites whose concentrations in grains were significantly altered by *Fusarium* treatment relative to controls. The univariate analysis showed that out of the 275 polar metabolites identified in the winter wheat grains, concentrations of 18 metabolites (6.55%) were significantly changed under *Fusarium* artificial inoculation compared to the corresponding controls at both experimental locations (Table 2). These polar metabolites were selected for further analyses.

The metabolites detected to vary between treatments significantly, belonged to diverse functional groups including amino acids and derivatives (2-piperidinecarboxylic acid or pipercolic acid, histidine, 5-hydroxytryptophan), small organic (carboxylic) acids (pyrrole-2-carboxylic acid, lactic acid dimer), polyphenols and their derivatives (4-hydroxybenzoic acid, 3-hydroxyflavone, 5,7-dihydroxyflavone, 3-(4-dihydroxyphenyl)propanoic acid, 2-hydroxyhippuric acid), saturated fatty acids (3-hydroxydodecanoic acid), carbohydrates and derivatives (turanose, sophorose, cellobiitol), nucleotides (guanosine, 2-deoxyguanosine), terpenoids (secologanin), and terpenols (α -tocopherol acetate).

PCA showed that principal component (PC) 1 accounted for 54.3%, and PC2 for 17.6% of the total variation (Figure 12). Metabolites 3-(4-dihydroxyphenyl)-propanoic acid, histidine, 3-hydroxyflavone, sophorose, guanosine, and α -tocopherol acetate were the major contributors to PC1, while the main contributors for PC2 were piperidine-2-carboxylic acid, pyrrole-2-carboxylic acid, 4-hydroxybenzoic acid, histidine, cellobiitol, and 3-hydroxyflavone. Metabolites clustered together in the groups indicate a positive correlation between them. Furthermore, metabolites guanosine, 2-deoxyguanosine, secologanin, 5,7-dihydroxyflavone, and 3-hydroxydodecanoic acid were on the opposite side of the type II resistance/susceptibility on the PCA biplot, which indicates a negative correlation between these variables. The closest metabolites to the FHB resistance/susceptibility on the PCA biplot were sophorose, turanose, cellobiitol, 5-hydroxytryptophan, and lactic acid dimer, also showing the same direction as FHB resistance/susceptibility (Figure 11). Furthermore, the PCA biplot showed a clear separation of genotypes from the control group (natural infection) and artificially infected

genotypes from both locations, with control genotypes clustered together mainly on the left side of the PCA biplot and inoculated genotypes grouped mostly on the right side of the biplot.

Table 2. Significant metabolites in the grains of six winter wheat genotypes across different treatments at two locations together obtained by Mann-Whitney U test.

	Rank Sum Group 1	Rank Sum Group 2	U	Z	<i>p</i> value	Z adjusted	<i>p</i> value	Valid N Group 1	Valid N Group 2	Exact <i>p</i> value
2-piperidinecarboxylic acid	703	473	173	2.371	0.018	-2.372	0.018	24	24	0.01724 *
Pyrrole-2-carboxylic acid	468	708	168	-2.474	0.013	-2.475	0.013	24	24	0.01278 *
Lactic acid dimer	489	687	189	-2.041	0.041	-2.042	0.041	24	24	0.04149 *
4-hydroxybenzoic acid	492	684	189	-1.979	0.048	-1.980	0.048	24	24	0.04828 *
3-hydroxydodecanoic acid	684	492	192	1.979	0.048	1.980	0.048	24	24	0.04828 *
3-(2,4-dihydroxyphenyl) propanoic acid	485.5	698.5	185.5	-2.114	0.035	-2.114	0.035	24	24	0.03368 *
Histidine	474.5	701.5	180.5	-2.340	0.019	-2.341	0.019	24	24	0.01828 *
2-hydroxyhippuric acid	716.5	461.5	164.5	2.547	0.011	2.547	0.011	24	24	0.00997 **
Cellobiitol	476	700	176	-2.309	0.021	-2.310	0.021	24	24	0.02052 *
3-hydroxyflavone	459	699	177	-2.289	0.023	-2.289	0.023	24	24	0.02172 *
Turanose	490.5	685.5	190.5	-2.010	0.044	-2.010	0.044	24	24	0.04365 *
Sophorose	486	690	186	-2.103	0.035	-2.104	0.035	24	24	0.03551 *
5-hydroxytryptophan	457	718.5	157.5	2.601	0.009	2.601	0.007	24	24	0.00633 **
Glutamine	696.5	479.5	179.5	2.237	0.025	2.238	0.025	24	24	0.02430 *
2-deoxyguanosine	694.5	481.5	181.5	2.196	0.028	2.197	0.028	24	24	0.02715 *
Secologanin	689.5	486.5	186.5	2.093	0.036	2.094	0.036	24	24	0.03551 *
5,7-dihydroxyflavone	685.5	490.5	190.5	2.010	0.044	2.011	0.044	24	24	0.04366 *
α -tocopheryl acetate	489	687	189	-2.041	0.041	-2.042	0.041	24	24	0.04149 *

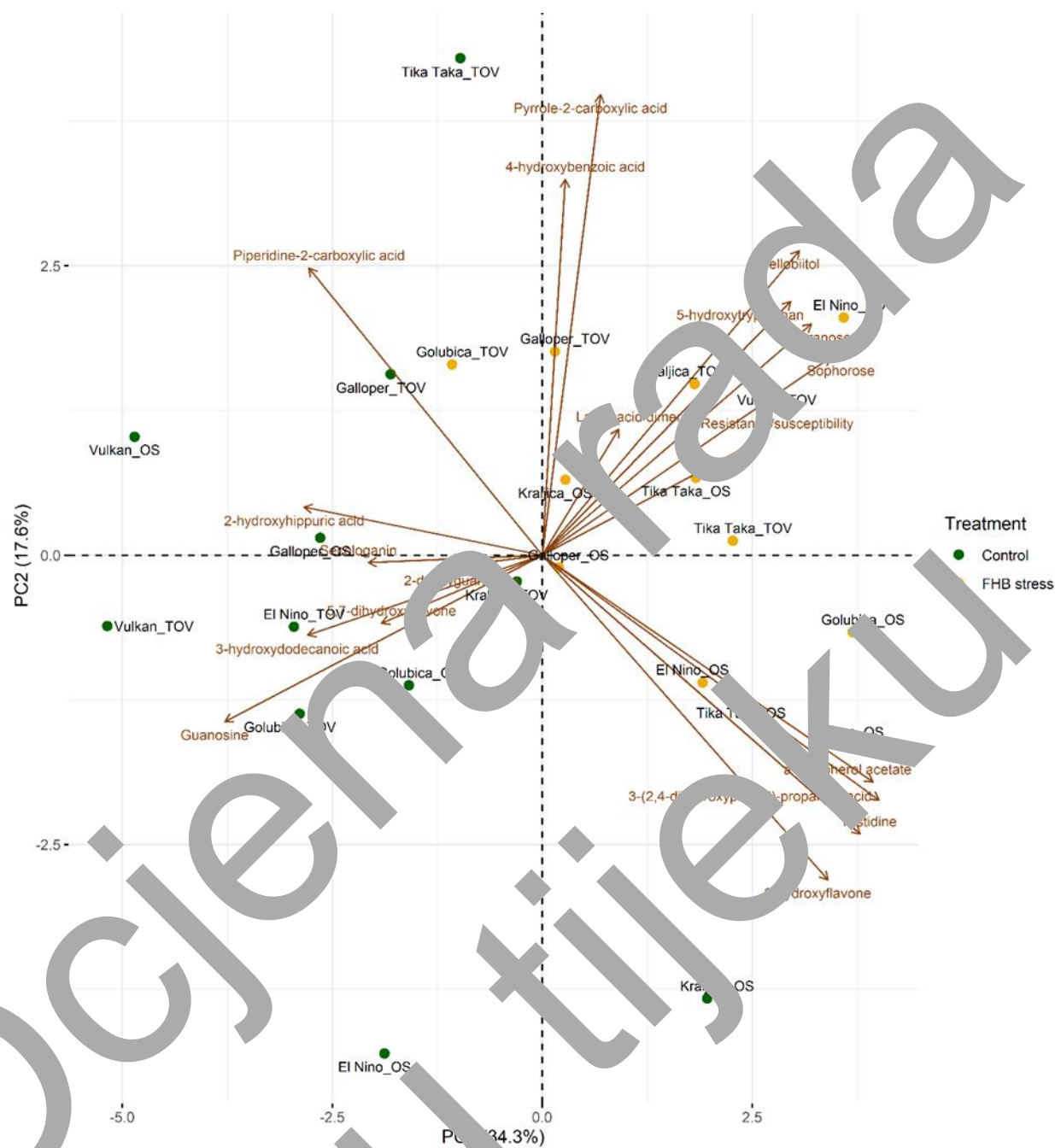


Figure 11. Principal component analysis (PCA) biplot of 18 wheat metabolites in control and Fusarium head blight (FHB) stressed grains of six winter wheat genotypes (El Nino, Galloper, Tika Taka, Vulkan, Kraljica, and Golubica) and general resistance/susceptibility to FHB at two experimental locations, Osijek (OS) and Tovarnik (TOV).

Spearman correlation coefficient showed that the most prominent significant positive correlations were between sophorose and 5-hydroxytryptophan, sophorose and cellobiitol, sophorose and turanose, between 5-hydroxytryptophan and cellobiitol, 5-hydroxytryptophan and turanose, cellobiitol and turanose, as well as between histidine and 3-hydroxyflavone, histidine and 3-(2,4-dihydroxyphenyl)-propanoic acid, and histidine and α -tocopherol acetate, between 3-hydroxyflavone and 3-(2,4-dihydroxyphenyl)-propanoic acid, and 3-hydroxyflavone and α -tocopherol acetate, and between 3-(2,4-dihydroxyphenyl)-propanoic acid and α -tocopherol acetate. The most distinguished significant negative correlations were between guanosine and sophorose, guanosine and 5-hydroxytryptophan, as well as between guanosine and cellobiitol. However, neither of the metabolites significantly changed following inoculations showed a significant correlation with FHB resistance in the Spearman correlation matrix (Figure 12) (Supplementary table 1).

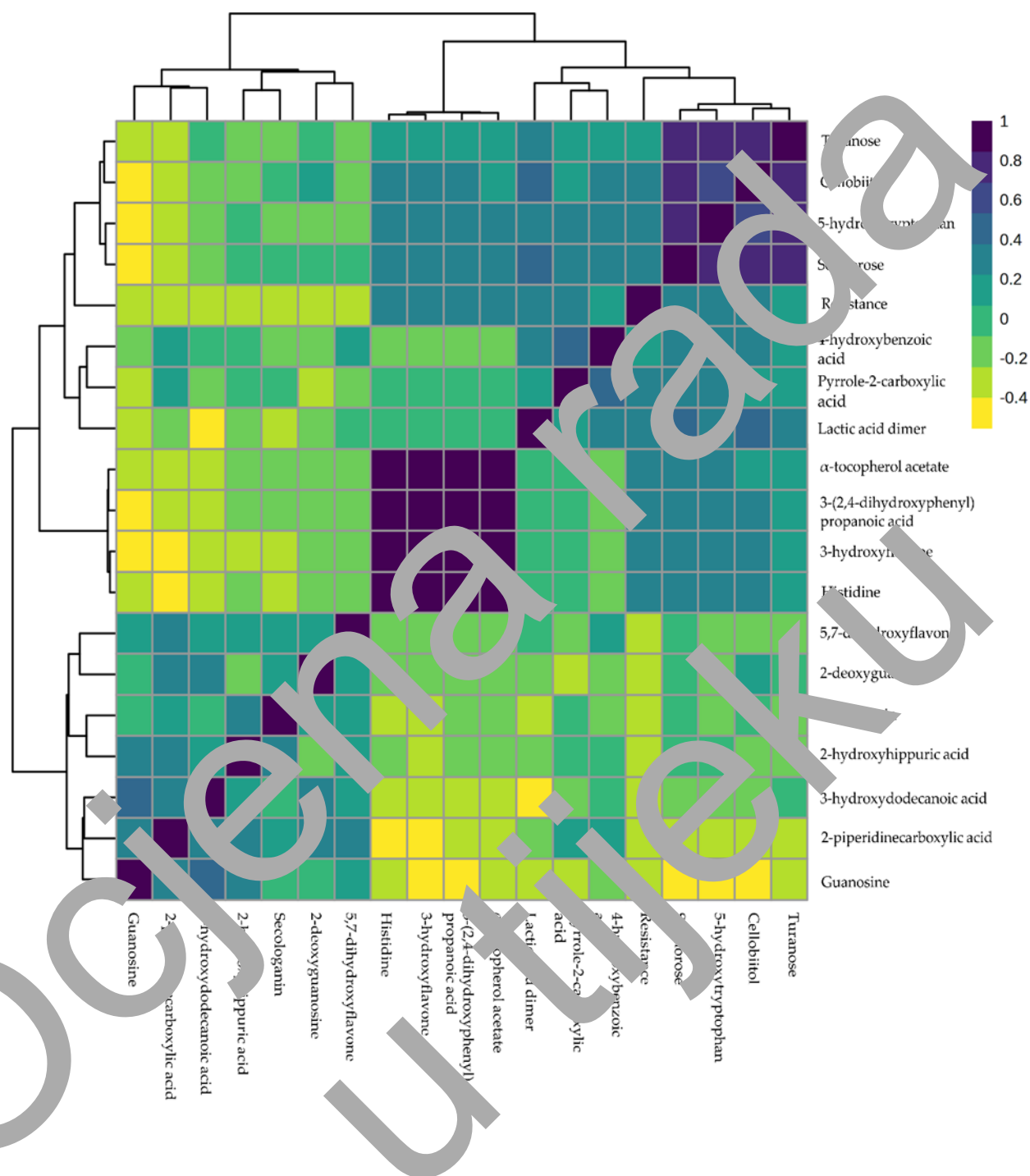


Figure 12. Graphical Spearman correlation matrix of 18 wheat metabolites in grains and resistance to *Fusarium*. Spearman correlation r values were determined using MetaboAnalyst. Colours are added for better visualization. The colours span from dark purple to yellow, where dark purple denotes an r value of 1 and yellow indicates an r value of -0.4 .

3.2. Controlled conditions (greenhouse)

3.2.1. Type II resistance to Fusarium head blight

On 10th dpi, nearly all genotypes exhibited distinctly visible spike bleaching (Figure 13). Table 3 shows the average number of infected spikelets for each variety on 10th dpi. Genotype Golubica exhibited the highest disease spread within the spike, with an average of 3.7 infected spikelets per spike. Genotypes Tika Taka and El Nino exhibited reduced disease spread in comparison to Golubica, with values of 3.5 and 2.5, respectively. In the genotypes Kraljica and Galloper, disease spread was lower compared to Golubica, Tika Taka, and El Nino, with an average of 1.9 infected spikelets per spike for Kraljica and 1.8 for Galloper. Genotype Vulkan demonstrated the lowest disease spread, with only one spikelet showing FHB symptoms on 10th dpi.

Table 3. Values for type II resistance to Fusarium head blight (resistance to disease spread within the spike) of six winter wheat genotypes. Data are average values of six independent biological replicates \pm SD. Different letters indicate significant differences between varieties ($p < 0.05$).

Genotype	Number of infected spikelets on 10 th dpi \pm SD
Golubica	3.7 \pm 0.7 a
Tika Taka	3.5 \pm 0.76 ab
El Nino	2.5 \pm 0.6 bc
Galloper	1.8 \pm 1.46 cd
Kraljica	1.9 \pm 0.58 cd
Vulkan	1 \pm 0.82 d



Figure 13. Fusarium head blight (FHB) symptoms of the spike bleaching in the genotype (a) Golubica, (b) Tika Taka, (c) El Nino, (d) Kraljica, (e) Galloper, and (f) Vulkan on 10th day post inoculation (dpi) in the greenhouse (author: Katarina Šunić Budimir).

3.2.2. Photosynthetic efficiency

3.2.2.1. Chlorophyll *a* fluorescence

Parameter TR_0/ABS was not significantly affected by artificial infection on the first two measurement points (1 dpi and 3 dpi) compared to the corresponding controls (Figure 14a-f). However, on 7 dpi and 10 dpi a significant decline of TR_0/ABS in FHB treatment was recorded, and the most prominent decrease had genotype Golubica, which decreased TR_0/ABS by 93.4% on the 7 dpi and 96.5% on the 10 dpi, compared to the 3 dpi (Figure 14f). The second most distinguished decrease of the TR_0/ABS on 7 dpi and 10 dpi compared to the 3 dpi had genotype Tika Taka, which decreased it by 96.3% and 92.7%, respectively (Figure 14c). The rest of the genotypes responded similarly to genotypes Tika Taka and Golubica. A decline in FHB inoculated treatment was observed in spikes of the genotype El Nino with TR_0/ABS significantly decreasing on 7 dpi and 10 dpi compared to 3 dpi (69.5% and 93.9%) (Figure 14a). Genotype Kraljica decreased TR_0/ABS in the FHB-stressed spikes on 7 dpi and 10 dpi by 61.3% and 49.3%, respectively, compared to the 3 dpi (Figure 14e). In addition, genotype Galloper significantly decreased the same parameter by 38.4 and 64.2% on the same measurement points compared to the measurement on 3 dpi, respectively (Figure 14b). Changes in TR_0/ABS in FHB-stressed spikes of the genotype Vulkan were much less pronounced than in the other genotypes investigated (Figure 14d). This parameter decreased significantly in FHB treatment by 23.9% and 27.3% on the same measurement points compared to the second measurement point, respectively.

When comparing FHB treatment and control, TR_0/ABS in FHB-stressed spikes decreased significantly on 7 and 10 dpi. In the genotype Golubica, the decrease in FHB treatment was 93.7% and 96.4% compared to the control measurements, respectively (Figure 14f). Similar to the genotype Golubica, genotype Tika Taka decreased TR_0/ABS at stressed spikes on 7 dpi (96.3%) and 10 dpi (92.5%) compared to the corresponding control measurements (14c). Significant decrease in the FHB-stressed spikes of the genotype El Nino was 69.2% on 7 dpi and 93.4% on 10 dpi compared to the controls (Figure 14a). In the genotype Kraljica, the same parameter decreased significantly only on the third measurement point (7 dpi) by 63.1% (Figure 14e). Similarly was obtained for genotype Vulkan where a significant decrease was recorded only on 7 dpi (24.9%) in FHB treated spikes, compared to corresponding control measurements (Figure 14d), while in the

stressed spikes of the genotype Galloper a significant decrease in TR_0/ABS was recorded on 10 dpi by 61.8%, compared to controls (Figure 14b).

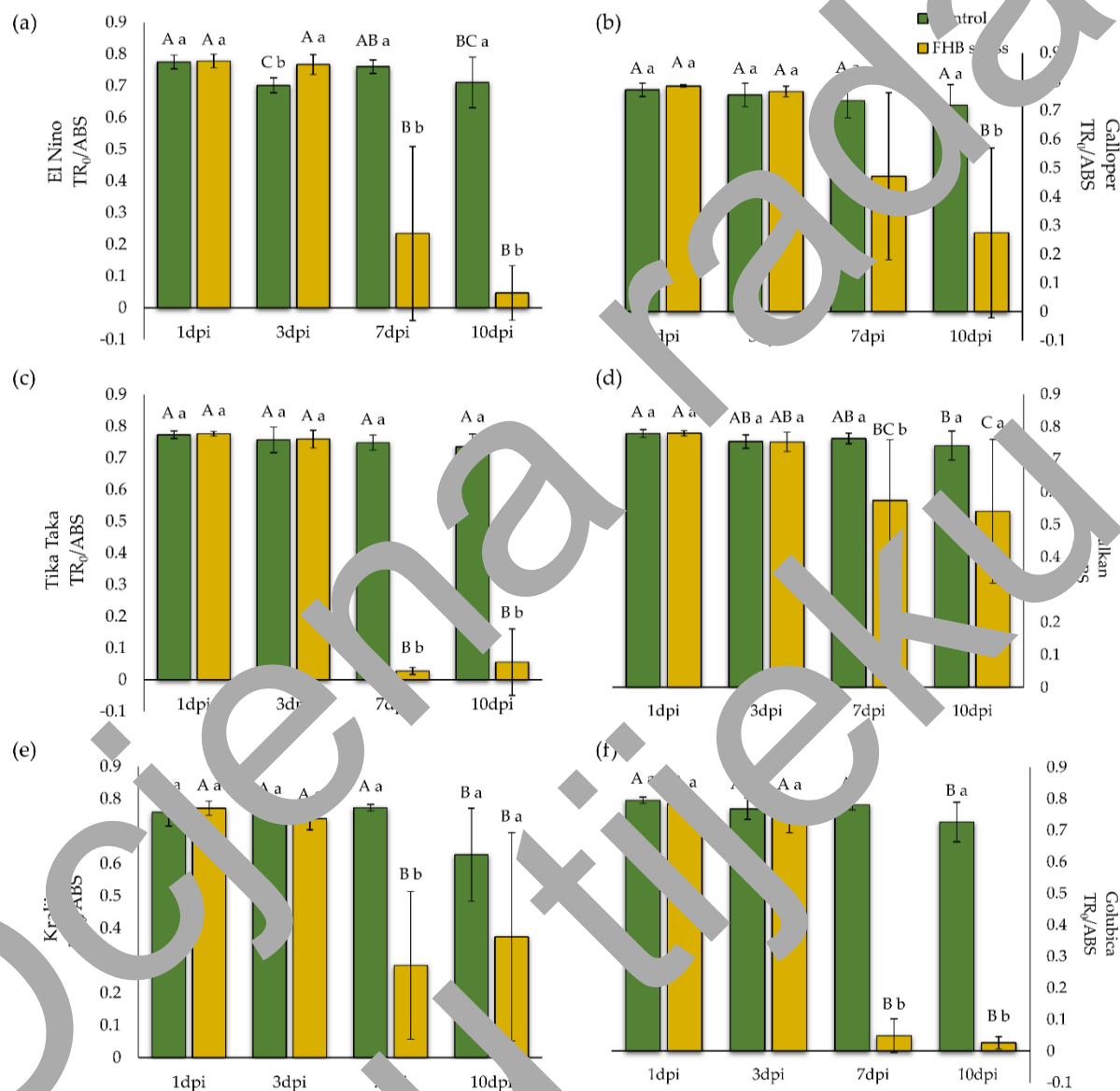


Figure 14. Maximum quantum yield of primary photochemistry (TR_0/ABS) in control and FHB-stressed spikes of six winter wheat genotypes (a) El Nino, (b) Galloper, (c) Tika Taka, (d) Vulkan, (e) Kraljica, and (f) Golubica. Bars represent mean values of six independent biological replicates \pm SD. Different small letters indicate significant differences between treatments on each measurement point separately (1 day post inoculation (dpi), 3 dpi 7 dpi, and 10 dpi) ($p < 0.05$). Different capital letters indicate differences among measurement points in each treatment separately ($p < 0.05$).

Similarly as TR_0/ABS , in the PI_{abs} , there were no recorded significant changes on the first two measurement points (1 and 3 dpi) of the FHB treatment, while on the last two measurement points (7 and 10 dpi), a significant decline of PI_{abs} in almost all genotypes studied was observed, compared to the first two measurements (Figure 15a–f). However, in the genotype Galloper, a significant decrease of PI_{abs} in the FHB treatment was observed on 7 dpi compared to 1 dpi (56.4%) and on 10 dpi compared to 1 dpi (78.2%) and 3 dpi (74.9%) (Figure 15b). Genotype Golubica decreased the measured parameter on 7 dpi (99.5%) and 10 dpi (100%) when compared to the same measured parameter measured on 3 dpi (Figure 15f). Genotype El Nino decreased PI_{abs} on 7 dpi and 10 dpi by 78.4% and 99.6% when compared to the 3 dpi, respectively (Figure 15a). Tika Taka had a significant decrease of PI_{abs} on 7 dpi and 10 dpi (100% and 99.2% compared to the 3 dpi, respectively (Figure 15c). Genotype Kraljica reduced it by 84.5% and 83.5% on the third and fourth measurement points compared to the second measurement point, respectively (Figure 15e). Genotype Vulkan had a less prominent decrease compared to the other genotypes and reduced PI_{abs} by 45.1% and 52% on 7 dpi and 10 dpi compared to the 3 dpi, respectively (Figure 15d).

PI_{abs} in control and artificially inoculated spikes at each measurement point separately showed a similar trend when comparing PI_{abs} between different measurement points. Genotype Tika Taka decreased this parameter by 100% and 97.6% on 7 and 10 dpi compared to the corresponding controls, respectively (Figure 15c). Genotype Golubica decreased PI_{abs} in the same measurement points by 99.6% and 100% when compared to the controls, respectively (Figure 15f), while genotype El Nino decreased it by 80.1% and 99.5% on 7 and 10 dpi compared to the corresponding controls on the same measurement points, respectively (Figure 15a). Significant decreases of the PI_{abs} in the genotypes Kraljica and Vulkan were observed only on 7 dpi by 90.7% and 57.6% compared to the controls, respectively, while no significant changes were observed on the last measurement point (10 dpi) (Figure 15e). In the FHB-stressed spikes of the genotype Galloper, this parameter significantly decreased only on 10 dpi by 75.4% (Figure 15b).

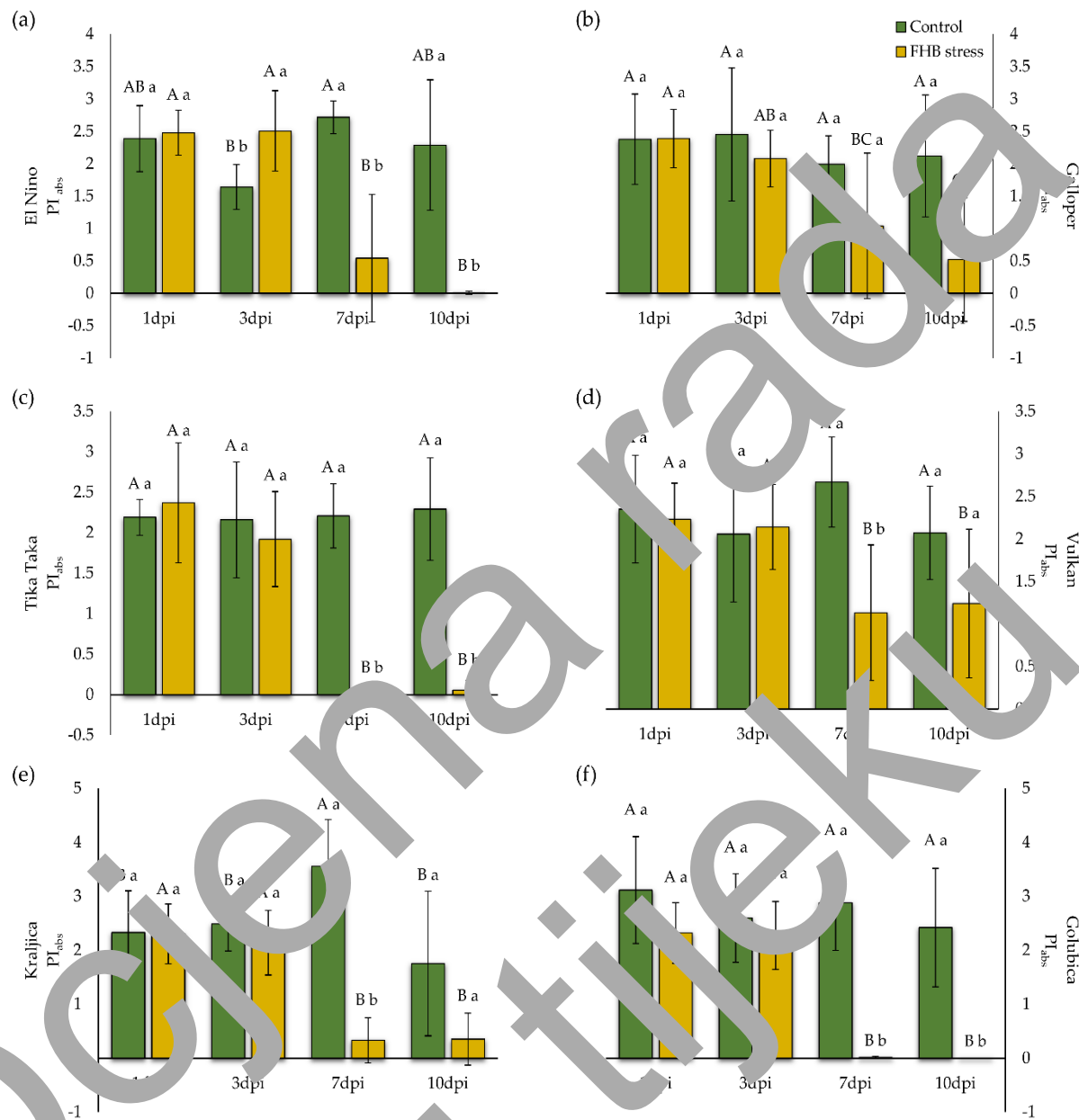


Figure 15. Performance index on absorption basis (PI_{abs}) in control and FHB-stressed spikes of six winter wheat genotypes (a) El Nino, (b) Gallop, (c) Tika Taka, (d) Vulkan, (e) Kraljica, and (f) Golubica. Bars represent mean values of six independent biological replicates \pm SD. Different small letters indicate significant differences between treatments on each measurement point separately (1 day post inoculation (dpi), 3 dpi, 7 dpi, and 10 dpi) ($p < 0.05$). Different capital letters indicate differences among measurement points in each treatment separately ($p < 0.05$).

3.2.2.2. Photosynthetic pigments content

Chl *a* content did not exhibit a uniform increasing or decreasing pattern among tested genotypes. Genotypes Vulkan, Tika Taka, Galloper, and Kraljica reduced Chl *a* content in FHB-stressed spikes. However, the reduction was significant only in genotypes Vulkan and Tika Taka, which reduced it by 17.6% and 12.5% compared to the corresponding controls, respectively. Genotypes El Nino and Golubica increased Chl *a* content by 4.6% and 14.2% compared to the corresponding control spikes, respectively (Figure 16).

Chl *b* content followed the same non-uniform decrease or increase trend as Chl *a*. Genotypes Tika Taka, Galloper, and Vulkan all decreased Chl *b* content. However, the decrease was only significant in genotypes Tika Taka and Vulkan, which reduced it by 27% and 16%, respectively. Although increased Chl *b* levels were recorded in genotypes Kraljica, Golubica, and El Nino, a significant increase was only recorded in genotype Golubica, which increased it by 20.5% (Figure 17).

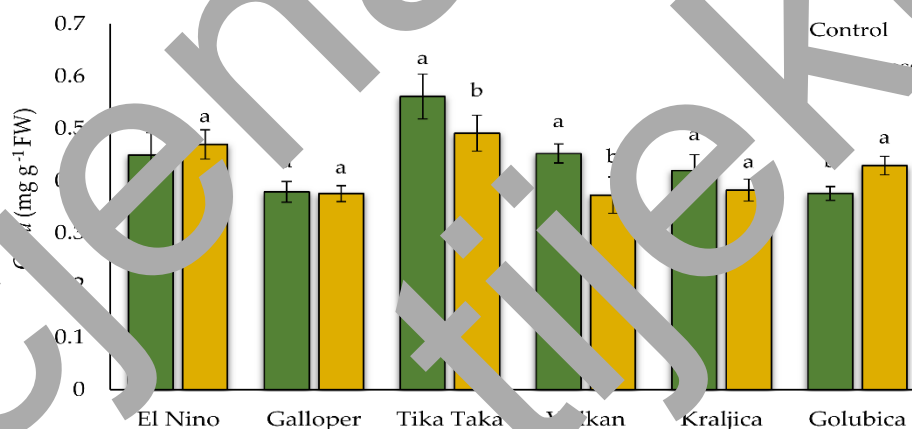


Figure 16. Content of chlorophyll *a* (Chl *a*) in control and FHB-stressed spikes of six winter wheat genotypes (El Nino, Galloper, Tika Taka, Vulkan, Kraljica, and Golubica). Bars represent mean values of six independent biological replicates \pm SD. Different letters indicate significant differences among treatments in each genotype separately ($p < 0.05$).

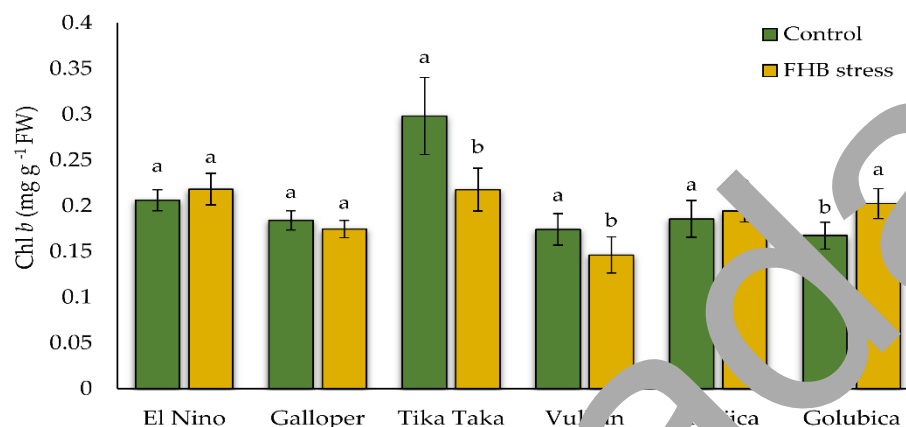


Figure 17. Content of chlorophyll *b* (Chl *b*) in control and FHB-stressed spikes of six winter wheat genotypes (El Nino, Galloper, Tika Taka, Vulkan, Kraljica, and Golubica). Bars represent mean values of six independent biological replicates \pm SD. Different letters indicate significant differences among treatments in each genotype separately ($p < 0.05$).

Genotypes Kraljica, Vulkan, and Galloper showed a decreasing trend in Car concentration. However, the decrease was significant only in FHB-stressed spikes of genotypes Kraljica and Vulkan, which reduced it by 12.9% and 20.2% compared to corresponding control spikes, while the decrease in genotype Galloper was not significant. Genotypes El Nino, Tika Taka, and Golubica increased Car levels in inoculated spikes by 1.7%, 5.3%, and 19.3% respectively, although increase in genotype Tika Taka was not significant. (Figure 18).

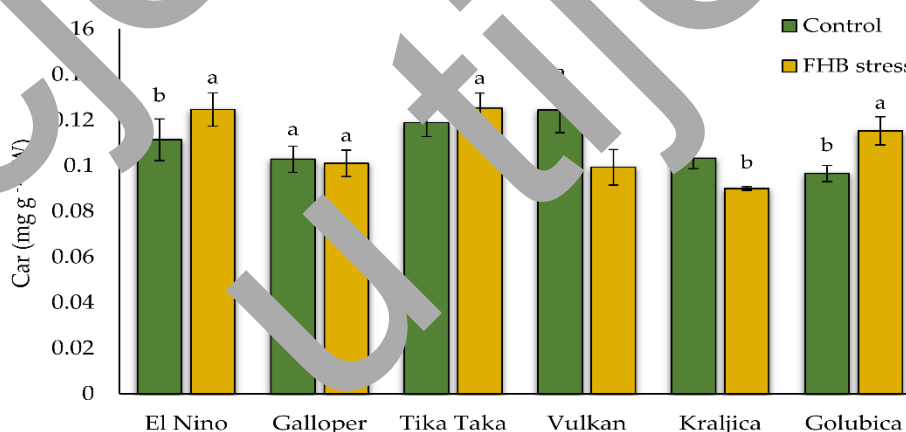


Figure 18. Content of carotenoids (Car) in control and FHB-stressed spikes of six winter wheat genotypes (El Nino, Galloper, Tika Taka, Vulkan, Kraljica, and Golubica). Bars represent mean values of six independent biological replicates \pm SD. Different letters indicate significant differences among treatments in each genotype separately ($p < 0.05$).

A decrease in Chl *a* to Chl *b* ratio (Chl *a*/Chl *b*) was recorded in genotypes El Nino, Vulkan, Kraljica, and Golubica, while genotypes Galloper and Tika Taka showed an increase in Chl *a*/Chl *b*. However, significant changes were recorded only in genotype Vulkan and Kraljica, which decreased this ratio by 7% and 16% compared to the control spikes, respectively. The recorded significant increase in FHB-stressed spikes of the genotype Tika Taka was 22.7%, compared to the corresponding controls (Figure 19).

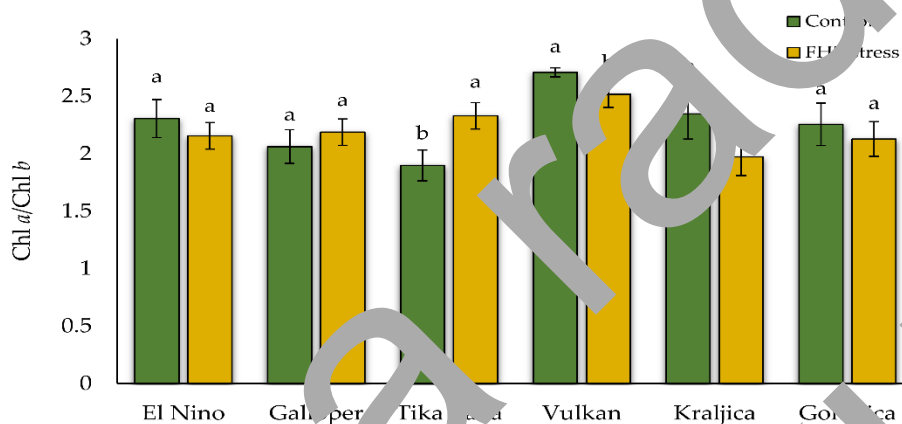


Figure 19. Chlorophyll *a/b* ratio in control and FHB-stressed spikes of six winter wheat genotypes (El Nino, Galloper, Tika Taka, Vulkan, Kraljica, and Golubica). Bars represent mean values of six independent biological replicates \pm SD. Different letters indicate significant differences among treatments in each genotype separately ($p < 0.05$).

Genotypes Galloper and Kraljica significantly decreased the Car to total Chl ratio (Car/Chl *a* + Chl *b*), by 4.6 and 13.6%, respectively, while this ratio increased in the rest of the genotypes (Figure 20). The increase in Car/Chl *a* + Chl *b*, which was the highest and at the same time only significant, was recorded in genotype Tika Taka, which increased it by 40.1%. The lowest increase in Car/Chl *a* + Chl *b* ratio was recorded in genotype Vulkan, which increased it by 2.3%.

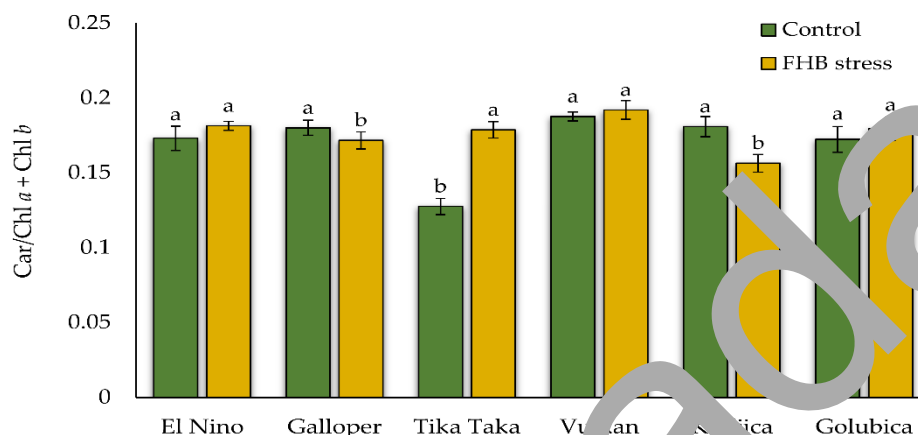


Figure 20. Carotenoids/total chlorophyll ratio (Car/Chl $a + \text{Chl } b$) in control and FHB-stressed spikes of six winter wheat genotypes (El Nino, Galloper, Tika Taka, Vulkan, Kraljica, and Golubica). Bars represent mean values of six independent biological replicates \pm SD. Different letters indicate significant differences among treatments in each genotype separately ($p < 0.05$).

3.2.3. Oxidative status

3.2.3.1. Lipid peroxidation level

The oxidative status of wheat spikes was assessed by determining the level of lipid peroxidation by measuring the amount of TBARS. All studied winter wheat genotypes had increased TBARS content in FHB-stressed spikes compared to control ones. However, a significant increase was recorded only in genotypes El Nino, Tika Taka, and Golubica, which increased it by 35.6%, 54.0%, and 61.5%, respectively (Figure 21).

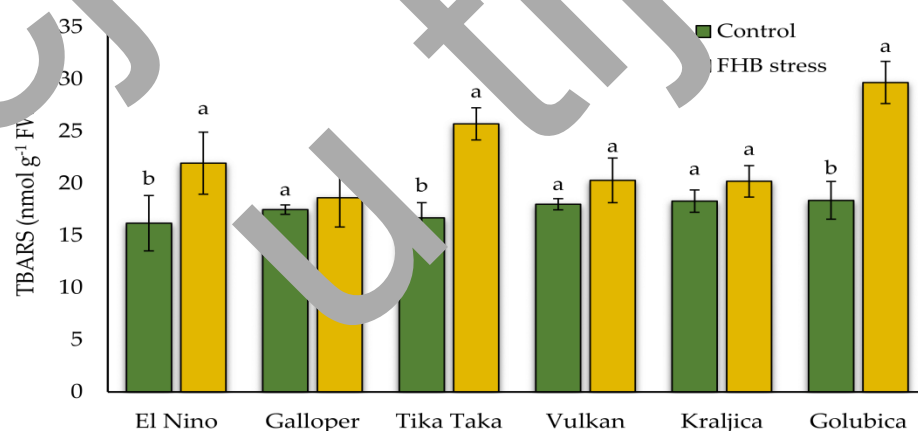


Figure 21. Content of thiobarbituric reactive substances (TBARS) in control and FHB-stressed spikes of six winter wheat genotypes (El Nino, Galloper, Tika Taka, Vulkan, Kraljica, and Golubica). Bars represent mean values of four independent biological replicates \pm SD. Different letters indicate significant differences among treatments in each genotype separately ($p < 0.05$).

3.2.3.2. Hydrogen peroxide content

In addition to the lipid peroxidation level, the oxidative status of winter wheat spikes was also monitored by measuring the amount of H_2O_2 . The same as for MDA content, the increase of H_2O_2 content in FHB-stressed spikes was also recorded in all studied genotypes. Furthermore, the increase was significant in almost all genotypes except genotype Vulkan, which increased H_2O_2 content in FHB-stressed spikes by 15.1% compared to control ones. Genotypes El Nino, Galloper, Tika Taka, Kraljica, and Golubica increased H_2O_2 by 53.8%, 50.0%, 89.5%, 41.2%, and 94.1% compared to control spikes, respectively. The most prominent increase in H_2O_2 had genotype Golubica (Figure 22).

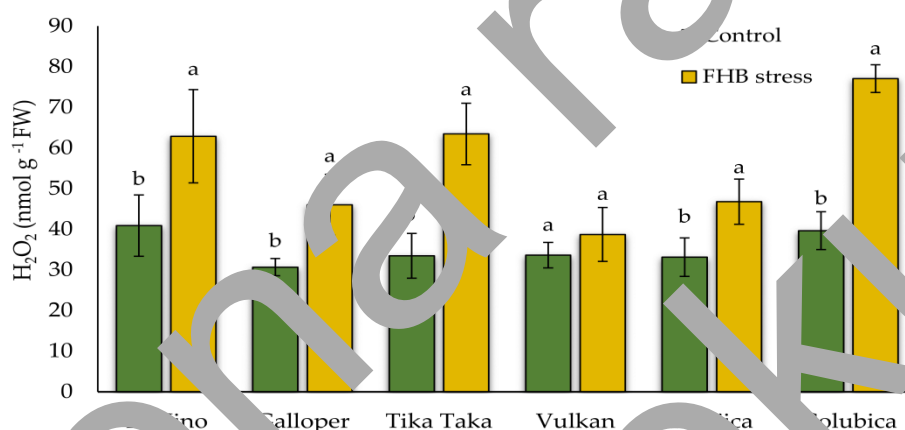


Figure 22. Content of hydrogen peroxide (H_2O_2) in control and FHB-stressed spikes of six winter wheat genotypes (El Nino, Galloper, Tika Taka, Vulkan, Kraljica, and Golubica). Bars represent mean values of four independent biological replicates \pm SD. Different letters indicate significant differences among treatments in each genotype separately ($p < 0.05$).

3.2.4. Antioxidative status

3.2.4.1. Ascorbate-glutathione cycle

3.2.4.1.1. Ascorbate peroxidase activity

In the artificially inoculated spikes of the Tika Taka and Golubica genotypes, APX activity significantly decreased by 78.5% and 51.7% compared to the corresponding control spikes, respectively. Genotypes Galloper, Vulkan, and Kraljica increased APX activity. The highest significant increase was in genotype Kraljica, which increased APX activity by 92.4%, followed by genotypes Galloper (73.4%) and Vulkan (32.8%) (Figure 23).

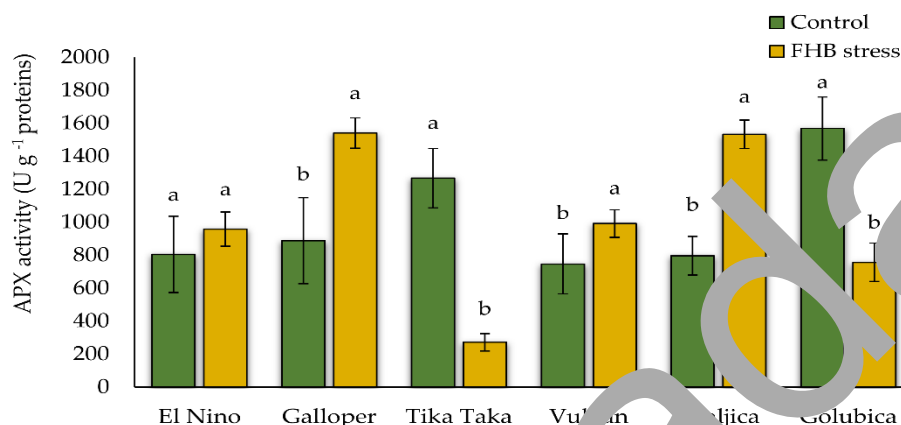


Figure 23. The activity of ascorbate peroxidase (APX) in control and FHB-stressed spikes of six winter wheat genotypes (El Nino, Galloper, Tika Taka, Vulkan, Kraljica, and Golubica). Bars represent mean values of six independent biological replicates \pm SD. Different letters indicate significant differences among treatments in each genotype separately ($p < 0.05$).

3.2.4.1.2. Monodehydroascorbate reductase activity

FHB stress decreased MDHAR activity in spikes of almost all winter wheat genotypes tested (Figure 24). The most prominent significant decrease in MDHAR activity was recorded in the genotype Golubica, which was reduced by 33.3%. The rest of the genotypes reduced it by 22.4% (Galloper), 26.9% (Tika Taka) and 15.5% (El Nino). In the artificially inoculated spikes of the genotype Kraljica MDHAR activity significantly increased by 49.1% compared to the corresponding control spike.

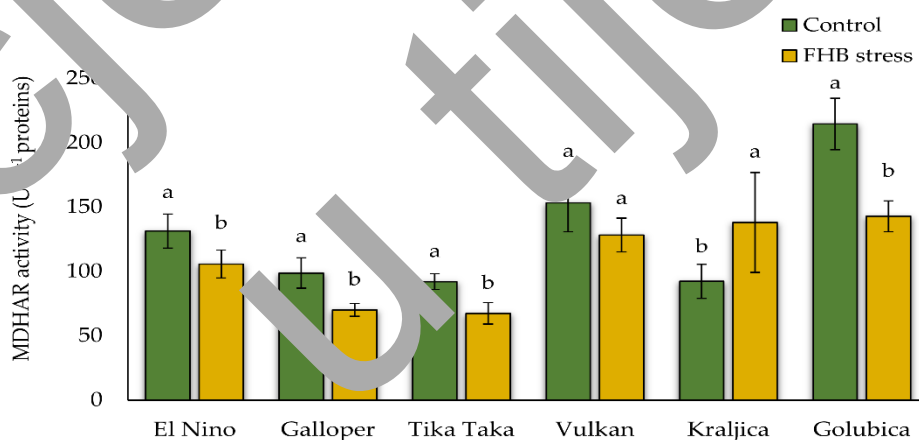


Figure 24. The activity of monodehydroascorbate reductase (MDHAR) in control and FHB-stressed spikes of six winter wheat genotypes (El Nino, Galloper, Tika Taka, Vulkan, Kraljica, and Golubica). Bars represent mean values of six independent biological replicates \pm SD. Different letters indicate significant differences among treatments in each genotype separately ($p < 0.05$).

3.2.4.1.3. Dehydroascorbate reductase activity

DHAR activity, similar to that recorded in the MDHAR, mostly decreased due to FHB stress (Figure 25). Genotype El Nino significantly reduced DHAR activity in the FHB-stressed spikes by 38.4% compared to the control ones, followed by genotypes Golubica (30.6%), Galloper (29.9%), and Tika Taka (21.1%). Genotypes Kraljica and Vulkan significantly increased DHAR activity in artificially infected spikes by 34% and 19.6%, respectively, compared to the corresponding control spikes.

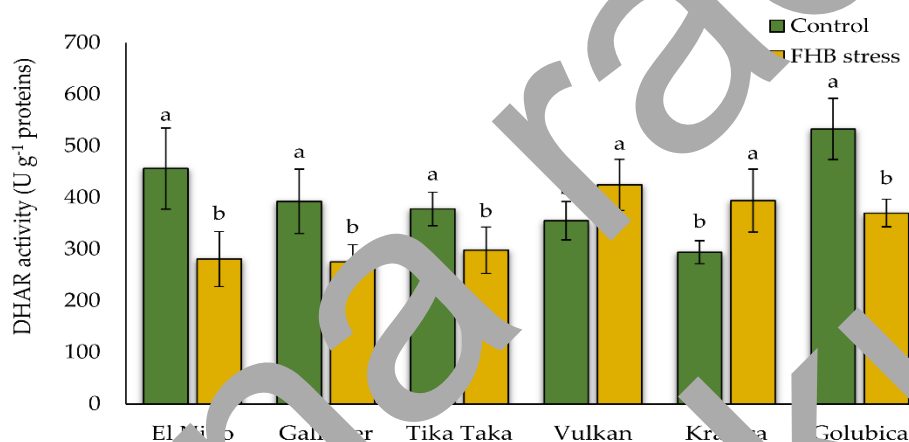


Figure 25. The activity of dehydroascorbate reductase (DHAR) in control and FHB stressed spikes of six winter wheat genotypes (El Nino, Galloper, Tika Taka, Vulkan, Kraljica, and Golubica). Bars represent mean values of six independent biological replicates \pm SD. Different letters indicate significant differences among treatments in each genotype separately ($p < 0.05$).

3.2.4.1.4. Glutathione reductase activity

Compared to the MDHAR and DHAR activities, which were mainly decreased, FHB stress increased GR activity in the spikes of almost all genotypes tested (Figure 26). The recorded increase was significant in all genotypes, where genotype Kraljica had the most distinguished increase (65.2%). Genotypes El Nino, Tika Taka, Golubica, and Galloper increased it by 49.3%, 39.1%, 25.2%, and 20.6%, respectively.

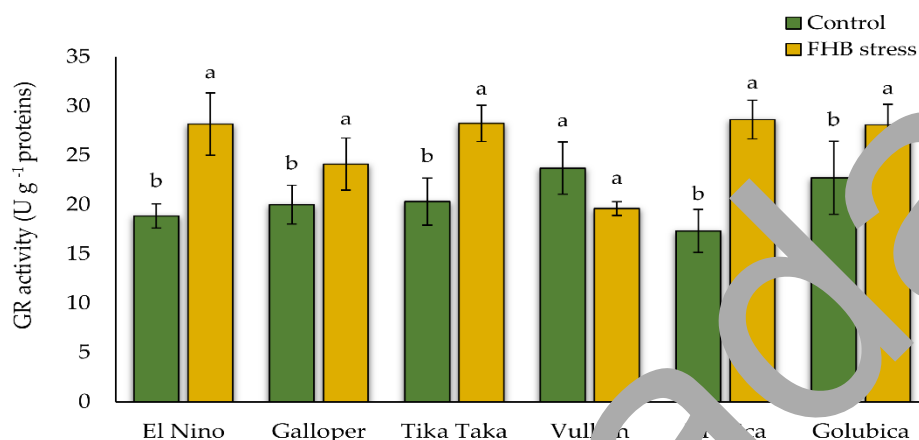


Figure 26. The activity of glutathione reductase (GR) in control and FHB-stressed spikes of six winter wheat genotypes (El Nino, Galloper, Tika Taka, Vulkan, Kraljica and Golubica). Bars represent mean values of six independent biological replicates \pm SD. Different letters indicate significant differences among treatments in each genotype separately ($p < 0.05$).

3.2.4.1.5. Reduced and oxidised glutathione content

The content of GSH in FHB-stressed spikes was not significantly affected in most of the tested genotypes (Figure 27a). Significant changes were only recorded in the FHB-stressed spikes of the Tika Taka and Golubica genotypes, which showed a 29.3% and 15.8% increase in GSH content compared to the corresponding controls, respectively.

Compared to the GSH content, all genotypes tested showed an increasing trend of GSSG in FHB-stressed spikes compared to the corresponding controls (Figure 27b). The recorded increase was significant in all genotypes tested except for the genotype Vulkan. Genotype Golubica had the most prominent significant increase of the GSSG content compared to the corresponding control (99.9%), followed by genotypes Kraljica (63.9%), El Nino (40.5%), Tika Taka (33%), and Galloper (21.3%).

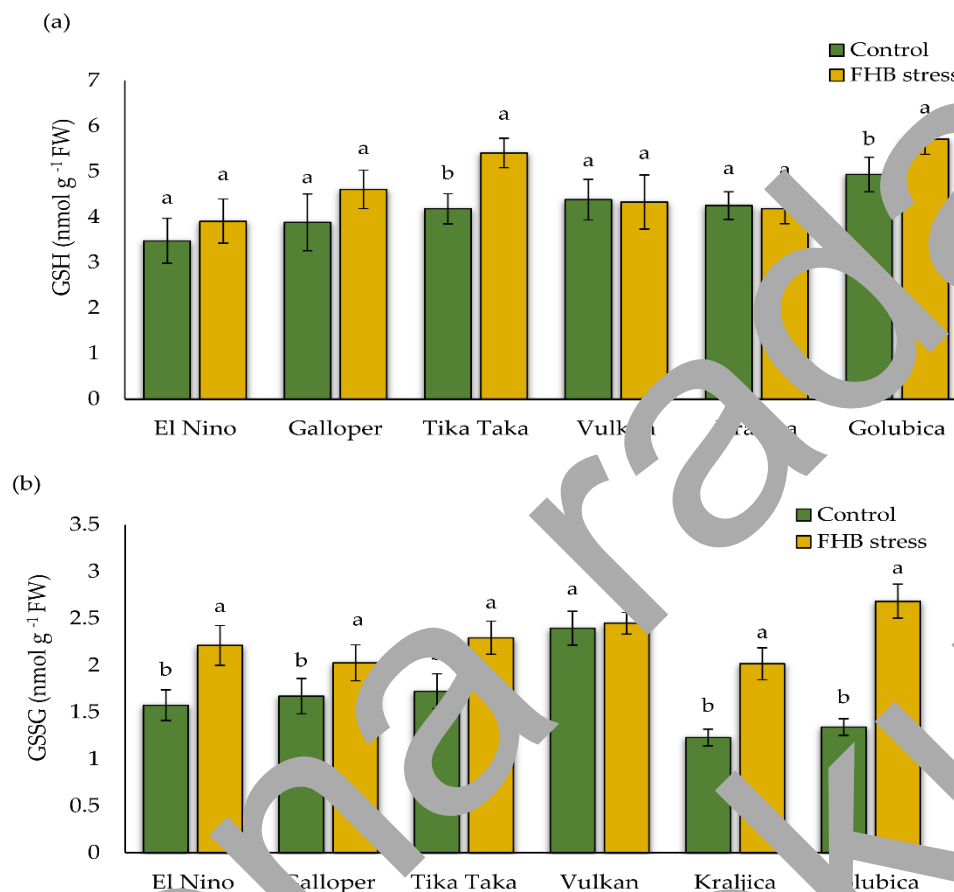


Figure 27. Content of (a) reduced glutathione (GSH) and (b) oxidized glutathione (GSSG) in control and FHB-stressed spikes of six winter wheat genotypes (El Nino, Galloper, Tika Taka, Vulkan, Kraljica, and Golubica). Bars represent mean values of six independent biological replicates \pm SD. Different letters indicate significant differences among treatments in each genotype separately ($p < 0.05$).

3.2.4.2. Catalase activity

Stress induced by FHB inoculations differentially affected CAT activity in the spikes of winter wheat genotypes studied. CAT activity increased only in FHB-stressed spikes of genotypes Galloper (15.7%) and Kraljica (12.5%). The rest of the genotypes decreased CAT activity in FHB-stressed spikes compared to the corresponding control spikes, where the decrease was significant in genotypes Tika Taka (16.3%), Vulkan (19.6%), and Golubica with the most prominent decrease (26.7%) (Figure 28).

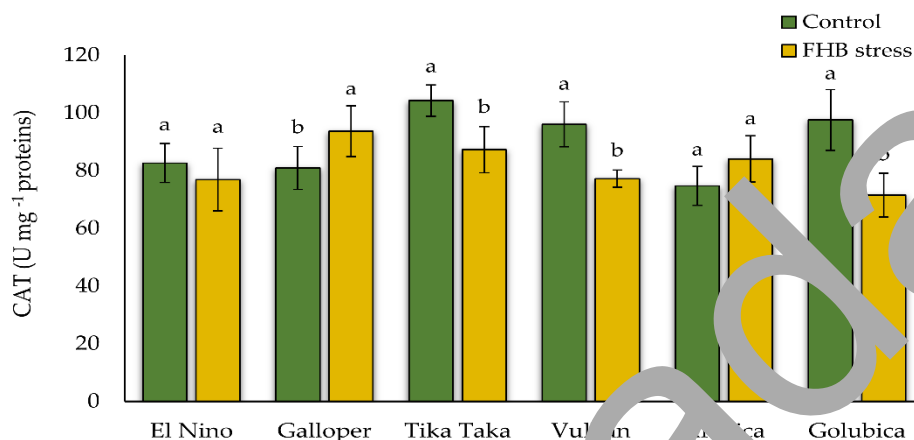


Figure 28. The activity of catalase (CAT) in control and FHB-stressed spikes of six winter wheat genotypes (El Nino, Galloper, Tika Taka, Vulkan, Kraljica, and Golubica). Bars represent mean values of six independent biological replicates \pm SD. Different letters indicate significant differences among treatments in each genotype separately ($p < 0.05$).

3.2.4.3. Glutathione S-transferase activity

FHB stress induced GST activity in almost all studied genotypes. However, the increase in GST activity was significant in only three out of five genotypes. Genotype Galloper increased GST activity in FHB-stressed spikes by 47.7%, genotype Vulkan by 27.7%, and genotype Kraljica by 16.6% compared to the corresponding controls. Only genotype Golubica significantly decreased GST activity in FHB-stressed spikes by 16% compared to the control spikes (Figure 29).

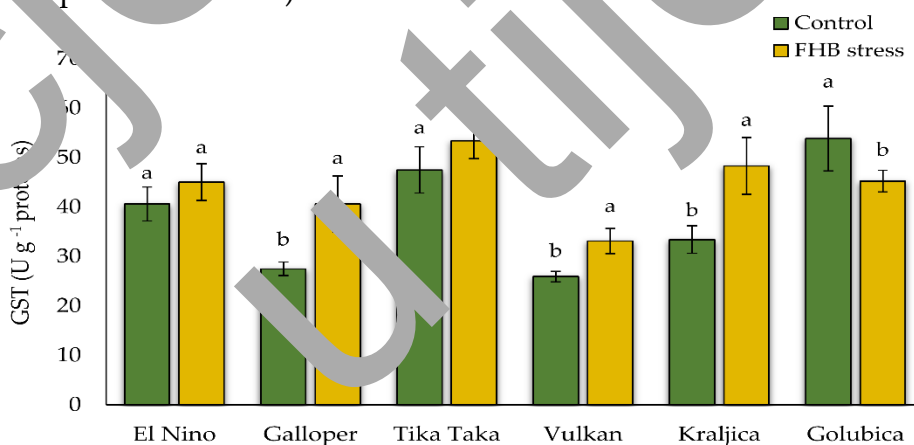


Figure 29. The activity of glutathione S-transferase (GST) in control and FHB-stressed spikes of six winter wheat genotypes (El Nino, Galloper, Tika Taka, Vulkan, Kraljica, and Golubica). Bars represent mean values of six independent biological replicates \pm SD. Different letters indicate significant differences among treatments in each genotype separately ($p < 0.05$).

3.2.4.4. Guaiacol peroxidase activity

FHB inoculations increased GPOD activity in almost all studied genotypes. The increase in GPOD activity was the most prominent in genotypes Galloper, Kraljica, El Nino, and Tika Taka which increased by 54.1%, 53.4%, 46.4%, and 22.8% compared to the control spikes, respectively. FHB stress did not cause changes in GPOD activity of genotypes Vulkan and Golubica (Figure 30).

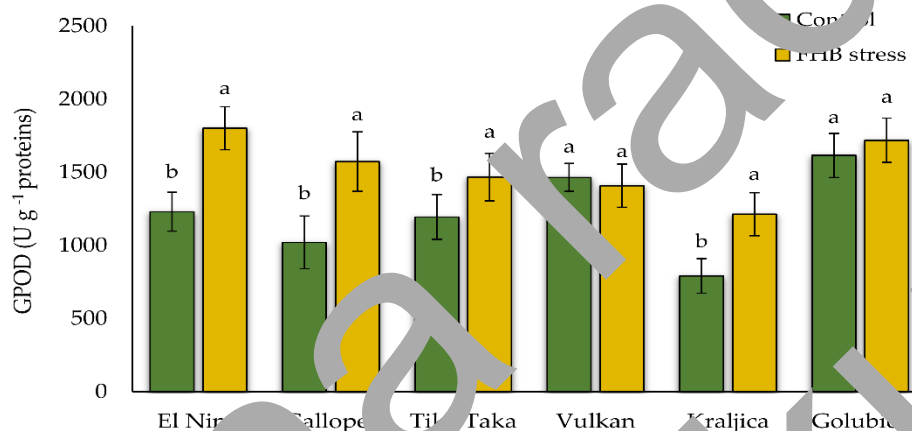


Figure 30. The activity of guaiacol peroxidase (GPOD) in control and FHB stressed spikes of six winter wheat genotypes (El Nino, Galloper, Tika Taka, Vulkan, Kraljica, and Golubica). Bars represent mean values of six independent biological replicates \pm SD. Different letters indicate significant differences among treatment in each genotype separately ($p < 0.05$).

3.2.5. Abscisic acid and salicylic acid content

Content of ABA was significantly increased in the FHB-stressed spikes of all winter wheat genotypes tested compared to corresponding controls. Genotype Golubica showed the most prominent significant ABA increase in FHB stressed spikes by 485.3%, followed by genotype Tika Taka with a 453.9% increase compared to the controls. Genotypes Galloper increased it by 218%, El Nino by 139%, and Vulkan by 126.9%, while the lowest increase was recorded for the genotype Kraljica (48.4%) (Figure 31).

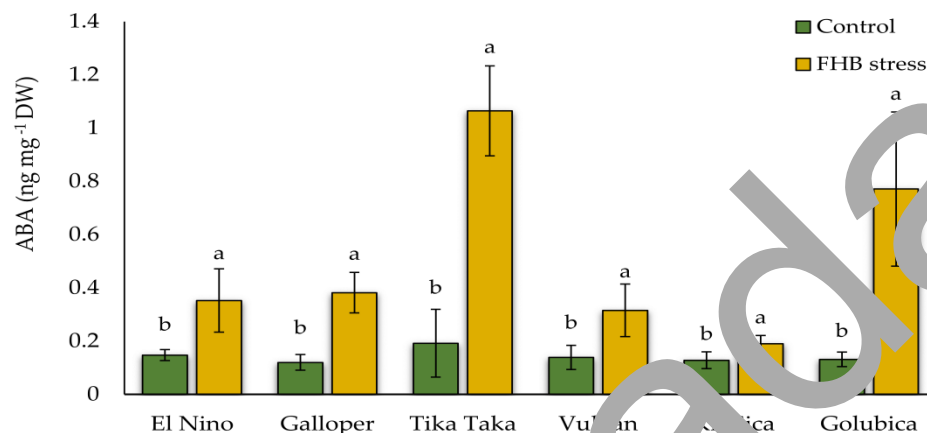


Figure 31. Content of abscisic acid (ABA) in control and FHB-stressed spikes of six winter wheat genotypes (El Nino, Galloper, Tika Taka, Vulkan, Kraljica, and Golubica). Bars represent mean values of six independent biological replicates \pm SD. Different letters indicate significant differences among treatments in each genotype separately ($p < 0.05$).

The content of SA in spikes of tested genotypes showed a non-uniform trend of decrease or increase. In most of the genotypes, observed SA content changes were insignificant. A significant increase in SA content in FHB-stressed spikes was recorded only in the genotype El Nino, which increased it by 54.6% compared to control spikes. On the contrary, genotype Vulkan showed a significant decrease in SA content in FHB-stressed spikes by 34.2% compared to the corresponding control spike (Figure 32).

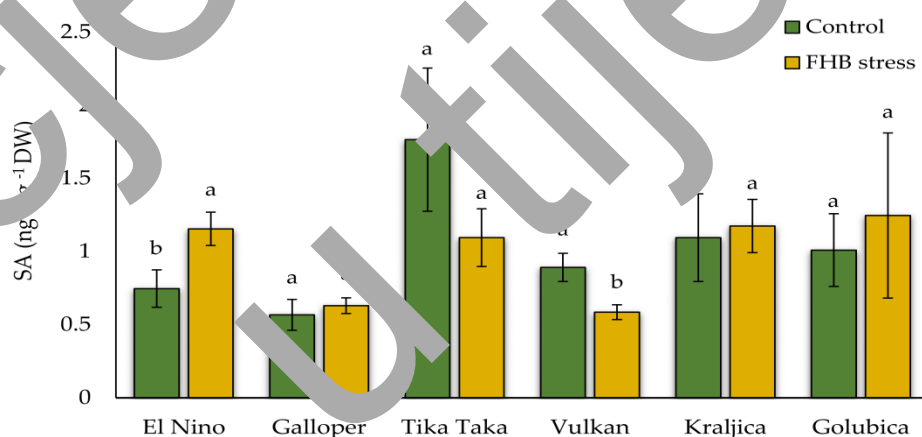


Figure 32. Content of salicylic acid (SA) in control and FHB-stressed spikes of six winter wheat genotypes (El Nino, Galloper, Tika Taka, Vulkan, Kraljica, and Golubica). Bars represent mean values of six independent biological replicates \pm SD. Different letters indicate significant differences among treatments in each genotype separately ($p < 0.05$).

3.2.5. Genes relative expression levels

3.2.5.1. *NPR1* relative expression

Relative expression of *NPR1* was differentially affected by FHB inoculations of the winter wheat spikes (Figure 33). The highest significant induction of the *NPR1* expression was recorded in the genotypes Vulkan and Tika Taka, both of which increased it by 86.9% compared to the corresponding control. The significant induction of the *NPR1* expression was also recorded in the genotype Kraljica, which increased it by 77% compared to the controls. The rest of the genotypes non-significantly increased the expression of *NPR1*.

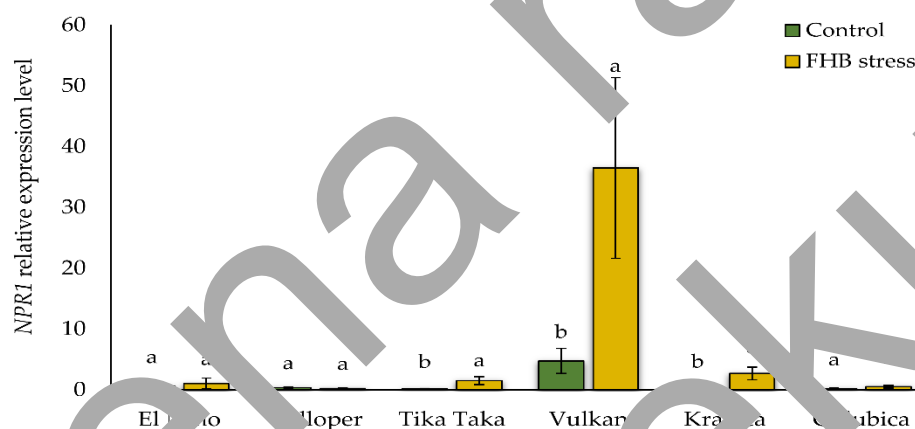


Figure 33. The relative expression level of the *NPR1* gene in control and FHB-stressed spikes of six winter wheat genotypes (El Nino, Galloper, Tika Taka, Vulkan, Kraljica, and Golubica). Bars represent mean values of six independent biological replicates \pm SD. Different letters indicate significant differences among treatments in each genotype separately ($p < 0.05$).

3.2.5.2. *TGA2* relative expression

Stress induced by FHB inoculations differentially affected *TGA2* expression (Figure 34). *TGA2* expression was significantly induced in genotypes El Nino, Golubica, and Galloper, which increased it by 74.8%, 66.8%, and 39.2% compared to the corresponding controls, respectively. FHB stress in the spikes of the genotype Tika Taka also induced *TGA2* expression, but non-significantly. In the FHB-stressed spikes of the genotypes Vulkan and Kraljica, *TGA2* expression was not influenced by the treatment.

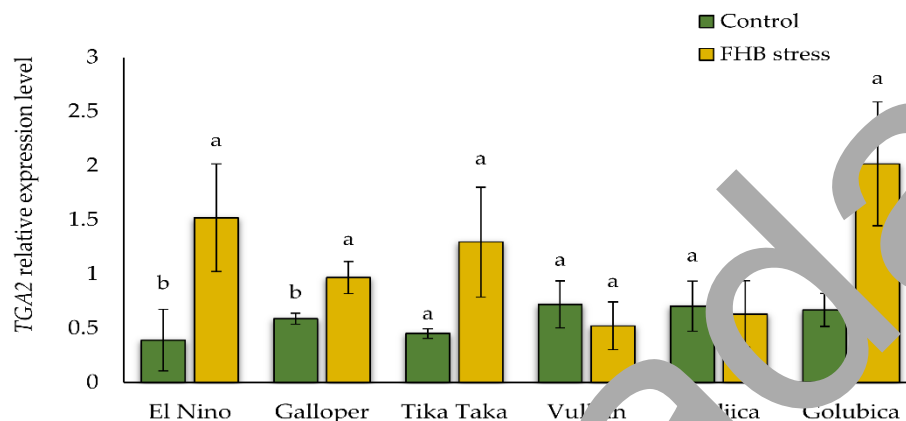


Figure 34. The relative expression level of the *TGA2* gene in control and FHB-stressed spikes of six winter wheat genotypes (El Nino, Galloper, Tika Taka, Vulkan, Kraljica, and Golubica). Bars represent mean values of six independent biological replicates \pm SD. Different letters indicate significant differences among treatments in each genotype separately ($p < 0.05$).

3.2.5.3. *PR1* relative expression

FHB stress significantly up-regulated expression of the gene encoding pathogenesis-related 1 (*PR1*) protein in the spikes of all studied winter wheat genotypes (Figure 35). The most prominent increase was recorded in the genotype Galloper, which induced the expression of *PR1* gene by 98.2% compared to the corresponding control. Genotypes Tika Taka, El Nino, Golubica, Kraljica, and Vulkan increase relative expression levels of *PR1* gene by 94.2%, 94.2%, 94.2%, 91.2%, and 78.6%, respectively.

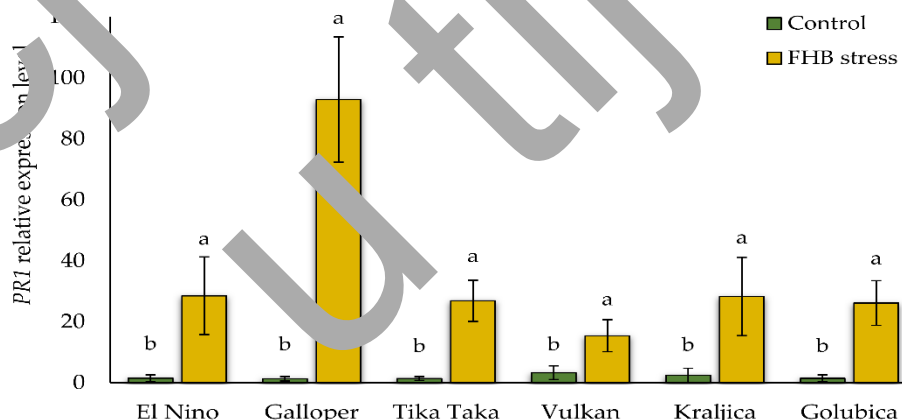


Figure 35. The relative expression level of the *PR1* gene in control and FHB-stressed spikes of six winter wheat genotypes (El Nino, Galloper, Tika Taka, Vulkan, Kraljica, and Golubica). Bars represent mean values of six independent biological replicates \pm SD. Different letters indicate significant differences among treatments in each genotype separately ($p < 0.05$).

3.2.5.4. *PR3* relative expression

The expression of the gene encoding pathogenesis-related 3 (*PR3*) protein showed the same trend of increase as the expression of the *PR1* gene (Figure 36). All studied winter wheat genotypes had a significant induction of the *PR3* expression in the spikes of FHB-inoculated plants compared to the control ones. The highest expression, also for the *PR1*, was recorded in the genotype Galloper (91.3%), followed by genotype El Nino (91.1%), Tika Taka (85.8%), Golubica (85.3%), and Kraljica (77.2%), and Vulkan (66.2%).

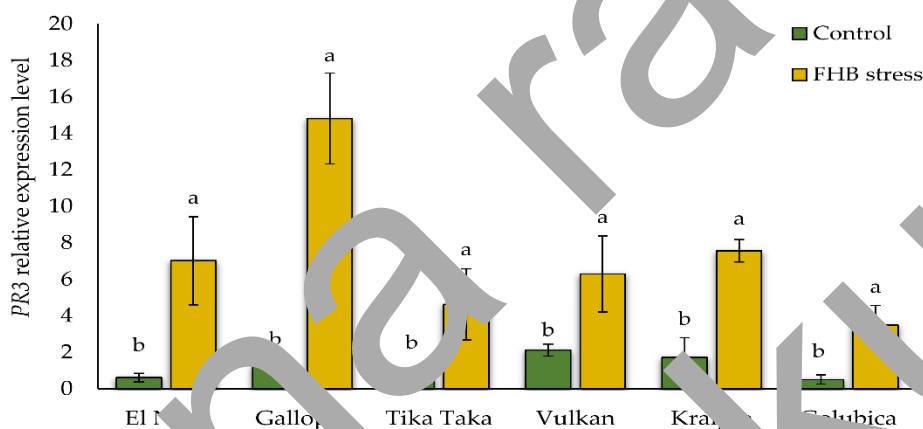


Figure 36. The relative expression level of the *PR3* gene in control and FHB-stressed spikes of six winter wheat genotypes (El Nino, Galloper, Tika Taka, Vulkan, Kraljica, and Golubica). Bars represent mean values of six independent biological replicates \pm SD. Different letters indicate significant differences among treatments in each genotype separately ($p < 0.05$).

3.2.5.5. *PR5* relative expression

FHB stress significantly induced the expression of pathogenesis related 5 (*PR5*) protein (Figure 37). The expression of the *PR5* gene was again the highest in the inoculated spikes of the genotype Galloper, which increased it by 99.3% compared to the corresponding control. The second highest expression was recorded in the genotype Golubica (99.2%), followed by genotypes Tika Taka (98.6%), Vulkan (98%), Kraljica (97.4%), and El Nino (96.6%).

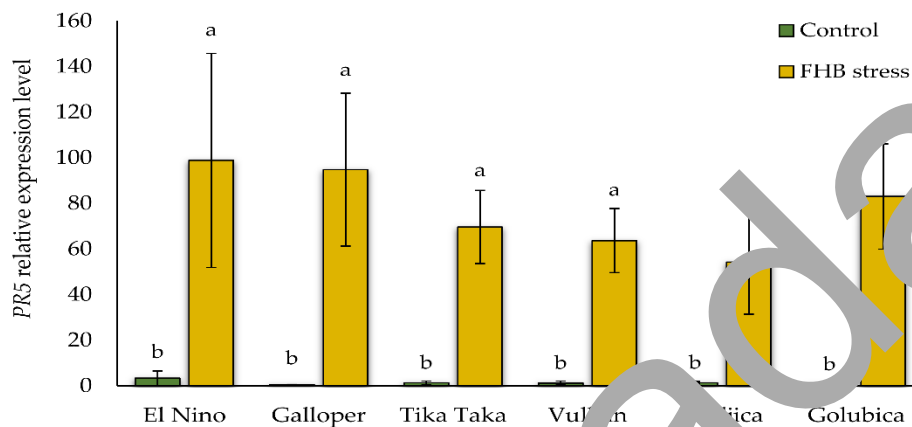


Figure 37. The relative expression level of the *PR5* gene in control and FHB-stressed spikes of six winter wheat genotypes (El Nino, Galloper, Tika Taka, Vulkan, Kraljica, Golubica). Bars represent mean values of six independent biological replicates \pm SD. Different letters indicate significant differences among treatments in each genotype separately ($p < 0.05$).

Ocjena rada
u tijeku

4. DISCUSSION

Developing wheat genotypes with a high degree of resistance to FHB is considered to be one of the most efficient methods of disease management. However, breeding FHB-resistant wheat genotypes is challenging due to the intricate wheat genome, quantitative inheritance, phenotypic variability, and ambiguous resistance mechanisms in host-pathogen interactions (Wu et al., 2022). Moreover, developing FHB-resistant genotypes with favourable agronomic traits is difficult due to the negative correlation between FHB resistance and agronomic traits. Several previous studies have focused on the different responses of winter wheat to FHB stress, either exclusively under field or controlled conditions, but rarely under both. Despite considerable effort to identify the processes involved in the wheat defence response to FHB, much remains to be clarified. Therefore, this study aimed to extend the existing knowledge on the metabolic, physiological, biochemical and molecular responses of winter wheat to FHB by investigating its response under both field and controlled conditions. Mycotoxin and polar metabolite content, general and type I resistance were determined on the genotypes grown in the field experiment, while type II resistance to FHB, photosynthetic efficiency, photosynthetic pigments, oxidative stress biomarkers, enzyme activities, GSH and GSSG content, stress-responsive gene expression, and plant hormones content were determined on the genotypes grown in the greenhouse.

The assessment of the general (disease severity) and type I (disease incidence) resistance was conducted using spray inoculation with *Fusarium* species. Disease severity indicates the proportion of infected spikelets either in a small or large spike population, while disease incidence refers to the number of spikes having one or more infected spikelets. Both disease severity and incidence, which describe the plant's reaction to spray inoculation, are estimated as a percentage, and this method has become the standard approach for evaluating FHB. According to AUDPC values for general resistance at both experimental locations, genotypes El Nino and Golubica could be characterised as highly susceptible, while AUDPC values for general resistance indicate genotypes Galloper and Vulkan at experimental location Osijek, and genotypes Galloper and Kraljica as FHB-resistant. Since genotypes El Nino and Golubica at experimental location Osijek and genotypes El Nino and Tika Taka at experimental location Tovarnik had the highest AUDPC values for type I resistance, they could be characterised as FHB-susceptible. On the other hand, genotypes Galloper and Vulkan at the experimental location Osijek and genotypes Vulkan and Kraljica had the lowest AUDPC values for type I resistance, indicating high type I resistance.

The extent of FHB spread inside an infected spike fluctuates according to the degree of host resistance. The pathogen may effectively initiate infection in any wheat genotype when spores are point-inoculated into a single floret of a spike. In a highly resistant genotype, FHB infection is often restricted to the inoculated spikelet or floret and does not spread to adjacent spikelets, while in a highly susceptible genotype, symptoms progress to uninoculated neighbouring spikelets until the whole spike is infected. The proliferation of FHB is contingent upon different factors, such as host genotypes and the environmental conditions under which the plants are cultivated (Ribichich et al., 2000; Bai et al., 2018). To evaluate FHB spread within the spike, the number of infected spikelets per spike was quantified at 10 dpi prior to tissue sampling. Symptoms of the infection became apparent at the 7th dpi, at which point the majority of spikes displayed FHB symptoms. Results of evaluating type II resistance in the current study indicate that genotypes Golubica and Tika Taka could be characterized as FHB-susceptible. Genotype El Nino possessed low type II resistance and could be characterized as FHB moderately susceptible. On the other hand, genotypes Kraljica and Galloper, according to the number of infected spikelets at 10 dpi could be characterized as FHB moderately resistant while genotype Vulkan possessed high type II resistance and could be identified as FHB-resistant.

4.1. Influence of Fusarium head blight on the winter wheat mycotoxin content

Fungi of the genus *Fusarium* are considered to be one of the world's most harmful pathogens, possessing high toxicity potential, and the mycotoxins synthesised by these pathogens rank among the five most significant mycotoxins in Europe and globally (Mielniczuk & Skwaryło-Bednarz, 2020). Mycotoxin contamination relies on several factors, such as climatic conditions, cultivation practices, harvesting techniques and timing, as well as the resistance of genotypes to FHB (Nganje et al., 2004; Golinski et al., 2017; Salgado et al., 2011, 2014; Bernhardt et al., 2012; Mielniczuk & Skwaryło-Bednarz, 2020). Previous studies demonstrated that mycotoxins DON and ZEN are the most frequently encountered mycotoxins in wheat, produced mainly by the species *F. graminearum*, *F. culmorum*, and *F. avenaceum* (Bottalico & Perrone, 2002). Nevertheless, numerous secondary metabolites produced by *Fusarium* species are insufficiently investigated, and as such, they are still not subject to legislation or monitoring (Stanciu et al., 2015).

Since mycotoxigenic fungi simultaneously synthesise numerous secondary metabolites (Streit et al., 2012), this study demonstrated the impact of epidemic FHB conditions on the levels of well-known mycotoxins and a range of fungal secondary metabolites synthesised by *Fusarium* species isolates. The total of 13 *Fusarium* metabolites and their concentrations were determined in the grains of six naturally infected and artificially inoculated genotypes (Vulkan, Kraljica, Galloper, Tika Taka, FENIKS and Grahovica) in this study. Since the use of fungicides and specific management practices can partly reduce losses caused by FHB, fungicides were excluded in this study, and field experiments were done according to the standard agronomical procedures.

In addition, growth of fungi and their capacity to produce mycotoxins are significantly affected by the intricate interplay of various environmental factors, primarily temperature and humidity (Llorens et al., 2004). The precipitation levels at the two experimental locations varied, with experimental location Tovarnik exhibiting higher precipitation rates and temperatures compared to experimental location Osijek. Consequently, the levels of *Fusarium* metabolites analysed were greater at Tovarnik than at Osijek. It is already previously reported that certain environmental factors such as temperature, water activity, and growth time directly impact DCM production in *F. culmorum*, *F. graminearum*, and *F. meridionale* (Llorens et al., 2004; Hope et al., 2005; Rybecky et al., 2018). Llorens et al. (Llorens et al., 2004) reported optimal temperature for *F. graminearum* and *F. culmorum* growth to be in the range between 20 °C and 32 °C, while reduction in the fungal growth was observed at the temperature of 15 °C and lower. Consequently, the most favourable temperature for DCM production was observed to be around 28 °C, while NIV synthesis was suggested to depend on the species, strain, and temperature (Llorens et al., 2004). Although toxin levels are found to be significantly elevated in the regions where pathogens are subjected to elevated temperatures and increased rainfall, mycotoxin synthesis can be increased even during a period of prolonged drought (Perincherri et al., 2019). For instance, the infection caused by *F. verticillioides* exacerbates throughout the flowering stage, and increased toxin accumulation is more likely to occur during warm conditions of approximately 30–35 °C with less rainfall (Perincherri et al., 2019). However, certain studies indicate that the impact of temperature and water availability on mycotoxin synthesis by *Fusarium* fungi is likely not direct but rather contingent upon the effects of these parameters on fungal growth (Popovski & Celar, 2013).

F. graminearum is globally distributed, including in Croatia, and is the primary DON producer (Spanic et al., 2010). The current results are in accordance with previous studies indicating that DON is the predominant mycotoxin in wheat grains (Vandecasteele, Fels-Klerx et al., 2012; Stanciu et al., 2017). Accumulation of DON in this study was recorded even in naturally infected grains of FHB-susceptible genotypes (Golubica, Trifun, Taka, and El Nino) at experimental location Tovarnik where it did not exceed the EU maximum limit of $1,250 \mu\text{g kg}^{-1}$ for unprocessed cereals (European Commission, 2006b). Similar results were obtained in a previous research where concentrations of DON in randomly selected cereal samples under natural infection from six Croatian regions (including Osječko-baranjska County) were below the maximum allowed concentration for human consumption (Pleadin et al., 2013). Nevertheless, artificially infected samples were far more contaminated with DON and exceeded maximum levels for DON contamination 10-fold at experimental location Osijek and 15-fold at experimental location Tovarnik. Such results are in accordance with similar previous studies showing the wide variety of fungal mycotoxins present in the field conditions in Croatia under *Fusarium* inoculation and under natural infection, where all *Fusarium* inoculated samples exceeded the maximum allowed levels for DON contamination (Spanic et al., 2020). Numerous studies have indicated a positive correlation between FHB incidence and DON levels (Snijders & Perkowski, 1990; Barać et al., 2011). However, there are also studies indicating that there was no significant correlation between DON concentration and FHB severity (Champeil et al., 2004). Nevertheless, the accumulation of DON is a significant element in the overall FHB pathogenesis and such opposite findings in previous investigations may be due to the differences in the genotypes, pathogen populations, weather conditions, or management practices (Ji et al., 2015).

D3G is one of the main DON metabolites known as “masked” mycotoxin (Kovač et al., 2017). Since these mycotoxin forms may be reactivated under specific conditions, such as within the gastrointestinal tract, the consumption of foods containing D3G raises concerns (Berthiller et al., 2011, 2012). D3G was present in artificially infected samples at both experimental locations, while in naturally infected samples, it was observed in susceptible genotypes only at the experimental location Tovarnik. Similar results were obtained in the previous study reporting the occurrence of DON and D3G in durum wheat in Italy (Dall’Asta et al., 2013). Similarly, as in the current study, Spanic et al. (Spanic et al., 2019) also reported that D3G in naturally infected (control) samples was below the detection limit in wheat samples before and after malting. However, in this

study, D3G concentrations in artificially infected grains were much lower than DON concentrations. Such findings are in accordance with previous reports, which indicated that D3G usually comes in lower concentrations compared to concentrations of DON (Lemmens et al., 2016; Bryła et al., 2018). While evidence regarding the prevalence of modified mycotoxins is emerging globally, for Croatia, there are limited findings regarding “masked” mycotoxin concentrations in cereal grains (Marković et al., 2013; Kovač et al., 2018).

Mycotoxin 3ADON has generally been reported to occur together with DON (European Food Safety Authority (EFSA), 2013). The current study detected 3ADON in artificially infected samples at both experimental locations. Previous studies reported that 3ADON was one of the most abundant naturally occurring mycotoxins (Miedaner et al., 2001; Zhao et al., 2021). In the study by Spanić et al. (Spanić et al., 2019), 3ADON was also found in 19 out of 25 naturally infected samples. However, such results were not the case in the current study, where 3ADON was observed in only one FHB-susceptible genotype.

Although NIV is less prevalent in food compared to DON, it exhibits higher toxicity in animal studies (Cheat et al., 2013; Bryła et al., 2018). In the current study, NIV at the experimental location Osijek was observed only in artificially infected grains of the susceptible genotypes, while it was not detected in the naturally infected grains. However, at the experimental location Tovarisk, NIV was also found in the naturally infected grains of the susceptible genotype Golubica. Similar results were previously reported in the research by Spanić et al. (Spanić et al., 2019), in which NIV was found in the grains of only one naturally infected genotype. Bryła et al. (Bryła et al., 2018) detected naturally occurring NIV in 29.5% of the samples in concentrations ranging from 5.1 to 37.5 $\mu\text{g kg}^{-1}$. Furthermore, previous studies indicated that NIV concentrations in the organic wheat samples from Italy ranged between 12 and 106 $\mu\text{g kg}^{-1}$ (Juan et al., 2013). This is in accordance with the current study, where NIV concentrations in artificially infected grains were within a similar range, while in naturally infected grains, NIV was present in the lower concentrations.

In the current study, ZEN levels recorded in both artificially and naturally infected were within the permissible range and did not exceed applicable regulations of the maximum allowed levels in unprocessed cereals other than maize (wheat, oat, and barley) of 100 $\mu\text{g kg}^{-1}$ (European Commission, 2006b). Among all metabolites studied, ZEN concentrations were the lowest at both experimental locations and both treatments. Similar findings

were observed in the studies by Spanic et al. (Spanic et al., 2019; Spanic et al., 2020), where ZEN was observed only in artificially infected samples and usually in lower concentrations, although ZEN was found in the susceptible genotypes under natural infection. Such findings align with prior research indicating that ZEN concentrations in wheat rarely exceed $50 \mu\text{g kg}^{-1}$ (Klarić et al., 2009; Stanciu et al., 2015). Such results could be the consequence of ZEN being predominantly found in cooler climates of northern Europe, so its absence is anticipated in cereals from middle and southern European countries (Bottalico & Perrone, 2002; Quarta et al., 2005). However, although in lower concentrations, ZEN is often co-produced with DON by different *Fusarium* species (Jestoi, 2008).

New evidence suggests CUL as an “emerging” mycotoxin. The function of CUL in *Fusarium* infection of plants is not fully understood. However, unlike insects and animals, wheat coleoptile tissues are reported to be sensitive to CUL (Wang & Miller, 1988). In the current study, CUL was found in artificially infected grains of all genotypes studied at both experimental locations. Similar results are reported in the study of Spanic et al. (Spanic et al., 2020). CUL was accumulated in much higher concentrations in the artificially infected grains of susceptible genotypes. In addition, at the experimental location Tovarnik it was found in almost all genotypes under natural infection. Previous studies reported high CUL levels in all naturally contaminated grain samples of three types of cereals (barley, wheat, and oats) which also had high DON concentrations (Ghebremeskel & Longworth, 2001). Such results are in accordance with the current study, where naturally infected genotypes at the experimental location Tovarnik contaminated with DON, were also contaminated with CUL. The same case was for the genotype Tika at the experimental location Osijek, which was the only genotype studied that was contaminated with both DON and CUL. Wheat samples exhibiting increased DON concentrations exhibited higher CUL concentrations, suggesting that CUL may have a potential role in *Fusarium* virulence. Similar studies previously reported that CUL levels were generally positively correlated with DON levels (Uhlig et al., 2013; Mousavi Khaneghah et al., 2019;).

Modified CUL metabolites such as 15-hydroxyculmorin, 15-hydroxyculmoron, and 5-hydroxyculmorin were also detected in the grains of the genotypes studied at both experimental locations. Beccari et al. (Beccari et al., 2018) reported about different *F. graminearum* and *F. culmorum* strains producing 15-hydroxyculmorin, 15-

hydroxyculmoron, and 5-hydroxyculmorin in durum wheat samples harvested in central Italy. In the previous research, 15-hydroxyculmorin was the most abundant CUL derivative, and 5-hydroxyculmorin was second most abundant in samples artificially inoculated with *F. culmorum* (Ghebremeskel & Langseth, 2001). The same pattern in the current research was observed at the experimental location Osijek, while at the experimental location Tovarnik, it was the opposite, with 5-hydroxyculmorin being the most abundant CUL derivative and second most abundant being 15-hydroxyculmorin. The results from the current study are in accordance with a previous study indicating that in naturally infected wheat samples from Croatia the concentrations of CUL and 15-hydroxyculmorin are comparable to those of DON, suggesting a correlation between DON and CUL as well as CUL derivatives (Štifier et al., 2021). Similar results were observed in the study by Spanic et al. (Spanic et al., 2020), where, except CUL, its derivatives also had elevated levels in the grains of artificially infected genotypes compared to the naturally infected samples.

In addition, newly discovered metabolites such as aurofusarin, butenolide, chrysogin, and fusarin C were detected in the current study. However, considering the fact that these metabolites have only been recently discovered, they are far less investigated compared to the other *Fusarium* metabolites (Stanciu et al., 2015). The red pigment aurofusarin, synthesised by *F. graminearum*, *F. culmorum*, and *F. pseudograminearum*, is a dimeric polyketide classed with the aromatic polyketide group of naphthoquinones (Malz et al., 2005). Under increased FHB pressure, aurofusarin was detected in the grains of all artificially infected genotypes at both experimental locations, but it was mostly not observed in naturally infected samples. At the experimental location Osijek, the average level of aurofusarin was in accordance with the previous study by Spanic et al. (Spanic et al., 2020). There was an even higher concentration of aurofusarin detected, up to 140,000 $\mu\text{g g}^{-1}$ in Italian samples of durum wheat (Beccari et al., 2018). While other studies indicate the co-occurrence of aurofusarin and rubrofusarin (Frandsen et al., 2011), rubrofusarin in the present study was not detected.

Butenolide (4-acetamido-4-hydroxy-2-butenic acid gamma-lactone) is a secondary metabolite synthesised by various *Fusarium* species and is synthesised concurrently with DON in cereal grains worldwide. Butenolide exhibits low toxicity. However, only a small amount of occurrence and exposure data are available (Woelflingseder et al., 2020). There are no reports about chrysogin activity in the scientific literature, and similarly, the

toxicity of fusarin C has not been extensively studied either. Nonetheless, the International Agency for Research on Cancer has identified it as a potential human carcinogen, and the mutagenic impact is likely associated with the interaction of the epoxide group with DNA (Stępień et al., 2020). Since both *F. graminearum* and *F. culmorum* produce butenolide and fusarin C, these metabolites were expected in the current study. Butenolide and chrysogin levels in the current study were lower than previously reported by Spanic et al (Spanic et al., 2020). Similar results as in the study by Spanic et al. (Spanic et al., 2020) were also observed in the study by Beccari et al. (Beccari et al., 2018), where higher concentrations of fusarin C, chrysogin, and butenolide were detected in naturally infected durum wheat samples. When considering only fusarin C and chrysogin, results from the current study are in accordance with results obtained by Garcia-Cela et al. (Garcia-Cela et al., 2018), where levels of fusarin C and chrysogin were increased in *Fusarium* inoculated wheat samples compared to the naturally stored wheat. In addition, Spanic et al. (Spanic et al., 2023) in their study during three consecutive years also observed chrysogin in all wheat samples but in concentrations lower than in the current study.

4.2. Influence of *Fusarium* head blight on the winter wheat polar metabolite content

Metabolomics is a powerful bioanalytical tool for the thorough analysis and monitoring of the plant metabolome. Nevertheless, its utilisation for monitoring plant metabolism regulation in response to biotic stress is still emerging. However, its utilization could yield significant insights for applications in plant biotechnology, biomarker-assisted selection, and the agrochemical, food, and pharmaceutical sectors, hence enhancing agricultural production (Calderini et al., 2014). In plant-pathogen interactions, a series of chemical, molecular, and mechanical events occur, resulting in disease development (Dodds & Ratjen, 2010). Previous research has identified a substantial array of metabolites that may function in cereals to mitigate *Fusarium* infection and minimise mycotoxin accumulation (Siranidou et al., 2002; Bullina et al., 2011; Gunnaiah & Kushalappa, 2014). These metabolites originate from primary and secondary plant metabolism and can be broadly categorised into six principal groups: fatty acids, amino acids and their derivatives, carbohydrates, amines and polyamines, terpenoids, and phenylpropanoids (Atanasova-Penichon et al., 2016).

The Mann–Whitney U test results in this study indicated that exposure to FHB substantially influenced 18 wheat grain metabolites across two locations among 275 polar

metabolites identified. The current research aimed to obtain metabolite profiles of wheat grains as the final products of plant development while also determining the potential association of resistance-related metabolites in wheat grains with FHB resistance or susceptibility. Metabolites that were found to be significantly changed between treatments belonged to the groups such as amino acids and derivatives (2-piperidinecarboxylic acid or pipercolic acid, histidine, 5-hydroxytryptophan), small organic (carboxylic) acids (pyrrole-2-carboxylic acid, lactic acid dimer), polyphenols and their derivatives (4-hydroxybenzoic acid, 3-hydroxyflavone, 3,7-dihydroxyflavone, 3-(2,4-dihydroxyphenyl)propanoic acid, 2-hydroxyhippuric acid), saturated fatty acids (3-hydroxydodecanoic acid), carbohydrates (turansose, sophorose, cellobiitol), nucleotides (guanosine, 2-deoxyguanosine), terpenoids (ecologanin) and tocots (α -tocopherol acetate).

FHB-resistant and moderately resistant genotypes Vulkan, Kraljica, and Galloper from the experimental location Tovarnik, as well as moderately resistant genotypes Kraljica and Galloper from the experimental location Osijek, were mostly grouped on the upper right quadrant of the PCA biplot, while resistant genotype Vulkan from experimental location Osijek was placed further from the rest of the moderately resistant and resistant genotypes from both experimental locations, in the lower right quadrant of the PCA biplot and near metabolites α -tocopherol acetate, histidine, 3-hydroxyflavone, and 3-(2,4-dihydroxyphenyl)propanoic acid. Genotypes Vulkan and Kraljica from the experimental location Tovarnik were placed close to carbohydrates and derivatives (sophorose, turansose, and cellobiitol) on the PCA biplot. This could indicate that these metabolites could have a potential role in their resistance to FHB. These metabolites also increased their peak intensities as a response to artificial inoculation, compared to the corresponding controls. A similar case was observed at the experimental location Osijek, where the same genotypes increased peak intensities of the abovementioned metabolites as a response to FHB inoculations. Increased carbohydrates following FHB inoculations may be the consequence of the cell wall structure alterations in response to pathogen invasion. Similar results were reported earlier in the study by (Cuperlovic-Culf et al., 2016), where authors concluded that an increase in carbohydrate concentrations may serve as a reinforcement of the cell wall barrier to inhibit *F. graminearum* penetration. Furthermore, carbohydrates and their derivatives are recognised for their involvement in cell signalling, particularly in the upregulation of various defence-related genes as well as in membrane biogenesis (Paranidharan et al., 2008). According to Morkunas and

Ratajczak (Morkunas & Ratajczak, 2014), the induction of carbohydrates in response to biotic stresses, referred to as “high sugar plant resistance,” may enhance glycolysis and the tricarboxylic acid cycle, facilitating the production of energy and secondary metabolites essential for plant defence. In addition, the metabolic profile of wheat spikelets indicated that sugars may contribute to wheat's resistance against *F. graminearum* and the accumulation of DON (Gauthier et al., 2017). In addition, sophorose was listed as one of the main contributors to PC1, while cellobiitol was one of the main contributors to PC2. However, although sophorose, turanose, and cellobiitol showed a high positive significant Spearman correlation coefficient, these metabolites were not significantly correlated to FHB resistance.

Metabolites 5-hydroxytryptophan and histidine, belonging to the group amino acids and amines, were placed near FHB moderately resistant and resistant genotypes. These metabolites' peak intensities were notably increased in response to FHB inoculations in resistant and moderately resistant genotypes compared to the corresponding controls. Similar results were obtained in the study by Návarová et al. (Návarová et al., 2013), who observed that *Arabidopsis* plants infected with SAR-inducing *Pseudomonas syringae* had significantly higher amounts of free amino acids, including branched-chain amino acids (valine, leucine, isoleucine), aromatic amino acids (phenylalanine, tyrosine, tryptophan), and lysine. Amino acids serve as essential building blocks for several biosynthetic pathways and are crucial in signalling processes and plant stress responses, in addition to their fundamental involvement in peptide and protein synthesis (Beyer & Aumann, 2008; Hildebrand et al., 2015). Previous studies indicate that the accumulation of certain amino acids or their metabolic by-products activates resistance responses against pathogens, which may occur through SA- and ROS-mediated defence pathways or independently of them (Kumudini et al., 2018). Although 5-hydroxytryptophan and histidine significantly correlated with several metabolites, there was no significant correlation with FHB resistance. Histidine was also one of the main contributors to the PC1 and PC2. Although piperidine-2-carboxylic acid (pipecolic acid), a non-protein amino acid that regulates SAR and mediates plant defence priming (Zeier, 2013), was also found to be significantly changed between treatments in the current study, it was placed further from the rest of the amino acids and their derivatives, on the opposite side of histidine at the PCA biplot.

Tocopherols are lipid-soluble chemicals classified as members of the vitamin E group. They are potent non-enzymatic antioxidants that protect lipids from oxidation by eliminating lipid peroxyl radicals and singlet molecular oxygen (Mansoor et al., 2020). Although their antifungal and antimycotoxin efficacy against *Fusarium* is not fully understood (Atanasova-Penichon et al., 2016), recent studies have shown that sub-lethal concentrations of α -tocopherol greatly influenced fumonisin production (Pilot et al., 2013). Furthermore, Cela et al. (Cela et al., 2018) observed that upon exposure to fungal infections, both mutant *Arabidopsis* plants lacking key enzymes in the tocopherol synthesis exhibited increased susceptibility to *Botrytis cinerea*, characterised by a fast increase in MDA levels and fungal biomass relative to wild-type plants, implicating alterations in membrane fatty acid composition. Metabolite α -tocopherol acetate also showed no significant correlation with FHB resistance in the Spearman correlation matrix.

Metabolite 3-hydroxyflavone and 3-(2,4-dihydroxyphenyl)-propanoic acid belonging to the group of polyphenols and their derivatives were also placed next to the resistant genotype Vulkan from experimental location Osijek. Phenols originate from the phenylpropanoid pathway and are regarded as the primary contributors to the overall antioxidant capacity of cereal grains (Atanasova-Penichon et al., 2016). The phenylpropanoid pathway leads to the formation of many compound families, including phenylpropanoid flavonoids, lignins, monolignols, phenolic acids, stilbenes, and coumarins. The flavonoid family comprises subfamilies of molecules categorised by their structural characteristics, such as flavones, isoflavones, anthocyanidins, flavonols, flavanols, flavanones, aurones, and chalcones (Ramirez et al., 2022). In the research by Zhou et al. (Zhou, 2010), elevated concentrations of flavonoids and phenylpropanoids were observed in barley resistant lines compared to susceptible lines after infection with *Fusarium*. Results of the previous study indicated that among other groups of metabolites, flavonoids exhibited significant alterations in synthesis after infection with *F. graminearum* in three Chinese wheat genotypes (Dong et al., 2023). Although 5,7-dihydroxyflavone, 4-hydroxybenzoic acid, and 2-hydroxyhippuric acid were also in this group of metabolites, they were placed further away, indicating that more important role in FHB resistance had 3-hydroxyflavone and 3-(2,4-dihydroxyphenyl)-propanoic acid. Although these metabolites correlated significantly with others, there was no significant correlation with FHB resistance in the correlation matrix.

Except 5,7-dihydroxyflavone, which was placed on the opposite side of most of the grouped moderately resistant and resistant genotypes on the PCA biplot, near were also nucleotides (guanosine, 2-deoxyguanosine), terpenoids (secologanin), and saturated fatty acids (3-hydroxydodecanoic acid). The role of nucleotides in regulating plant immunity has not yet been reported (Wang et al., 2022), although some previous studies concluded that guanosine phosphate nucleotides have a major impact on plant pathogen interactions and response to plant hormones like ABA, jasmonic acid, ethylene, and SA (Takahashi et al., 2004; Abdelkefi et al., 2018). Secologanin, a secopiridoing glucoside, plays a pivotal role as a terpenoid intermediate in the biosynthesis of monoterpenoids and indole alkaloids (Powell et al., 2017). A previous study investigating double haploid barley lines with varying sensitivity to FHB revealed that secologanin was consistently produced in resistant lines (Chamarthi et al., 2014). Secologanin may exhibit a direct antifungal effect or serve as a precursor for the synthesis of other compounds, such as phytoalexins, that mediate defense against fungal pathogens. Furthermore, alkaloids play a significant role in defense mechanisms. Nevertheless, relatively few alkaloid compounds have been identified in wheat. Although secologanin in the current study was on the opposite side of the FHB resistance, identifying the complete range of phytoalexins and other antifungal metabolites produced by wheat may provide a pathway for developing innovative disease resistance strategies (Powell et al., 2017). In addition to nucleotides and secologanin, previous research indicated that around 40 identified metabolites linked to fatty acid metabolic pathways may influence cereal resistance to *Fusarium* (Havrlentová et al., 2022). Although such metabolites may play a role in basal immunity and gene-mediated resistance in plants (Kachroo & Kachroo, 2006), 3-hydroxydodecanoic acid placed on the opposite side of the FHB-resistant and moderately resistant genotypes on the PCA biplot indicates that results are contrary to these previously obtained. Even though their exact function in plant stress response is still insufficiently understood, some small organic (carboxylic) acids are recognised as crucial in plant responses to biotic stress (Panchal et al., 2021). For instance, lower concentrations of certain small organic acids can improve plant host innate immunity against fungal pathogens by altering signalling and structural protein expression (Ghosh et al., 2016). However, small organic acids in the current study were placed further from the resistant and susceptible genotypes, possibly implying their less relevant function in wheat response to FHB stress.

4.3. Biochemical, physiological, and molecular response of winter wheat to *Fusarium* head blight

Understanding the processes and mechanisms involved in FHB defence responses is limited, and developing resistant genotypes is deemed the most effective strategy for controlling FHB (Buerstmayr et al., 2020). The first phases of *Fusarium* infection were documented as asymptomatic. After a proliferation of mycelium along the rachis and into the spikelets, the spike axis degrades, and symptoms manifest as bleaching (Leslie et al., 2021). Type II resistance has been well characterised and used in breeding programs due to its stability and ease of assessment in wheat compared to other resistance types. Type II resistance is often assessed using single flower (spikelet) inoculation, which involves injecting inoculum into a central spikelet of a spike during greenhouse experiments or through grain-spawn inoculation in field conditions (Bai et al., 2018).

The infection with fungal pathogens has a strong connection with alterations in many metabolic pathways, one of which is photosynthesis (Yang et al., 2016). However, a limited number of researches attempted to investigate the physiological response of wheat to *Fusarium* inoculation and the impact of FHB resistance on this response. Chl *a* fluorescence measurements are recognised as non-invasive, efficient, rapid, and sensitive. Additionally, the OJIP-test is extensively utilised to assess the effect of various stress types (Masuf et al., 2010). The response of the photosynthetic apparatus to varying conditions is typically assessed through the analysis of several OJIP-test parameters, such as the TR_0/ABS and the PI_{abs} , which quantifies the overall functionality of the electron flow through photosystem II (Ceusters et al., 2015). In the current study, TR_0/ABS and PI_{abs} measurements indicated that severe FHB stress adversely impacted photosynthetic efficiency in wheat spikes across nearly all tested genotypes, particularly in those susceptible to FHB (Golubica, Tikanjka, and El Nino). These genotypes had the highest decrease in TR_0/ABS and PI_{abs} on 7 and 10 dpi when compared to corresponding control spikes. Similar results were reported in the study by Katanić et al. (Katanić et al., 2021), in which susceptible genotypes showed a decrease in selected OJIP-test parameters at the beginning of symptom development. TR_0/ABS value is usually close to 0.8, and a reduced value signifies damage to a part of photosystem II reaction centres, a phenomenon referred to as photoinhibition, commonly observed in plants experiencing abiotic and biotic stress (Cheaib & Killiny, 2024). According to previous studies, infection by hemibiotrophic fungal pathogens typically leads to a decline in photosynthesis prior to

the manifestation of symptoms (Bilgin et al., 2010; Hu et al., 2020). The reason for this decline in incompatible reactions may result from the resources used for defence (Kangasjärvi et al., 2012). On the other hand, in compatible reactions, a decline in photosynthetic capacity could originate from the damage caused by pathogen infection on the host (Ma et al., 2015).

The photosynthetic apparatus consists of two main pigment groups - Chl and Car. It is generally agreed that elevated oxidative stress decreases photosynthetic pigments synthesis. Chl may, however, be important in the signalling network associated with stress responses (Agathokleous et al., 2020). In addition to Chl, Car are also crucial in various plant processes and serve as antioxidants during periods of plant stress. They function as light harvesters, quenchers, and scavengers of triplet state Chl and singlet oxygen species, dissipating damaging energy during stress conditions and stabilising membranes (Mohapatra & Mittra, 2007; Parrota et al., 2018). In cereals, Car are one of the main secondary metabolites with antioxidant activity (Boutigny et al., 2008). However, their antifungal and antimycotoxin activities against *Fusarium* spp. are not fully understood (Atanasova-Penichon et al., 2016). In the current study, FHB-susceptible genotypes Golubica and El Nino increased Chl *a* concentration in the artificially inoculated spikes, while in the rest of the genotypes studied Chl *a* content was decreased or it was not changed. Chl *b* showed a similar trend as for Chl *a*. Except for the susceptible genotypes Golubica and El Nino, genotype Kraljica also increased Chl *b* content in the artificially inoculated spikes. A previous study by Agathokleous et al. (Agathokleous et al., 2020) suggested that this phenomenon represents a conditioned defence mechanism in which adaptive responses characterised by elevated Chl concentrations triggered by low-dose stress can prevent Chl degradation or inhibition of Chl synthesis. Car also showed a similar trend in the artificially inoculated spikes of FHB-susceptible and moderately susceptible genotypes. Genotypes Golubica, Tika Taka, and El Nino increased Car content in the artificially inoculated spikes when compared to the control spikes. Such increased Car content in FHB-susceptible genotypes may indicate the employment of alternative defence mechanisms against the pathogen. Targeted approaches designed to correlate the lipophilic antioxidant composition of grains with resistance to *Fusarium* have been performed. However, they revealed either positive or negative correlation based on the specific group of compounds examined, either carotenoids or tocopherols (Atanasova-Penichon et al., 2016). The Chl *a*/Chl *b* ratio

exhibited varying patterns in our study relative to the contents of Chl *a* and Chl *b*. This ratio was especially evident in the FHB-resistant genotype Vulkan.

Different environmental stresses, including FHB, result in the formation of ROS in cells, leading to significant oxidative damage to the plants and consequently inhibiting growth and reducing grain yield. The balance between ROS generation and removal is known as redox homeostasis, but when ROS generation exceeds ROS scavenging, disrupting cellular redox equilibrium, it leads to a state known as oxidative stress (Caverzan et al., 2016). Lipid peroxidation is regarded as a characteristic of oxidative stress-induced cell damage. It results in extensive damage to cell membranes by altering the composition, assembly, structure, and dynamics of lipid bilayers. Lipid-derived radicals, being highly reactive compounds, facilitate further ROS generation, which interact with nucleic acids and proteins. In lipid peroxidation, polyunsaturated fatty acids such as linoleic, linolenic, arachidonic, and docosahexaenoic acids found in membrane phospholipids are particularly prone to oxidation. Radicals like $O_2^{\cdot-}$ and $^{\cdot}OH$ interact with polyunsaturated fatty acids, forming peroxides that extend the chain reaction and yield several additional reactive species. Elevated lipid peroxidation results in increased membrane rigidity and permeability, turning membrane-localized enzymes, ion channels, and receptors non-functional (Sahu et al., 2022). In the current study, all genotypes tested exhibited increased lipid peroxidation levels. However, the highest increase was recorded in the FHB-susceptible genotypes Golubica, Tika Taka, and El Nino. Similar results were obtained in the previous studies. Khaledi et al. (Khaledi et al., 2017) observed increased lipid peroxidation levels in inoculated spikes of wheat genotypes after infection by *Fusarium* spp. isolates until the milk stage and decreases afterwards. Furthermore, Gorahinobar et al. (Gorahinobar et al., 2016) also reported significantly elevated lipid peroxidation levels after treatment of wheat genotypes of varying levels of FHB resistance with *F. graminearum*. Chen et al. (Chen et al., 2015) also reported about increased lipid peroxidation in two wheat genotypes infected with stripe rust, with more susceptible genotype having more pronounced level of lipid peroxidation. The most prominent increase of the lipid peroxidation level in the genotypes Golubica, Tika Taka, and El Nino indicate more cellular damage than in other genotypes. On the other hand, lower lipid peroxidation in the rest of the genotypes studied implies a stronger antioxidative response in these genotypes.

Among the many ROS, H_2O_2 is one of the most prevalent and stable in aerobic biological systems of higher plants, exhibiting great reactivity and toxicity (Caverzan et al., 2016). Chloroplasts are a significant source of H_2O_2 production. In the absence of transition metal ions, H_2O_2 exhibits low reactivity with most organic molecules and may readily diffuse across the cell membrane to distant locations beyond its site of formation. An increasing body of research indicates that H_2O_2 is essential for the defence systems of plants under biotic stress (Yergaliyev et al., 2016). Elevated H_2O_2 content was observed in all genotypes studied. However, only the FHB-resistant genotype Vulkan showed non-significant increase, while susceptible genotypes showed the most prominent H_2O_2 increase. Increased H_2O_2 content in genotype infected with *Fusarium* species was reported in the previous studies. Sorahinobar et al. (Sorahinobar et al., 2016) reported elevated H_2O_2 concentration in both, FHB-resistant and susceptible wheat genotypes following inoculation with *F. graminearum*. Furthermore, Khaledi et al. (Khaledi et al., 2016) in their study performed histochemical analyses of the presence of H_2O_2 in the leaves of two wheat genotypes at various time points after inoculation with *Fusarium* isolates. The result indicates connection between increased cell death and the formation of ROS. Previous research suggested that ROS have a dual function in interactions between plants and pathogens (Feng et al., 2014). However, the importance of ROS for plant defence mechanisms depends on their concentration (Fittler et al., 2004). A low concentration of ROS activates protective antioxidant systems and triggers a systemic response, while a moderate to high concentration of ROS can be detrimental (Chen et al., 2015). Results of the current study indicate that a low amount of H_2O_2 in FHB-resistant genotype Vulkan activated defence mechanisms and there was no severe oxidative damage, while its high amounts in the susceptible genotypes imply high oxidative damage and cell death.

Plants have developed a sophisticated antioxidant defence system to detoxify the accumulation of excessive ROS and mitigate their harmful effects, which includes enzymatic and non-enzymatic antioxidants (Chen et al., 2015; Spanic et al., 2017). The assessment of the antioxidative response in wheat spikes after *Fusarium* inoculations in this study involved determining the levels of GSH and GSSG and activities of the enzymes CAT, GST, GPOD, and enzymes of the AsA-GSH pathway - APX, MDHAR, DHAR, and GR. GSH, a major cellular redox buffer, is one of the most important non-enzymatic antioxidants and one of the crucial factors in the stress tolerance of different plants, including wheat (Kuzniak et al., 2018). In non-stressed cells, GSH appears mostly

in its reduced form at around 90% and oxidised form at about 10%. Stressful conditions, such as plant infections by pathogens, often provoke oxidative stress, resulting in alterations in GSH levels and the ratio of GSH and GSSG (Zechmann, 2020). Given the critical importance of the reduced form of GSH in maintaining the redox potential in various reactions and cellular processes, it is important to maintain its level in cells by reducing GSSG to GSH by the enzyme GR in the presence of NADPH as a reducing agent (Deponte, 2013). In the current study, increased content of GSH was observed in FHB-susceptible and moderately susceptible genotypes, while GSSG content was significantly higher in all genotypes except Vulkan. According to Zechman (Zechmann, 2020), fluctuations in GSH levels are expected to be frequently noted during the initial phases of fungal infections, given that GSH neutralises ROS. A significant elevation of GSH and AsA levels in the apoplast of oat and barley plants correlated with resistance to the biotrophic fungus powdery mildew (*Blumeria graminis*) (Vanacker et al., 2000). However, in the current research, elevated GSH levels in FHB-susceptible genotypes may result from *de novo* GSH synthesis, implying elevated cytosol oxidation (Foyer & Noctor, 2005). In addition, significantly increased GSSG concentrations in nearly all genotypes in the current study indicate higher GSH consumption and inadequate GSH recycling under FHB stress despite increased GR activity. Such increased GSSG concentrations could be explained by GSH participation in direct or the indirect removal of ROS in wheat cells, as well as in maintaining other antioxidants, such as AsA and α -tocopherol, in a reduced state. Furthermore, enzymes such as glyoxalase I, glutathione peroxidases, and GST, also use GSH in their detoxification reactions. Almost each of these reactions, with the exception of reactions catalyzed by GST and glyoxalase I, results in the formation of GSSG (Deponte, 2013).

The activity of the AsA-GSH cycle significantly affects the steady-state concentration of ROS in cells, as well as the duration, localisation, and amplitude of ROS signals, collectively termed the ROS signature, which dictates the specificity of ROS signalling. In addition to AsA and GSH, enzymes of the AsA-GSH cycle - APX, MDHAR, DHAR, and GR - also play crucial functions and their activities are strongly correlated with the pools of GSH and AsA (Kuzniak et al., 2018). FHB inoculations significantly affected the activities of the enzymes of the AsA-GSH cycle. The first enzyme of the AsA-GSH cycle, APX, catalyses the detoxication of H_2O_2 using AsA as an electron donor. APX possesses a greater affinity for H_2O_2 compared to CAT and is more significant in regulating ROS-induced responses under stress. Increased APX expression in plants has been shown

under diverse stressful conditions (Syman et al., 2024). FHB-resistant and moderately resistant genotypes (Vulkan, Galloper, and Kraljica) in the present study increased APX activity in the inoculated spikes, while a significant reduction of the APX activity in the current study, caused by FHB inoculations-induced stress, was observed in the genotypes that can be characterized as FHB-susceptible (Golubica and Tik, Taka). Similar results were obtained in the study by Spanic et al. (Spanic et al., 2017), which observed a nonsignificant reduction of APX activity 336 hours after FHB inoculations in the susceptible genotype compared to the control, while more resistant genotypes showed an increase of APX activity on the same measuring point. In addition, in the experiment under field conditions, APX activity decreased quickly following FHB inoculations in the susceptible genotype (Spanic et al., 2020). The increase of the APX activity in the FHB-resistant and moderately resistant genotypes is in accordance with the study by Khaledi et al. (Khaledi et al., 2016), who measured the activities of the antioxidant enzymes in leaves and spikes inoculated with *F. graminearum* and *F. culmorum* in two genotypes varying in FHB resistance levels. Loss of APX activity in the susceptible genotype could be due to insufficient AsA recycling by other enzymes of the AsA-GSH cycle, consequently leading to high H_2O_2 accumulation under severe stress conditions (Shigeoka et al., 2002). In the process of APX-mediated detoxification of H_2O_2 , AsA is oxidised to MDHA, while MDHA is either enzymatically converted back to AsA through the action of the enzyme MDHAR or undergoes non-enzymatic disproportionation into AsA and DHA. DHA is then reduced back to AsA utilizing GSH as the electron donor by the action of the enzyme DHAR (Gallie, 2011; Pandey et al., 2015). In the current study, stress induced by artificial FHB inoculation decreased MDHAR activity in all studied genotypes, with the exception of the genotype Kraljica. The most prominent decrease in MDHAR activity was observed in the FHB-susceptible genotype Golubica. Similarly, as MDHAR, DHAR in the current study also showed a trend of decreasing activity in inoculated spikes. However genotype Kraljica and Vulkan, which can be characterised as FHB moderately resistant and resistant, respectively, showed increased activity of this enzyme following FHB inoculation. Burhenne and Gregersen (Burhenne & Gregersen, 2000), however, observed up-regulation of the MDHAR in barley leaves during powdery mildew infection in the compatible interaction when assayed 96 h after inoculation. However, in total leaf extracts of the barley genotype susceptible to powdery mildew 168 h after inoculation can be observed a decline of MDHAR activity. Kuźniak and Skłodowska (Kuźniak & Skłodowska, 2005) observed a characteristic biphasic pattern of

activity of the enzymes responsible for AsA recycling. In their study, the activities of MDHAR and DHAR in tomato plants inoculated with *B. cinerea* were induced only early during the infection, whereas the appearance of disease symptoms was characterised with a notable suppression of these enzymes. Such decline in MDHAR and DHAR activities in the more susceptible genotypes suggests that AsA is not effectively converted back to AsA by MDHAR and DHAR, while their increase in more resistant genotypes imply successful AsA recycling. In addition to AsA, GSSG produced during the detoxification of ROS is regenerated by the flavoprotein oxidoreductase GR, mainly localized in chloroplasts (Gill & Tuteja, 2010). When compared to other enzymes of the AsA-GSH cycle, stress induced by FHB artificial inoculations increased GR activity in all studied genotypes. Observed results imply greater GSH production and increased need for GSH recycling. However, such increased GR activity appeared to be insufficient to prevent the oxidation of the GSH pool, considering higher GSH consumption and consequently elevated GSSG content in inoculated spikes. Exception is genotype Vulkan which did not showed differences in GR activity compared to the control. Motallebi et al. (Motallebi et al., 2015) also showed elevated enzyme activity in the seedlings of resistant wheat genotypes infected with *F. culmorum*. Moreover, the authors observed a significantly earlier activation of antioxidant enzymes in FHB moderately resistant and resistant genotypes, followed by a decline in their activities over time. Such results showing early induction of antioxidant enzymes in plants with resistance to different pathogens may explain the reduction in enzyme activity in FHB inoculated spikes of moderately resistant and resistant genotypes on 10 dpi in the current study, aligning with the manifestation of disease symptoms.

In addition to APX, CAT is also one of the crucial enzymes that have the ability to break down H_2O_2 , making them essential for ROS detoxification (Syman et al., 2024). Similarly to the enzymes of the AsA-GSH cycle, CAT also showed decreased activity in all FHB-susceptible genotypes, while moderately resistant genotypes increased CAT activity. A similar was observed in the study by Khaledi et al. (Khaledi et al., 2016), where CAT activity decreased in the FHB-susceptible genotype Falat 72 h post-inoculations, while the same enzyme activity was higher in inoculated resistant genotype Gaskozhen. The authors concluded that enhanced activity of the antioxidant enzymes in leaves and spikes of wheat in Gaskozhen was correlated with a higher level of resistance in this genotype. Furthermore, Spanic et al. (Spanic et al., 2017) also observed higher (non-significant) CAT activity in the spikes of the resistant genotype 336 h after inoculations, while in the

susceptible genotype, CAT activity was significantly reduced on the same measuring point.

GSTs are enzymes that, except converting H_2O_2 , also catalyse the conjugation of GSH to various hydrophobic, electrophilic, and typically cytotoxic substrates (Manns, 1995). In addition to APX and CAT, an important role in the removal of H_2O_2 is also attributed to the enzyme GPOD, which is activated at significantly lower amounts of H_2O_2 compared to CAT and APX (Gadjev et al., 2008). Stress caused by artificial FHB inoculations induced activities of antioxidant enzymes GST and GPOD in almost all genotypes studied. A crucial element of GSH metabolism in plants affected by fungi is the detoxification of mycotoxins by the host plants' GSTs (Gullner et al., 2010). In the research by Gardiner et al. (Gardiner et al., 2010), treatment of barley spikes with DON resulted in significant up-regulation of gene transcripts encoding GSTs. The synthesis of DON-GSH conjugates was also noted, and the results indicated that GSH-conjugation facilitated by GSTs may mitigate the effects of trichothecenes. The results obtained in the current study were partially in accordance with the study by Khaledi et al. (Khaledi et al., 2016). In their study, authors observed increased GPOD activity in the spikes of the resistant wheat genotype compared to the susceptible genotype. Furthermore, GPOD activity significantly increased in the cells of cotton cotyledon undergoing hypersensitive response (Delannoy et al., 2003). Increased GPOD activity in most genotypes could, therefore, represent an alternative mechanism for H_2O_2 removal under conditions of excessive ROS production.

Phytohormones have a crucial role in the linkage between host-pathogen detection and the resulting cellular responses that activate defence pathways (Mishra et al., 2024). ABA plays a crucial role primarily in triggering adaptive responses to various abiotic stresses, including drought, low temperature, and salinity (Duvnjak et al., 2023). However, there is growing evidence that ABA affects biotic stress signalling (Mauch-Mani & Mauch, 2005). The highest increase of ABA content recorded in FHB-susceptible genotypes Golubica and Tika Taka in the current study is consistent with previous reports where increased levels of endogenous hormones such as ABA and related metabolites 4 days after inoculation with *F. graminearum* were observed (Qi et al., 2016). Research on ABA content after wheat inoculation with *Fusarium* spp. is limited. However, Qi et al. (Qi et al., 2019) examined transcriptome alterations of various phytohormones in wheat spikes, including ABA and observed that the pathogen invasion-induced ABA accumulation

likely lowers FHB tolerance by suppressing the expression of phenylalanine pathway genes. Inhibition of these genes reduced flavonoid and lignin biosynthesis, thereby compromising physical barriers against the fungus. Furthermore, the study by Buhrow et al. (Buhrow et al., 2016, 2021) demonstrated that ABA enhances gene expression associated with the early *F. graminearum* infection of wheat. Such results confirm results obtained in the current study, where two winter wheat genotypes displaying the highest FHB susceptibility exhibited the most significant elevation in ABA levels after *Fusarium* inoculations.

In recent decades, SA has been the subject of extensive research, particularly for its crucial function in plant immunity as a signalling molecule that triggers SAR to various phytopathogens (Rocheleau et al., 2019). In the current study, SA did not show a uniform trend of increase or decrease in response to artificial inoculations. Genotypes Tika Taka and Vulkan decreased SA, while an increase in SA content in the rest of the genotypes studied was recorded. The reason for decreased SA levels on 10 dpi could be explained by the fact that SA plays a crucial role in the early stages of infection (Graymar et al., 2015). Similar findings were observed in the previous study, where a biphasic phenomenon within the initial 24 h post-inoculation of wheat with *F. graminearum* was observed. The activation of the SA and Ca^{2+} pathway occurred within 6 h post-inoculation, followed by the activation of the JA-mediated pathway approximately 12 h post-inoculation (Feng et al., 2011). At the transcriptional level, a significant upregulation of genes involved in lignin biosynthesis was reported at 24 h post-inoculation, subsequently followed by down-regulation in the following 48 h (Zhang et al., 2015). Spanic et al. (Spanic et al., 2017) suggested that the rapid increase of H_2O_2 concentration in spikes of resistant winter wheat genotypes during the early stages of FHB infection may enhance FHB resistance, given that H_2O_2 functions as a signalling molecule for the induction of SAR. These findings might explain the observed results on 10 dpi in the current study. Nonetheless, the relation between SA and ROS, namely H_2O_2 , remains complex (Dat et al., 2000). Since previous investigations indicate that several *Fusarium* species may metabolise SA (Dodge & Wackett, 2005; Qi et al., 2019), this may explain why exogenous SA treatments of wheat spikes do not influence FHB resistance in some studies (Li & Yen, 2008; Qi et al., 2012). Li and Yen (Li & Yen, 2008) observed the absence of the effect of SA on FHB symptom levels. On the other hand, several reports indicate that SA is essential in this pathosystem, providing protection against FHB (Makandar et al., 2012). Previous studies confirmed that soil drench treatment with SA can enhance the resistance of wheat

genotypes to *F. graminearum* infection (Sorahinobar et al., 2016a; 2016b). Furthermore, the same authors indicated that wheat seed priming with SA led to induced resistance against *F. graminearum* seedling blight and concluded that seed priming is an effective method to mitigate the occurrence of *F. graminearum* infection by activating plant defence mechanisms (Sorahinobar et al., 2022). However, the effect of SA on wheat defence mechanisms that regulate FHB is still poorly understood (Qi et al., 2022).

The regulation of plant immunity via downstream SA-responsive genes encompasses several critical components that collectively optimise the complex defence mechanisms (Mishra et al., 2024). To evaluate the modulation of defence responses in wheat spikes following artificial inoculations, qPCR analysis was conducted to quantify the expression of defined defence-related genes 10 dpi with *F. graminearum* and *F. culmorum*. In the current study, the strongest upregulation of the *NPR1* gene was recorded in the artificially inoculated spikes of the FHB-resistant genotype Vulkan and FHB-susceptible genotype Tika Taka. These results are partially in accordance with the results obtained by Pan et al. (Pan et al., 2018), which observed an upregulation of differentially expressed genes associated with the SA pathway in response to *Fusarium* inoculation. A stronger upregulation was observed in the FHB-susceptible genotype. Another study showed that loss-of-function mutations in the *Arabidopsis thaliana NPR1* (*AtNPR1*) gene impaired the activation of SAR and increased susceptibility to multiple pathogens (Dong, 2004), demonstrating that *NPR1* is an effective candidate for controlling FHB. In the study by Thapa et al. (Thapa et al., 2018), leucine-rich receptor-like kinase gene (*TaLRRK-6D*) was upregulated in wheat following DON exposure during the initial phase of *F. graminearum* infection and silencing of *TaLRRK-6D* lowered wheat resistance to *F. graminearum* by downregulating the expression of SA signalling genes, one of which is also *NPR1*. However, certain studies showed that overexpression of wheat *NPR1* led to increased susceptibility to FHB (Rommens & Kuchare, 2000).

NPR1 lacks a DNA binding domain and hence exerts its transcriptional activity via interactions with other transcription factors. These transcription factors, also known as *NPR1*-interacting proteins, exhibit similarity to the basic domain leucine zipper motif and are categorised within the TGA family (Mishra et al., 2024). The majority of understanding about TGAs was derived from research conducted on *A. thaliana*. In *Arabidopsis*, TGAs consist of 10 members, categorised into five clades based on their sequence similarity (Gatz, 2013). *AtTGA2*, together with *AtTGA5* and *AtTGA6*, is

classified under clade II, exhibiting redundant functions in pathogen resistance and serving as co-activators of *NPR1* to stimulate *PR* gene expression (Zhang et al., 2003). TGA factors, similar to *NPR1*, are essential for SAR (Gao et al., 2015). In the current study, the strongest upregulation of the *TGA2* gene was recorded in the artificially inoculated spikes of the FHB-susceptible genotypes, while in the resistant genotypes, it was not significantly changed. Such results are contradictory to the results obtained in the study by Zhang et al. (Zhang et al., 2003), which showed that *tga2-tga5-tga6* triple mutant is non-responsive to SA and shows an impairment in SAR. Zander et al. (Zander et al., 2010) elucidated the critical function of TGA transcription factors (TGA2, TGA5, and TGA6) in the initiation of SA-mediated defence against biotrophic pathogens and the activation of ethylene-jasmonic acid-mediated defence against necrotrophic pathogens in *Arabidopsis*. In addition, transcription factors belonging to the basic domain leucine zipper motif family exhibited significant down-regulation in susceptible wheat genotypes infected with FHB (Erayman et al., 2015). Such results indicate that TGA factors may play both negative and positive functions in plant defence responses.

The induction of *PR* genes is a primary mechanism by which SA affects the immune response to pathogens at the transcriptional level (Mishra et al., 2014). In the current study, genes encoding *PR1*, *PR3*, and *PR5* proteins were upregulated in all studied genotypes in response to artificial inoculations. The results of our investigation are in accordance with results obtained by Pritsch et al. (Pritsch et al., 2000, 2001), who observed transcripts of several defence response genes encoding peroxidase, *PR1*, *PR2*, *PR3*, *PR4*, and *PR5* accumulated in wheat spike tissues of FHB-susceptible and resistant genotypes. In addition, the authors observed that the accumulation of *PR4* and *PR5* gene transcripts was higher and earlier in the resistant genotype compared to the susceptible one. However, authors concluded that the systemic molecular response in uninfected spike tissues of *F. graminearum* point inoculated wheat spikes is not directly linked to type II resistance mechanisms but rather reflects a universal host response to infection manifested in both infected and neighbouring uninfected tissues (Pritsch et al., 2001). In the study by Qi et al. (Qi et al., 2012), an increase in expression of *PR1* and *PR4* genes was observed in response to wheat inoculation with *F. graminearum*, suggesting that SA, as well as ethylene-jasmonic acid defence pathways, were involved. Pan et al. (Pan et al., 2018) also reported about the upregulation of *PR1*, *PR1-1*, and *PR4* genes following *Fusarium* inoculations. However, authors concluded that none of them were expressed higher in any resistant genotype than in the susceptible one. The identification of many

differentially expressed genes across genotypes suggests that plant defence mechanisms against FHB infection involve a complicated regulatory network. This network comprises genes linked to signal transduction, metabolism, transport facilitation and cellular defence, as well as genes with unknown roles.

Ocjena rada
u tijeku

5. CONCLUSIONS

- Considering the fact that experimental location Tovarnik had higher precipitation and higher temperatures in the winter wheat flowering stage compared to the experimental location Osijek, epidemic FHB conditions caused by artificial inoculations in the field experiment led to the more pronounced disease symptoms and consequently higher levels of *Fusarium* mycotoxins at experimental location Tovarnik. Elevated mycotoxin levels were particularly increased in the genotypes susceptible to FHB.
- CUL and hydroxyculmorin levels were higher in winter wheat genotypes with higher DON concentrations, suggesting that CUL may play a certain role in *Fusarium* virulence, which was most noticeable in genotypes with more pronounced FHB infection.
- Artificial *Fusarium* inoculations in the field experiment led to the separation of 18 polar metabolites, which varied among treatments at both experimental locations compared to the corresponding controls. PCA of metabolite profiles showed that most of the *Fusarium* inoculated wheat genotypes were separated from the control genotypes, indicating a clear difference between metabolite profiles of FHB inoculated and control genotypes.
- Metabolites placed near the FHB moderately resistant and resistant genotypes on the PCA biplot are considered to have a certain impact on FHB resistance. These metabolites belonged to the functional groups of carbohydrates and derivatives, amino acids and derivatives, and polyphenols and derivatives.

Since the decrease in the values of both main indicators of photosynthetic efficiency (TR_0/ABS , PI_{abs}) was more pronounced in genotypes susceptible to FHB, it can be concluded that severe FHB stress adversely impacted photosynthetic efficiency in wheat spikes across nearly all tested genotypes, particularly in those susceptible to FHB.

- Although Chl *a* and *b* did not show a uniform trend of response to inoculations, an increase of Car caused by FHB stress in FHB-susceptible genotypes might imply the utilisation of alternative defence mechanisms against the pathogen attack.

- The significant elevation of lipid peroxidation levels in the FHB-susceptible genotypes suggests greater cellular damage compared to other genotypes. This is also supported by the fact that resistant genotypes had lower H_2O_2 increases compared to susceptible genotypes, where genotype Vulcan showed no changes in H_2O_2 content, implying a more effective antioxidative response.
- Decreased CAT and APX activity in FHB-susceptible genotypes implies that a more important role in ROS scavenging is attributed to GPOD, which maintained its high activity levels in almost all genotypes studied. Decreased MDHAR and DHAR activities in FHB-susceptible and moderately susceptible genotypes may imply insufficient AsA recycling. The reduction of certain enzyme activities in FHB inoculated spikes of moderately resistant and resistant genotypes 10 dpi may be due to their earlier activation. Increased GST activity in all genotypes except the most susceptible one might imply that GST plays an important role in plants affected by fungi by detoxifying *Fusarium* mycotoxins.
- Increased GSH levels only in FHB-susceptible genotypes, despite increased GR activity and significantly increased GSSG concentrations in nearly all genotypes might indicate that GSSG has not been successfully reduced. Increased GSH levels in FHB-susceptible genotypes may result from *de novo* GSH synthesis, implying greater GSH need and consumption, as well as elevated cytosol oxidation. Apart from the reactions of the AsA-GST cycle, the increased GSH consumption could also be a consequence of GSH participation in direct or the indirect removal of ROS in wheat cells, as well as in maintaining other antioxidants, such as AsA and α -tocopherol, in a reduced state. Furthermore, enzymes such as glyoxalase I, glutathione peroxidases, and GST, also use GSH in their detoxification reactions. Almost each of these reactions, with the exception of reactions catalyzed by GST and glyoxalase I, results in the formation of GSSG.
- FHB-susceptible genotypes in the current study had the most pronounced increase in the ABA levels, implying that ABA accumulation likely lowers FHB tolerance. Inconsistent SA levels in the studied genotypes could indicate that SA plays a crucial role in the early stages of FHB infection, following the activation of the jasmonic acid-mediated pathway.

- Since the induction of PR genes is a primary mechanism by which SA affects the immune response to pathogens, genes encoding PR1, PR3, and PR5 proteins were upregulated in all studied genotypes in response to artificial inoculations. Expression of *TGA2* was upregulated only in FHB-susceptible genotypes, and expression of the *NPR1* gene only in resistant genotypes. Since it has been shown that *NPR3*, which promotes *NPR1* degradation, has a low affinity for SA, low SA levels should reduce *NPR1* degradation. Thus, lower SA levels in the FHB-resistant genotype in the current study might be the reason why there was an increase of *NPR1* in the resistant genotype even on 10 d after inoculation.

Ocjena rada
u tijeku

6. REFERENCES

- Abdelkefi, H., Sugliani, M., Ke, H., Harchouni, S., Soubigou-Taconnat, L., Citerne, S., Mouille, G., Fakhfakh, H., Robaglia, C., & Field, B. (2018). Guanosine tetraphosphate modulates salicylic acid signalling and the resistance of *Arabidopsis thaliana* to Turnip mosaic virus. *Molecular Plant Pathology*, 19(6), 634–646. <https://doi.org/10.1111/MPP.12548>
- Aebi, H. (1984). Catalase in Vitro. *Methods in Enzymology*, 105(C), 121–126. [https://doi.org/10.1016/S0076-6879\(84\)05016-3](https://doi.org/10.1016/S0076-6879(84)05016-3)
- Agathokleous, E., Feng, Z. Z., & Peñuelas, J. (2020). Chlorophyll Fluorescence: Are chlorophylls major components of stress biology in higher plants? *Science of the Total Environment*, 726, 138637. <https://doi.org/10.1016/j.scitotenv.2020.138637>
- Alassane-Kpembi, I., Kolf-Clauw, M., Gauthier, M., Abrami, R., Abiola, F. A., Oswald, I. P., & Puel, O. (2013). New insights into mycotoxin mixtures: The toxicity of low doses of Type B trichothecenes on intestinal epithelial cells is synergistic. *Toxicology and Applied Pharmacology*, 272(1), 19–28. <https://doi.org/10.1016/j.taap.2012.05.023>
- Aldon, D., Mbengue, M., Mazars, C., & Galand, J. P. (2018). Calcium signalling in plant biotic interactions. *International Journal of Molecular Sciences*, 19(1), 1–19. <https://doi.org/10.3390/ijms19010665>
- Ali, S., Ganai, B. A., Khatili, A. N., Bhat, A. A., Mir, Z. A., Bhat, J. A., Syagi, A., Islam, S. T., Mushtaq, M., Adnan, P., Rawat, S., & Goveer, A. (2019). Pathogenesis-related proteins and peptides as promising tools for engineering plants with multiple stress tolerance. *Microbiological Research*, 212–213, 29–35. <https://doi.org/10.1016/j.micres.2018.04.008>
- Alifan, K. A., Faubert, D., & Jabaji, S. (2014). A Metabolic Profiling Strategy for the Detection of Plant Defense against Fungal Pathogens. *PLoS ONE*, 9(11). <https://doi.org/10.1371/journal.pone.0111930>
- Arcey, M., Audenaert, K., Zutter, M., Steppe, K., Van Meulebroek, L., Vanhaecke, L., De Vleeschauwer, D., Maesaert, G., & Smagghe, G. (2015). Priming of wheat with the green leaf volatile Z-3-hexenyl acetate enhances defense against *Fusarium Graminearum* but boosts deoxynivalenol production. *Plant Physiology*, 167(4), 1671–1684. <https://doi.org/10.1104/pp.15.00107>
- Anderson, J. A., Chao, S., & Liu, S. (2007). Molecular breeding using a major QTL for *Fusarium* head blight resistance in wheat. *Crop Science*, 47. <https://doi.org/10.2135/cropsci2007.04.0006IPBS>

- Arif, Y., Sami, F., Siddiqui, H., Bajguz, A., & Hayat, S. (2020). Salicylic acid in relation to other phytohormones in plant: A study towards physiology and signal transduction under challenging environment. *Environmental and Experimental Botany*, 175, 104040. <https://doi.org/10.1016/j.envexpbot.2020.104040>
- Arruda, M. P., Brown, P. J., Lipka, A. E., Krill, A. M., Thurber, C., & Kolb, J. L. (2015). Genomic Selection for Predicting Fusarium Head Blight Resistance in Wheat Breeding Program. *The Plant Genome*, 8(3). <https://doi.org/10.3835/plantgenome2015.01.0003>
- Asselbergh, B., De Vleeschauwer, D., & Höfte, M. (2008). Guard cell switches and fine-tuning-ABA modulates plant pathogen defence. *Molecular Plant-Microbe Interactions*, 21(6), 709–719. <https://doi.org/10.1094/MPMI-21-6-0709>
- Atanasova-Penichon, V., Barreau, C., & Richard-Fortet, F. (2016). Antioxidant secondary metabolites in cereals: Potential involvement in resistance to Fusarium and mycotoxin accumulation. *Frontiers in Microbiology*, 7, 1–16. <https://doi.org/10.3389/fmicb.2016.00562>
- Bai, G. H., Plattner, R., DeJardins, A., Jones, J. D. G., & Jones, S. S. (2001). Resistance to fusarium head blight and deoxynivalenol accumulation in wheat. *Plant Breeding*, 120(1), 1–6. <https://doi.org/10.1046/J.1439-0523.2001.00562.X>
- Bai, G., & Shan, G. (2004). Management and resistance in wheat and barley to fusarium head blight. *Annual Review of Phytopathology*, 42, 137–161. <https://doi.org/10.1146/annurev.phyto.42.040803.140311>
- Bai, G., Su, Z., & Cao, J. (2018). Wheat resistance to Fusarium head blight. *Canadian Journal of Plant Pathology*, 40(3), 336–346. <https://doi.org/10.1080/07060661.2018.1476111>
- Baron, R., & Jones, J. D. G. (2009). Role of plant hormones in plant defence responses. *Plant Molecular Biology*, 70(4), 473–488. <https://doi.org/10.1007/s11103-008-9435-0>
- Beccari, G., Colasante, V., Tini, F., Scudore, M. T., Prodi, A., Sulyok, M., & Covarelli, L. (2018). Causal agents of Fusarium head blight of durum wheat (*Triticum durum* Desf.) in central Italy and their in vitro biosynthesis of secondary metabolites. *Food Microbiology*, 70, 17–27. <https://doi.org/10.1016/J.FM.2017.08.016>
- Berger, S., Sinha, A. K., & Roitsch, T. (2007). Plant physiology meets phytopathology: Plant primary metabolism and plant-pathogen interactions. *Journal of Experimental Botany*, 58(15–16), 4019–4026. <https://doi.org/10.1093/jxb/erm298>

- Bernhoft, A., Torp, M., Clasen, P., Løes, A., & Kristoffersen, A. B. (2012). Influence of agronomic and climatic factors on *Fusarium* infestation and mycotoxin contamination of cereals in Norway. *Food Additives & Contaminants: Part A: Chemistry, Analysis, Control, Exposure & Risk Assessment*, 29(7), 1129–1140. <https://doi.org/10.1080/19440049.2012.672476>
- Berthiller, F., Crews, C., Dall'Asta, C., Saeger, S. De, Haesaert, G., Krska, R., Oswald, I. P., Seefelder, W., Speijers, G., & Stroka, J. (2011). Masked mycotoxins: A review. *Molecular Nutrition and Food Research*, 57(1), 165–180. <https://doi.org/10.1002/mnfr.201100764>
- Berthiller, F., Krska, R., Domig, K. J., Kneifel, W., Lange, M., Schramacher, R., & Adam, G. (2011). Hydrolytic fate of deoxynivalenol-3-glucoside during digestion. *Toxicology Letters*, 206(3), 264–267. <https://doi.org/10.1016/j.toxlet.2011.08.006>
- Beyer, M., & Aumann, J. (2008). Effect of *Fusarium* infection on the amino acid composition of winter wheat grain. *Food Chemistry*, 111(3), 750–754. <https://doi.org/10.1016/j.foodchem.2008.04.047>
- Bilgin, D. D., Zavala, J. A., Zhu, Y., Clement, S. J., Ort, D. R., & Deluc, E. H. (2010). Biotic stress globally down-regulates photosynthesis genes. *Plant, Cell, and Environment*, 33(10), 1597–1613. <https://doi.org/10.1111/J.1365-3040.2010.02377.X>
- Bollina, V., Kusalar, A. C., Choo, T. M., Dion, Y., & Riou, S. (2011). Identification of metabolites related to mechanisms of resistance in barley against *Fusarium graminearum*, based on mass spectrometry. *Plant Molecular Biology*, 77(4–5), 355–370. <https://doi.org/10.1007/s11103-011-9811-3>
- Bottalico, A., & Perrone, G. (2002). Toxigenic *Fusarium* species and mycotoxins associated with head blight in small-grain cereals in Europe. *European Journal of Plant Pathology*, 108(7), 611–621. <https://doi.org/10.1023/A:1020635214971>
- Boutigny, A. L., Richard-Forget, F., & Bureau, C. (2008). Natural mechanisms for cereal resistance to the accumulation of *Fusarium* trichothecenes. *European Journal of Plant Pathology*, 121(4), 411–423. <https://doi.org/10.1007/s10658-007-9266-x>
- Boutigny, A. L., Ward, T. J., Van Coller, G. J., Flett, B., Lamprecht, S. C., O'Donnell, K., & Viljoen, A. (2011). Analysis of the *Fusarium graminearum* species complex from wheat, barley and maize in South Africa provides evidence of species-specific differences in host preference. *Fungal Genetics and Biology*, 48(9), 914–920. <https://doi.org/10.1016/j.fgb.2011.05.005>

- Bradford, M. M. (1976). A rapid and sensitive method for the quantitation of microgram quantities of protein utilizing the principle of protein-dye binding. *Analytical Biochemistry*, 72, 248–254. [https://doi.org/10.1016/0003-2697\(76\)90527-3](https://doi.org/10.1016/0003-2697(76)90527-3)
- Brauer, E. K., Subramaniam, R., & Harris, L. J. (2020). Regulation and dynamics of gene expression during the life cycle of fusarium graminearum. *Phytopathology*, 110(8), 1368–1374. <https://doi.org/10.1094/PHYTO-03-20-0080-IA>
- Broekaert, N., Devreese, M., De Baere, S., De Backer, P., & Crombels, S. (2015). Modified Fusarium mycotoxins unmasked: From occurrence in cereals to animal and human excretion. *Food and Chemical Toxicology*, 80, 17–37. <https://doi.org/10.1016/j.fct.2015.02.015>
- Bryła, M., Ksieniewicz-Woźniak, E., Waśkiewicz, A., Szymczyk, K., & Jędrzejczak, R. (2018). Natural occurrence of nivalenol, deoxynivalenol, and deoxynivalenol-3-glucoside in polish winter wheat. *Toxins*, 10(2). <https://doi.org/10.3390/toxins10020015>
- Buerstmayr, H., Ban, T., & Anderson, J. A. (2009). QTL mapping and marker-assisted selection for Fusarium head blight resistance in wheat: a review. *Plant Breeding*, 128(1), 1–26. <https://doi.org/10.1111/j.1439-0523.2008.01550.x>
- Buerstmayr, M., Steiner, B., & Buerstmayr, H. (2020). Breeding for Fusarium head blight resistance in wheat—Progress and challenges. *Plant Breeding*, 139(3), 429–454. <https://doi.org/10.1111/pbr.12797>
- Buhr, L. M., Cram, D., Tulpan, D., Foroud, N. A., & Loewen, M. C. (2016). Exogenous abscisic acid and gibberellic acid elicit opposite effects on Fusarium graminearum infection in wheat. *Phytopathology*, 106(9), 986–993. <http://doi.org/10.1094/PHYTO-01-16-0033-R>
- Buhr, L. M., Liu, Z., Cram, D., Sharma, T., Foroud, N. A., Pan, Y., & Loewen, M. C. (2021). Wheat transcriptome profiling reveals abscisic and gibberellic acid treatments regulate early-stage phytohormone defense signaling, cell wall fortification, and metabolic switches following Fusarium graminearum-challenge. *BMC Genomics*, 22(1), 1–21. <https://doi.org/10.1186/s12864-021-08069-0>
- Burhenne, K., & Gregersen, P. L. (2000). Up-regulation of the ascorbate-dependent antioxidative system in barley leaves during powdery mildew infection. *Molecular Plant Pathology*, 1(5), 303–314. <https://doi.org/10.1046/j.1364-3703.2000.00034.x>
- Cainong, J. C., Bockus, W. W., Feng, Y., Chen, P., Qi, L., Sehgal, S. K., Danilova, T. V.,

- Koo, D. H., Friebe, B., & Gill, B. S. (2015). Chromosome engineering, mapping, and transferring of resistance to Fusarium head blight disease from *Elymus tsukushiensis* into wheat. *Theoretical and Applied Genetics*, 128(6), 1019–1027. <https://doi.org/10.1007/s00122-015-2485-1>
- Castro-moretti, F. R., Gentzel, I. N., Mackey, D., & Alonso, A. P. (2020). Metabolomics as an emerging tool for the study of plant–pathogen interactions. *Metabolites*, 10(2), 1–23. <https://doi.org/10.3390/metabo10020052>
- Caverzan, A., Casassola, A., & Brammer, S. P. (2016). Antioxidant responses of wheat plants under stress. *Genetics and Molecular Biology*, 39(7), 1–6. <https://doi.org/10.1590/1678-4685-GMB-2015-0109>
- Cela, J., Tweed, J. K. S., Sivakumaran, A., Lee, M. P. F., Muir, L. A. J., & Munné-Bosch, S. (2018). An altered tocopherol composition in chloroplasts reduces plant resistance to *Botrytis cinerea*. *Plant Physiology and Biochemistry*, 127, 200–210. <https://doi.org/10.1016/j.plaphy.2017.03.033>
- Ceusters, N., Valcke, R., Frans, M., Claes, J. E., Van den Ende, W., & Ceusters, J. (2019). Performance Index and PSI: Connectivity Under Drought and Contrasting Light Regimes in the CAM Orchid *Phalaenopsis*. *Frontiers in Plant Science*, 10, 461163. <https://doi.org/10.3389/fpls.2019.01012/BIBTEX>
- Chamarthi, S. K., Kumar, K., Gunnaiah, R., Kuchalappa, A. G., Dhan, Y., & Choo, T. M. (2014). Identification of fusarium head blight resistance related metabolites specific to double-haploid lines in barley. *European Journal of Plant Pathology*, 138(1), 67–78. <https://doi.org/10.1007/S10658-013-0302-8>
- Champeil, A., Fourbault, J. F., Doré, T., & Rossignol, L. (2004). Influence of cropping system on Fusarium head blight and mycotoxin levels in winter wheat. *Crop Protection*, 23(6), 531–537. <https://doi.org/10.1016/j.cropro.2003.10.011>
- Choudhary, A., & Killiny, N. (2014). Photosynthesis Responses to the Infection with Plant Pathogens. *Molecular Plant-Microbe Interactions*, 1–55.
- Cheat, S., Gerez, J. R., Cognié, J., Alassane-Kpembi, I., Bracarense, A. P. F. L., Raymond-Letron, I., Oswald, I. P., & Kolf-Clauw, M. (2015). Nivalenol has a greater impact than deoxynivalenol on pig jejunum mucosa in vitro on explants and in vivo on intestinal loops. *Toxins*, 7(6), 1945–1961. <https://doi.org/10.3390/toxins7061945>
- Chen, K., Li, G. J., Bressan, R. A., Song, C. P., Zhu, J. K., & Zhao, Y. (2020). Absciscic acid dynamics, signaling, and functions in plants. *Journal of Integrative Plant Biology*,

- 62(1), 25–54. <https://doi.org/10.1111/jipb.12899>
- Chen, Y. E., Cui, J. M., Su, Y. Q., Yuan, S., Yuan, M., & Zhang, H. Y. (2015). Influence of stripe rust infection on the photosynthetic characteristics and antioxidant system of susceptible and resistant wheat cultivars at the adult plant stage. *Frontiers in Plant Science*, 6, 1–11. <https://doi.org/10.3389/fpls.2015.00779>
- Choo, T. M. (2010). Breeding Barley for Resistance to Fusarium Head Blight and Mycotoxin Accumulation. In *Plant Breeding Reviews* (Vol. 30). <https://doi.org/10.1002/9780470650325.ch5>
- Colasuonno, P., Lozito, M. L., Marcotuli, I., Nigro, D., Giannaccaro, A., Mangini, G., De Vita, P., Mastrangelo, A. M., Pecchioni, N., Houston, K., Simeone, R., Gadaleta, A., & Blanco, A. (2017). The carotenoid biosynthetic and catabolic genes in wheat and their association with yellow pigments. *BMC Genomics*, 18(1), 1–18. <https://doi.org/10.1186/s12864-016-2395-6>
- Cuadros-Inostroza, Á., Caldana, C., Reyes, H., Kusano, M., Lisec, J., Peña-Correal, H., Willmitzer, L., & Hannah, M. A. (2009). TargetSearch - a Biocductor package for the efficient preprocessing of GC-MS metabolite profile data. *BMC Bioinformatics*, 10(1), 1–12. <https://doi.org/10.1186/1471-2105-10-428/TABLE1>
- Cuperlovic-Culf, M., Wang, L., Forseille, L., Boyle, K., Markiewicz, N., Burton, I., & Fobert, P. R. (2016). Metabolic biomarker panels of response to Fusarium head blight infection in cereal wheat varieties. *PLoS ONE*, 11(1), 1–16. <https://doi.org/10.1371/journal.pone.0153642>
- Curtis, T., & Halford, N. G. (2014). Food security: the challenge of increasing wheat yield and the importance of not compromising food safety. *Annals of Applied Biology*, 164(3), 354–372. <https://doi.org/10.1111/aab.12108>
- Dall'Asta, C., Dall'Era, A., Mantovani, P., Massi, A., & Galaverna, G. (2013). Occurrence of deoxynivalenol and deoxynivalenol-3-glucoside in durum wheat. *World Mycotoxin Journal*, 6(1), 83–91. <https://doi.org/10.3920/WMJ2012.1463>
- Das, K., & Roychoudhury, A. (2014). Reactive oxygen species (ROS) and response of antioxidants as ROS-scavengers during environmental stress in plants. *Frontiers in Environmental Science*, 2, 1–13. <https://doi.org/10.3389/fenvs.2014.00053>
- Dat, J., Vandenabeele, S., Vranová, E., Van Montagu, M., Inzé, D., & Van Breusegem, F. (2000). Dual action of the active oxygen species during plant stress responses. *Cellular and Molecular Life Sciences*, 57(5), 779–795.

- <https://doi.org/10.1007/s000180050041>
- Delannoy, E., Jalloul, A., Assigbetsé, K., Marmey, P., Geiger, J. P., Lherminier, J., Daniel, J. F., Martinez, C., & Nicole, M. (2003). Activity of Class III Peroxidases in the Defense of Cotton to Bacterial Blight. *Molecular Plant-Microbe Interactions*, 16(11), 1030–1038. <https://doi.org/10.1094/MPMI.2003.16.11.1030>
- Dempsey, D. A., Vlot, A. C., Wildermuth, M. C., & Klessig, D. F. (2011). Salicylic Acid Biosynthesis and Metabolism. *The Arabidopsis Book*, 9, e0156. <https://doi.org/10.1199/tab.0156>
- Deponte, M. (2013). Glutathione catalysis and the reaction mechanisms of glutathione-dependent enzymes. *Biochimica et Biophysica Acta - General Subjects*, 1830(5), 3217–3266. <https://doi.org/10.1016/j.bbagen.2012.06.018>
- Ding, L., Xu, H., Yi, H., Yang, L., Kong, Z., Zhang, L., Xue, S., Jia, H., & Ma, Z. (2011). Resistance to hemi-biotrophic *F. graminearum* infection is associated with coordinated and ordered expression of diverse defense signaling pathways. *PLoS ONE*, 6(4). <https://doi.org/10.1371/journal.pone.0019008>
- Dodds, P. N., & Rathjen, J. P. (2010). Plant immunity: towards an integrated view of plant–pathogen interactions. *Nature Reviews Genetics* 2010 11(8), 539–548. <https://doi.org/10.1038/nrg2812>
- Dodge, A. G., & Mckett, J. P. (2005). Metabolism of bismuth sulosalicylate and intracellular accumulation of bismuth by *Fusarium sporotrichi* BI. *Applied and Environmental Microbiology*, 71(2), 876–882. <https://doi.org/10.1128/AEM.71.2.876-882.2005>
- Li, Y., & Zhang, Y. (2004). NFK1, all things considered. *Current Opinion in Plant Biology*, 7(5), 547–552. <https://doi.org/10.1016/j.copbi.2004.07.005>
- Dong, Y., Xia, X., Ahmad, D., Wang, X., Zhang, X., Wu, L., Jiang, P., Zhang, P., Yang, X., Li, G., & He, Y. (2023). Investigating the Resistance Mechanism of Wheat Varieties to *Fusarium* Head Blight Using Comparative Metabolomics. *International Journal of Molecular Sciences*, 24(4). <https://doi.org/10.3390/ijms24043214>
- Duvnjak, J., Lončarić, A., Brkljačić, L., Šamec, D., Šarčević, H., Salopek-Sondi, B., & Španić, V. (2023). Morpho-Physiological and Hormonal Response of Winter Wheat Varieties to Drought Stress at Stem Elongation and Anthesis Stages. *Plants*, 12(3). <https://doi.org/10.3390/plants12030418>

- Dweba, C. C., Figlan, S., Shimelis, H. A., Motaung, T. E., Sydenham, S., Mwadzingeni, L., & Tsilo, T. J. (2017). Fusarium head blight of wheat: Pathogenesis and control strategies. *Crop Protection*, 91, 114–122. <https://doi.org/10.1016/j.cropro.2016.10.002>
- Ekwomadu, T. I., Akinola, S. A., & Mwanza, M. (2021). Fusarium mycotoxins, their metabolites (Free, emerging, and masked), food safety concerns, and health impacts. *International Journal of Environmental Research and Public Health*, 18(22). <https://doi.org/10.3390/ijerph182211741>
- Erayman, M., Turktas, M., Akdogan, G., Gurkok, T., Inan, E., Ishaq, M., E., Ilhan, E., & Unver, T. (2015). Transcriptome analysis of wheat inoculated with *Fusarium graminearum*. *Frontiers in Plant Science*, 6, 17–162. <https://doi.org/10.3389/FPLS.2015.00867/FTYPE>
- Erban, A., Schauer, N., Fernie, A. R., & Kopka, J. (2007). Nonsupervised construction and application of mass spectral and retention time index libraries from time-of-flight gas chromatography-mass spectrometry metabolite profiles. *Methods in Molecular Biology*, 358, 19–38. http://doi.org/10.1007/978-1-59745-244-1_2/CORRER
- Escrivá, L., Font, G., & Moyes, P. (2015). In vivo toxicity studies of Fusarium mycotoxins in the last decade: A review. *Food and Chemical Toxicology*, 78, 185–206. <https://doi.org/10.1016/j.fct.2015.02.005>
- European Commission. (2006a). Commission recommendation of 17 August 2006 on the prevention and reduction of Fusarium toxins in cereals and cereal products. *Official Journal of the European Union*, L 234, 35–40.
- European Commission. (2006b). Commission regulation (EC) No 1881/2006 of 19 December 2006 setting maximum levels for certain contaminants in foodstuffs. *Official Journal of the European Union*, 1881, 1–24.
- European Commission. (2013). Recommendations on the presence of T-2 and HT-2 toxin in cereals and cereal products. *Official Journal of the European Union*, L 91, 12–15.
- European Food Safety Authority (EFSA). (2013). Deoxynivalenol in food and feed: occurrence and exposure. *EFSA Journal* (Vol. 11, Issue 10). <https://doi.org/10.2903/J.EFSA.2013.3379>
- European Parliament and the Council of the European Union. (2002). 96/23/EC COMMISSION DECISION of 12 August 2002 implementing Council Directive 96/23/EC concerning the performance of analytical methods and the interpretation of results. *Official Journal of the European Communities*, L 221/8, 8–36.

<https://doi.org/10.1017/CBO9781107415324.004>

- Fabre, F., Rocher, F., Alouane, T., Langin, T., & Bonhomme, L. (2020). Searching for FHB Resistances in Bread Wheat: Susceptibility at the Crossroad. *Frontiers in Plant Science*, 11, 1–8. <https://doi.org/10.3389/fpls.2020.00731>
- Fang, C., Fernie, A. R., & Luo, J. (2019). Exploring the Diversity of Plant Metabolism. *Trends in Plant Science*, 24(1), 83–98. <https://doi.org/10.1016/j.tplants.2018.09.006>
- Feng, H., Wang, X., Zhang, Q., Fu, Y., Feng, C., Wang, P., Huang, L., & Kang, Z. (2014). Monodehydroascorbate reductase gene, regulated by the wheat PN-2013 miRNA, contributes to adult wheat plant resistance to stripe rust through ROS metabolism. *Biochimica et Biophysica Acta - Gene Regulatory Mechanisms*, 1839(1), 1–12. <https://doi.org/10.1016/j.bbagr.2013.11.001>
- Foyer, C. H., & Halliwell, B. (1976). The presence of glutathione and glutathione reductase in chloroplasts: A proposed role in ascorbic acid metabolism. *Planta*, 133(1), 21–25. <https://doi.org/10.1007/BF00386001>
- Foyer, C. H., & Kunert, K. (2002). The ascorbate-glutathione cycle coming of age. *Journal of Experimental Botany*, 53(9), 2682–2699. <https://doi.org/10.1093/jxb/erae023>
- Foyer, C. H., & Noctor, G. (2005). Oxidant and antioxidant signalling in plants: A re-evaluation of the concept of oxidative stress in a physiological context. *Plant, Cell and Environment*, 28(8), 1056–1071. <https://doi.org/10.1111/j.1365-3040.2005.01327.x>
- Foyer, C. H., & Noctor, G. (2011). Ascorbate and glutathione: The heart of the redox hub. *Plant Physiology*, 155(1), 2–18. <https://doi.org/10.1093/pp.110.167569>
- Hamann, R., N., Schütt, C., Lund, B. W., Stahl, D., Nielsen, J., Olsson, S., & Giese, H. (2011). Two novel classes of enzymes are required for the biosynthesis of beauvericin in *Fusarium graminearum*. *Journal of Biological Chemistry*, 286(12), 10419–10428. <https://doi.org/10.1074/jbc.M110.179853>
- Gadjev, I., Stone, J. M., & Gechev, T. S. (2008). Chapter 3: Programmed Cell Death in Plants. New Insights into Redox Regulation and the Role of Hydrogen Peroxide. In *International Review of Cell and Molecular Biology* (Vol. 270, Issue C). Elsevier Inc. [https://doi.org/10.1016/S1937-6448\(08\)01403-2](https://doi.org/10.1016/S1937-6448(08)01403-2)
- Gallie, D. R. (2013). The role of l-ascorbic acid recycling in responding to environmental stress and in promoting plant growth. *Journal of Experimental Botany*, 64(2), 433–443. <https://doi.org/10.1093/jxb/ers330>

- Gao, Q. M., Zhu, S., Kachroo, P., & Kachroo, A. (2015). Signal regulators of systemic acquired resistance. *Frontiers in Plant Science*, 6, 1–12. <https://doi.org/10.3389/fpls.2015.00228>
- García-Caparrós, P., De Filippis, L., Gul, A., Hasanuzzaman, M., Ozturk, M., Altun, V., & Lao, M. T. (2021). Oxidative Stress and Antioxidant Metabolism under Adverse Environmental Conditions: a Review. *Botanical Review*, 87(4), 421–466. <https://doi.org/10.1007/s12229-020-09231-1>
- Garcia-Cela, E., Kiaitsi, E., Medina, A., Sulyok, M., Krska, R., & Mesterhazy, N. (2018). Interacting environmental stress factors affects targeted metabolomic profiles in stored natural wheat and that inoculated with *F. graminearum*. *Toxins*, 10(2). <https://doi.org/10.3390/toxins10020056>
- Gardiner, S. A., Boddu, J., Berthiller, E., Hametner, J., Stupar, R. M., Adam, G., & Muehlbauer, G. J. (2010). Transcriptome Analysis of the Barley–Deoxynivalenol Interaction: Evidence for a Role of Glutathione in Deoxynivalenol Detoxification. *Molecular plant-microbe interactions*, 23(7), 962–976. <https://doi.org/10.1094/MPMI-23-7-0962>
- Gatz, C. (2013). From Players to Team Players: TGA Transcription Factors Provide a Molecular Link Between Different Stress Pathways. *Molecular plant-microbe interactions*, 26(2), 1–15. <https://doi.org/10.1094/MPMI-26-2-0078-IA>
- Gauthier, J., Attia-Gova-Fenichon, V., Chéreau, S., & Richard-Forget, F. (2015). Metabolomics decipher the Chemical Defense of Cereals against Fusarium graminearum and Deoxynivalenol Accumulation. *International Journal of Molecular Sciences*, 16(10), 24839–24872. <https://doi.org/10.3390/ijms161024839>
- Gebreab, M., & Langseth, W. (2001). The occurrence of culmorin and hydroxyculmorins in cereals. *Mycopathologia*, 152(2), 103–108. <https://doi.org/10.1023/A:101247823193>
- Ghosh, S., Narula, K., Sinha, A., Ghosh, K., Jawa, P., Chakraborty, N., & Chakraborty, S. (2016). Proteometabolomic analysis of transgenic tomato overexpressing oxalate decarboxylase uncovers novel proteins potentially involved in defense mechanism against Sclerotinia. *Journal of Proteomics*, 143, 242–253. <https://doi.org/10.1016/j.jprot.2016.04.047>
- Gietler, M., Fidler, J., Labudda, M., & Nykiel, M. (2020). Review abscisic acid—enemy or savior in the response of cereals to abiotic and biotic stresses? *International Journal of Molecular Sciences*, 21(13), 1–29. <https://doi.org/10.3390/ijms21134607>

- Gilbert, J., & Haber, S. (2013). Overview of some recent research developments in fusarium head blight of wheat. *Canadian Journal of Plant Pathology*, 35(2), 149–174. <https://doi.org/10.1080/07060661.2013.772921>
- Gill, S. S., & Tuteja, N. (2010). Reactive oxygen species and antioxidant mechanism in abiotic stress tolerance in crop plants. *Plant Physiology and Biochemistry*, 48(11), 909–930. <https://doi.org/10.1016/j.plaphy.2010.08.016>
- Gimenez, E., Salinas, M., & Manzano-Agugliaro, F. (2018). Worldwide research on plant defense against biotic stresses as improvement for sustainable culture. *Sustainability*, 10(2), 1–19. <https://doi.org/10.3390/su10020001>
- Golinski, P., Waskiewicz, A., Wisniewska, H., Kiecana, J., Michniczuk, E., Gromadzka, K., Kostecki, M., Bocianowski, J., & Rymanek, E. (2010). Reaction of winter wheat (*Triticum aestivum* L.) cultivars to infection with *Fusarium* spp.: Mycotoxin contamination in grain and chaff. *Food Additives and Contaminants - Part A*, 27(7), 1015–1024. <https://doi.org/10.1080/10440041003702208>
- Gordon, C. S., Rajagopalan, N., Risse-Lew, F. P., Surpin, M., Ball, F. J., Barker, C. J., Buhrow, L. M., Clark, S. M., Page, J. L., Todd, C. D., Aboums, S. R., & Leach, M. C. (2016). Characterization of *triticum aestivum* abscisic acid receptors and a possible role for these in mediating fusarium head blight susceptibility in wheat. *PLoS ONE*, 11(10), 1–23. <https://doi.org/10.1371/journal.pone.0164996>
- Goswami, P. S., & Kastler, H. C. (2004). Heading for disaster: *Fusarium graminearum* on cereal crops. *Molecular Plant Pathology*, 5(6), 515–525. <https://doi.org/10.1111/J.1364-5703.2004.00252.X>
- Guller, G., Kalmave, T., Király, L., & Schröder, P. (2018). Glutathione S-transferase enzymes in plant-pathogen interactions. *Frontiers in Plant Science*, 871, 427485. <https://doi.org/10.3389/FPLS.2018.01836/XML/NLM>
- Granaiah, R., & Kushalappa, A. C. (2014). Metabolomics deciphers the host resistance mechanisms in wheat cultivar Surmai-3, against trichothecene producing and non-producing isolates of *Fusarium graminearum*. *Plant Physiology and Biochemistry*, 83, 40–50. <https://doi.org/10.1016/j.plaphy.2014.07.002>
- Guo, J., Zhang, X., Hou, Y., Cai, J., Shen, X., Zhou, T., Xu, H., Ohm, H. W., Wang, H., Li, A., Han, F., Wang, H., & Kong, L. (2015). High-density mapping of the major FHB resistance gene *Fhb7* derived from *Thinopyrum ponticum* and its pyramiding with *Fhb1* by marker-assisted selection. *Theoretical and Applied Genetics*, 128(11), 2301–2316. <https://doi.org/10.1007/s00122-015-2586-x>

- Gustafson, P., Raskina, O., Ma, X., & Nevo, E. (2009). Wheat Evolution, Domestication, and Improvement. *Wheat Science and Trade*, 3–30. <https://doi.org/10.1002/9780813818832.ch1>
- Haas, M., Schreiber, M., & Mascher, M. (2019). Domestication and crop evolution of wheat and barley: Genes, genomics, and future directions. *Journal of Integrative Plant Biology*, 61(3), 204–225. <https://doi.org/10.1111/jipb.12737>
- Habig, W. H., Pabst, M. J., & Jakoby, W. B. (1974). Glutathione transferase. *Journal of Biological Chemistry*, 249, 7130–7139. [https://doi.org/10.1016/S0021-9258\(19\)42083-8](https://doi.org/10.1016/S0021-9258(19)42083-8)
- Han, X., Huangfu, B., Xu, T., Xu, W., Asakiya, C., He, X., & Huang, K. (2022). Research Progress of Safety of Zearalenone: A Review. *Toxins*, 14(6). <https://doi.org/10.3390/toxins14060386>
- Havrlentová, M., Šliková, S., Gregusová, V., Kováčsová, B., Lančaričová, A., Nemeček, P., Hendrichová, J., & Hozlár, J. (2021). The Influence of Artificial Fusarium Infection on Oat Grain Quality. *Microorganisms* 2021, 9(10), 2108. <https://doi.org/10.3390/MICROORGANISMS9102108>
- Hazard, B., Trafford, K., Lovegrove, A., Griffiths, S., Uauy, C., & Shewry, P. (2020). Strategies to improve wheat for human health. *Nature Food*, 1(1), 475–480. <https://doi.org/10.1038/s43016-020-0134-6>
- Hellin, F., Dederingherde, G., Duvivier, M., Scauftaire, Huybrichts, B., Callebaut, A., Munaut, F., & Lecomte, A. (2016). Relationship between *Fusarium* spp. diversity and deoxynivalenol contents of mature grains in southern Belgium. *Food Additives and Contaminants - Part A Chemistry, Analysis, Control, Exposure and Risk Assessment*, 33(7), 1223–1240. <https://doi.org/10.1080/19440043.2016.1185900>
- Hietaniemi, V., Rämö, S., Yli-Mattila, T., Jestoi, M., Peltonen, S., Kartio, M., Sieviläinen, E., Koivisto, T., & Parikka, P. (2016). Updated survey of *Fusarium* species and toxins in Finnish cereal grains. *Food Additives and Contaminants - Part A Chemistry, Analysis, Control, Exposure and Risk Assessment*, 33(5), 831–848. <https://doi.org/10.1080/19440043.2016.1162112>
- Hildebrandt, T. M., Nunes Nesi, A., Araújo, W. L., & Braun, H. P. (2015). Amino Acid Catabolism in Plants. *Molecular Plant*, 8(11), 1563–1579. <https://doi.org/10.1016/j.molp.2015.09.005>
- Hope, R., Aldred, D., & Magan, N. (2005). Comparison of environmental profiles for growth and deoxynivalenol production by *Fusarium culmorum* and *F.*

- graminearum on wheat grain. *Letters in Applied Microbiology*, 40(4), 295–300.
<https://doi.org/10.1111/j.1472-765X.2005.01674.x>
- Hossain, M. A., Nakano, Y., & Asada, K. (1984). Monodehydroascorbate reductase in spinach chloroplasts and its participation in regeneration of ascorbate for scavenging hydrogen peroxide. *Plant and Cell Physiology*, 25(3), 385–390.
<https://doi.org/10.1093/oxfordjournals.pcp.a076726>
- Hu, Y., Zhong, S., Zhang, M., Liang, Y., Gong, G., Chang, X., Tian, F., Yang, H., Qiu, X., Luo, L., & Luo, P. (2020). Potential Role of Photosynthesis in the Regulation of Reactive Oxygen Species and Defence Response to *Blumeria graminis* f. sp. *tritici* in Wheat. *International Journal of Molecular Sciences*, 21(16), 5767.
<https://doi.org/10.3390/IJMS21165767>
- Infantino, A., Santori, A., & Shah, D. A. (2012). Community structure of the *Fusarium* complex on wheat seed in Italy. *European Journal of Plant Pathology*, 132(4), 499–510.
<https://doi.org/10.1007/s10658-011-9802-1>
- Iqbal, Z., Iqbal, M. S., Hashem, A., Abdel-All, E. F., & Ansari, M. I. (2021). Plant Defense Responses to Biotic Stress and Its Interplay With Fluctuating Daylight Conditions. *Frontiers in Plant Science*, 12, 1–22.
<https://doi.org/10.3389/fpls.2021.631810>
- Jenkins, P., & Parry, D. W. (1994). Splash dispersal of conidia of *Fusarium culmorum* and *Fusarium avenaceum*. *Mycological Research*, 98(4), 506–510.
[https://doi.org/10.1016/S0953-7562\(09\)80468-1](https://doi.org/10.1016/S0953-7562(09)80468-1)
- Jestli, M. (2003). Emerging fusarium-mycotoxins: zearalenone, beauvericin, enniatins, and moniliformin - A review. *Critical Reviews in Food Science and Nutrition*, 48(1), 21–32.
<https://doi.org/10.1080/10408390601000021>
- Ji, F., He, D., Olaniran, A. O., Mokoch, M. P., Xu, J., & Shi, J. (2019). Occurrence, toxicity, production and detection of *Fusarium* mycotoxin: a review. *Food Production, Processing and Nutrition*, 1(1), 1–14. <https://doi.org/10.1186/s43014-019-0007-2>
- Ji, F., Wu, J., Zhao, H., Xu, J., & Shi, J. (2015). Relationship of deoxynivalenol content in grain, chaff, and straw with *Fusarium* head blight severity in wheat varieties with various levels of resistance. *Toxins*, 7(3), 728–742.
<https://doi.org/10.3390/toxins7030728>
- Juan, C., Ritieni, A., & Mañes, J. (2013). Occurrence of *Fusarium* mycotoxins in Italian

- cereal and cereal products from organic farming. *Food Chemistry*, 141(3), 1747–1755. <https://doi.org/10.1016/j.foodchem.2013.04.061>
- Junglee, S., Urban, L., Sallanon, H., Lopez-Lauri, F., Junglee, S., Urban, L., Sallanon, H., & Lopez-Lauri, F. (2014). Optimized Assay for Hydrogen Peroxide Determination in Plant Tissue Using Potassium Iodide. *American Journal of Analytical Chemistry*, 5(11), 730–736. <https://doi.org/10.4236/AJAC.2014.511081>
- Kachroo, A., & Kachroo, P. (2009). Fatty acid-derived signals in plant defense. *Annual Review of Phytopathology*, 47, 153–176. <https://doi.org/10.1146/annurev-phyto-080508-081820>
- Kang, Z., & Buchenauer, H. (2000). Cytology and ultrastructure of the infection of wheat spikes by *Fusarium culmorum*. *Mycological Research*, 104(9), 1083–1093. <https://doi.org/10.1017/S0953756200002495>
- Kangasjärvi, S., Neukermans, J., Li, S., Aarts, E. M., & Noctor, G. (2012). Photosynthesis, photorespiration, and light signalling and defence responses. *Journal of Experimental Botany*, 63(4), 1619–1636. <https://doi.org/10.1093/JXB/ERR402>
- Kassambara, A. (2020). *ggplot2: "ggplot2" Based Publication Ready Plots* (R package version 0.4.0.).
- Kassambara, A., & Märtens, F. (2020). *Factoextra: extract and visualize the results of multivariate statistical analyses* (R package version 1.0.7.).
- Katanić, Z., Marović, S., Katanić, N., Čosić, J., & Španić, V. (2021). Photosynthetic efficiency in flag leaves and ears of winter wheat during fusarium head blight infection. *Agronomy*, 11(12). <https://doi.org/10.3390/agronomy11122415>
- Kessler, A., & Kalske, A. (2018). Plant secondary metabolite diversity and species interactions. *Annual Review of Ecology, Evolution, and Systematics*, 49, 115–138. <https://doi.org/10.1146/annurev-ecolsys-110617-062406>
- Khaledi, N., Taheri, P., & Falahati-Rastegar, M. (2016). Reactive oxygen species and antioxidant system responses in wheat cultivars during interaction with *Fusarium* species. *Australasian Plant Pathology*, 45(6), 653–670. <https://doi.org/10.1007/s13313-016-0455-y>
- Khaledi, N., Taheri, P., & Falahati-Rastegar, M. (2017). Evaluation of resistance and the role of some defense responses in wheat cultivars to *Fusarium* head blight. *Journal of Plant Protection Research*, 57(4), 396–408. <https://doi.org/10.1515/jppr-2017-0054>

- Khalid, A., Hameed, A., & Tahir, M. F. (2023). Wheat quality: A review on chemical composition, nutritional attributes, grain anatomy, types, classification, and function of seed storage proteins in bread making quality. *Frontiers in Nutrition*, 10, 1–14. <https://doi.org/10.3389/fnut.2023.1053196>
- Kifer, D., Sulyok, M., Jakšić, D., Krska, R., & Šegvić Klarić, M. (2021). Fungus and their metabolites in grain from individual households in Croatia. *Food Additives and Contaminants: Part B Surveillance*, 14(2), 98–109. <https://doi.org/10.1080/19393210.2021.1883746>
- Kitahata, N., & Asami, T. (2011). Chemical biology of abscisic acid. *Journal of Plant Research*, 124(4), 549–557. <https://doi.org/10.1007/s10265-011-0415-0>
- Klarić, M. Š., Cvetnić, Z., Pepeljnjak, S., & Kosarić, I. (2009). Co-occurrence of aflatoxins, ochratoxin a, fumonisins, and zearalenone in cereals and feed, determined by competitive direct enzyme-linked immunosorbent assay and thin-layer chromatography. *Arhiv za Higijenu, Radu i Toksikologiju*, 60(4), 427–434. <https://doi.org/10.2478/10004-254650-2009-1975>
- Kovač, M., Šubarić, D., Burić, I., Kovačević, T., & Šarkanj, B. (2018). Yesterday masked, today modified; what do mycotoxins bring next? *Arhiv Za Higijenu, Radu i Toksikologiju*, 69(3), 190–214. <https://doi.org/10.2478/aiht-2018-003108>
- Kumudhni, B. S., Jayashoban, N. S., Patil, S. V., & Govardhan, M. (2018). Primary Plant Metabolism During Plant-Pathogen Interactions and Its Role in Defense. In *Plant Metabolism and Regulation under Environmental Stress*. Elsevier Inc. <https://doi.org/10.1016/B978-0-12-82689-9.00111-7>
- Kuzniak, E., Kopiczki, T., & Chojak-Kozłowska, J. (2018). Ascorbate-Glutathione cycle and biotic stress tolerance in plants. In *Ascorbic Acid in Plant Growth, Development and Stress Tolerance*. https://doi.org/10.1007/978-3-319-74057-7_8
- Kuzniak, E., & Skłodowska, M. (2005). Fungal pathogen-induced changes in the antioxidant systems of leaf peroxisomes from infected tomato plants. *Planta*, 222(1), 192–200. <https://doi.org/10.1007/s00425-005-1514-8>
- Lê, S., Josse, J., & Husson, F. (2008). FactoMineR: An R package for multivariate analysis. *Journal of Statistical Software*, 25(1), 1–18. <https://doi.org/10.18637/JSS.V025.I01>
- Lemmens, M., Steiner, B., Sulyok, M., Nicholson, P., Mesterhazy, A., & Buerstmayr, H. (2016). Masked mycotoxins: Does breeding for enhanced Fusarium head blight

- resistance result in more deoxynivalenol-3-glucoside in new wheat varieties? *World Mycotoxin Journal*, 9(5), 741–754. <https://doi.org/10.3920/WMJ2015.2029>
- Leplat, J., Friberg, H., Abid, M., & Steinberg, C. (2013). Survival of *Fusarium graminearum*, the causal agent of Fusarium head blight. A review. *Agronomy for Sustainable Development*, 33(1), 97–111. <https://doi.org/10.1007/s13593-012-0093-5>
- Leslie, J. F., Moretti, A., Mesterh, Á., Ameye, M., Audenaert, J., Singh, S. K., Richard-forget, F., Chulze, N., Ponte, E. M. Del, Chala, A., Battilana, P., & Lombrico, A. F. (2021). Key Global Actions for Mycotoxin Management in Wheat and Other Small Grains. *Toxins*, 13, 1–48. <https://doi.org/https://doi.org/10.3390/toxins13100725>
- Levy, A. A., & Feldman, M. (2022). Evolution and origin of bread wheat. *Plant Cell*, 34(7), 2549–2567. <https://doi.org/10.1093/plcell/koac130>
- Li, G., & Yen, Y. (2008). Jasmonate and ethylene signaling pathway may mediate Fusarium head blight resistance in wheat. *Crop Science*, 48(5), 1888–1896. <https://doi.org/10.2135/crops2008.02.0027>
- Li, J., Pang, Z., Trivedi, P., Chen, X., Zhang, X., Jia, H., & Wang, N. (2017). “*Candidatus liberibacter asiaticus*” encode a functional salicylic acid (SA) hydroxylase that degrades SA to suppress plant defenses. *Molecular Plant-Microbe Interactions*, 30(8), 620–630. <https://doi.org/10.1094/MPMI-12-16-0257-F>
- Li, N., Han, X., Peng, D., Yuan, D., & Huang, L. J. (2019). Signaling crosstalk between salicylic acid and ethylene/Jasmonate in plant defense: Do we understand what they are whispering? *International Journal of Molecular Sciences*, 20(3). <https://doi.org/10.3390/ijms20030671>
- Lightner, H. K. (1987). Chlorophylls and Carotenoids: Pigments of Photosynthetic Biomembranes. *Methods in Enzymology*, 148, 350–382. [https://doi.org/10.1016/0076-6879\(87\)48036-1](https://doi.org/10.1016/0076-6879(87)48036-1)
- Mezec, J., Schauer, N., Kopka, J., Willmitter, L., & Fernie, A. R. (2006). Gas chromatography mass spectrometry-based metabolite profiling in plants. *Nature Protocols*, 1(1), 387–396. <https://doi.org/10.1038/nprot.2006.59>
- Liu, S., Hall, M. D., Griffey, C. A., & McKendry, A. L. (2009). Meta-Analysis of QTL associated with fusarium head blight resistance in wheat. *Crop Science*, 49(6), 1955–1968. <https://doi.org/10.2135/cropsci2009.03.0115>
- Liu, T., Song, T., Zhang, X., Yuan, H., Su, L., Li, W., Xu, J., Liu, S., Chen, L., Chen, T.,

- Zhang, M., Gu, L., Zhang, B., & Dou, D. (2014). Unconventionally secreted effectors of two filamentous pathogens target plant salicylate biosynthesis. *Nature Communications*, 5. <https://doi.org/10.1038/ncomms5686>
- Llorens, A., Mateo, R., Hinojo, M. J., Valle-Algarra, F. M., & Jiménez, M. (2009). Influence of environmental factors on the biosynthesis of type B trichothecenes by isolates of *Fusarium* spp. from Spanish crops. *International Journal of Food Microbiology*, 94(1), 43–54. <https://doi.org/10.1016/j.ijfoodmicro.2003.12.017>
- Löffler, M., Schön, C. C., & Miedaner, T. (2009). Revealing the genetic architecture of FHB resistance in hexaploid wheat (*Triticum aestivum* L.) by QTL meta-analysis. *Molecular Breeding*, 23(3), 473–488. <https://doi.org/10.1007/s11032-008-9250-y>
- Ma, J., Qiu, D., Pang, Y., Gao, H., Wang, X., & Qian, Y. (2020). Diverse roles of tocopherols in response to abiotic and biotic stresses and strategies for genetic biofortification in plants. *Molecular Breeding*, 40(2), 1–15. <https://doi.org/10.1007/S11037-019-0007-X/FIGURES/2>
- Ma, L. J., Geiser, D. M., Proctor, R. H., Rooney, A. P., O'Donnell, K., Trail, F., Gardner, D. M., Manners, J. M., & Katan, R. (2013). *Fusarium* pathogenomics. *Annual Review of Microbiology*, 67, 409–416. <https://doi.org/10.1146/annurev-micro-092412-155650>
- Ma, L. X., Zhong, B. F., Qiu, D., Chen, W. Q., Liu, T. G., Li, X., Zhang, M., Ren, Z. L., Yang, J. Z., & Lu, P. G. (2015). Gene expression profile and physiological and biochemical characterization of hexaploid wheat inoculated with *Blumeria graminis* sp. nov. *Physiological and Molecular Plant Pathology*, 90, 39–48. <https://doi.org/10.1016/j.pmpp.2015.02.005>
- Ma, L., Xie, Q., Li, G., Jia, H., Zhou, J., Kong, Z., Li, N., & Yuan, Y. (2020). Germplasms, genomics and genomics for better control of devastating wheat *Fusarium* head blight. *Theoretical and Applied Genetics*, 133(5), 1541–1568. <https://doi.org/10.1007/s00122-019-03525-8>
- Makandar, R., Nalam, V. J., Lee, H., Triuk, H. N., Dong, Y., & Shah, J. (2012). Salicylic Acid Regulates Basal Resistance to *Fusarium* Head Blight in Wheat. *Molecular Plant-Microbe Interactions*, 25(3), 431–439. <https://doi.org/10.1094/MPMI-09-11-0232>
- Malz, S., Grell, M. N., Thrane, C., Maier, F. J., Rosager, P., Felk, A., Albertsen, K. S., Salomon, S., Bohn, L., Schäfer, W., & Giese, H. (2005). Identification of a gene cluster responsible for the biosynthesis of aurofusarin in the *Fusarium graminearum* species complex. *Fungal Genetics and Biology*, 42(5), 420–433. <https://doi.org/10.1016/j.FGB.2005.01.010>

- Mao, H., Jiang, C., Tang, C., Nie, X., Du, L., Liu, Y., Cheng, P., Wu, Y., Liu, H., Kang, Z., & Wang, X. (2023). Wheat adaptation to environmental stresses under climate change: Molecular basis and genetic improvement. *Molecular Plant*, 16(10), 1564–1589. <https://doi.org/10.1016/j.molp.2023.09.001>
- Mao, S. L., Wei, Y. M., Cao, W., Lan, X. J., Yu, M., Chen, Z. M., Chen, G. Y., & Zhang, Y. L. (2010). Confirmation of the relationship between plant height and Fusarium head blight resistance in wheat (*Triticum aestivum* L.) by QTL meta-analysis. *Euphytica*, 174(3), 343–356. <https://doi.org/10.1007/s10681-009-0128-7>
- Marrs, K. A. (1996). The functions and regulation of glutathione S-transferases in plants. *Annual Review of Plant Physiology and Plant Molecular Biology*, 47(1), 127–158. <https://doi.org/10.1146/annurev.arplant.47.1.127>
- Martin, C., Schöneberg, T., Vogelgsang, S., Vincent, F., Bertossa, M., Mauch-Mani, B., & Mascher, F. (2017). Factors of wheat grain resistance to Fusarium head blight. *Phytopathologia Mediterranea*, 56(1), 155–166. https://doi.org/10.14601/Phytopathol_Mediterr-20292
- Mauch-Mani, B., & Mauch, F. (2005). The role of abscisic acid in plant-pathogen interactions. *Current Opinion in Plant Biology*, 8(4), 409–414. <https://doi.org/10.1016/j.copbi.2005.05.015>
- Mesterházy, A. (2020). Updating the Breeding Philosophy of Wheat to Fusarium Head Blight (FHB) Resistance Components, QTL Identification, and Phenotyping - A Review. *Plants*, 9(102), 33. <https://doi.org/10.3390/plants91021702>
- Mesterházy, A. (1995). Types and components of resistance to Fusarium head blight of wheat. *Plant Breeding*, 114(5), 377–386. <https://doi.org/10.1111/j.1439-0523.1995.tb00816.x>
- Miedaner, Reinbrecht, Lauber, Schwenberger, & Geiger. (2001). Effects of genotype and genotype-environment interaction on deoxynivalenol accumulation and resistance to Fusarium head blight in rye, triticale, and wheat. *Plant Breeding*, 120(2), 97–105. <https://doi.org/10.1046/j.1439-0523.2001.00580.x>
- Mielniczuk, E., & Skwaryło-Bednarz, B. (2020). Fusarium head blight, mycotoxins and strategies for their reduction. *Agronomy*, 10(4), 509. <https://doi.org/10.3390/agronomy10040509>
- Mishra, S., Roychowdhury, R., Ray, S., Hada, A., Kumar, A., Sarker, U., Aftab, T., & Das, R. (2024). Salicylic acid (SA)-mediated plant immunity against biotic stresses:

- An insight on molecular components and signaling mechanism. *Plant Stress*, 11, 100427. <https://doi.org/10.1016/J.STRESS.2024.100427>
- Mittler, R., Vanderauwera, S., Gollery, M., & Van Breusegem, F. (2004). Reacting oxygen gene network of plants. *Trends in Plant Science*, 9(10), 490–498. <https://doi.org/10.1016/j.tplants.2004.08.009>
- Mittler, R., Vanderauwera, S., Suzuki, N., Miller, G., Tognetti, V. B., Van de poele, K., Gollery, M., Shulaev, V., & Van Breusegem, F. (2011). ROS signaling: The new wave? *Trends in Plant Science*, 16(6), 300–309. <https://doi.org/10.1016/j.tplants.2011.03.007>
- Mohapatra, S., & Mittra, B. (2017). Alleviation of Fusarium oxysporum induced oxidative stress in wheat by *Trichoderma viride*. *Archives of Phytopathology and Plant Protection*, 50(1–2), 84–96. <https://doi.org/10.1080/03235408.2016.1263052>
- Morkunas, I., & Ratajczak, L. (2014). The role of sugar signaling in plant defense responses against fungal pathogens. *Acta Physiologiae Plantarum*, 36(7), 1607–1619. <https://doi.org/10.1007/s11738-014-1559-z>
- Motallebi, P., Niknam, M., Ebrahimiadeh, H., Enferadi, S. T., & Hashemi, M. (2015). The effect of methyl jasmonate on enzyme activities in wheat genotypes infected by the crown and root rot pathogen *Fusarium culmorum*. *Acta Physiologiae Plantarum*, 37(11). <http://doi.org/10.1007/s11738-015-1988-3>
- Mousavi Khatameghini, A., Kamani, M. H., Fakhri, Y., Coppin, C. M., S. C., de Oliveira, C. A. F., & Sant'Ana, A. S. (2019). Changes in marked forms of deoxynivalenol and their co-occurrence with culmorin in cereal-based products: A systematic review and meta-analysis. *Food Chemistry*, 294, 587–596. <https://doi.org/10.1016/J.FOODCHEM.2019.05.034>
- Morshedi, A., Aghaei-Dargiri, S., Banati, B., Kadkhodaei, S., Wei, H., Sangari, S., Yang, L., & Xu, C. (2022). Plant Immunities Regulated by Biological, Genetic, and Epigenetic Factors. *Agronomy*, 12(10), 2790. <https://doi.org/10.3390/agronomy12112790>
- Murshed, R., Lopez-Lauri, F., & Sallanon, H. (2008). Microplate quantification of enzymes of the plant ascorbate-glutathione cycle. *Analytical Biochemistry*, 383(2), 320–322. <https://doi.org/10.1016/j.ab.2008.07.020>
- Muthamilarasan, M., & Prasad, M. (2013). Plant innate immunity: An updated insight into defense mechanism. *Journal of Biosciences*, 38(2), 433–449.

- <https://doi.org/10.1007/s12038-013-9302-2>
- Nakagawa, H., He, X., Matsuo, Y., Singh, P. K., & Kushiro, M. (2017). Analysis of the masked metabolite of deoxynivalenol and fusarium resistance in CIMM2 wheat germplasm. *Toxins*, 9(8). <https://doi.org/10.3390/toxins9080238>
- Nakano, Y., & Asada, K. (1981). Hydrogen peroxide is scavenged by ascorbate-specific peroxidase in spinach chloroplasts. *Plant and Cell Physiology*, 22(5), 867–880. <https://doi.org/10.1093/oxfordjournals.pcp.a076232>
- Návarová, H., Bernsdorff, F., Döring, A. C., & Zeier, P. (2017). Pipecolic acid, an endogenous mediator of defense amplification and priming, is a critical regulator of inducible plant immunity. *Plant Cell*, 29(12), 5123–5141. <https://doi.org/10.1105/tpc.112.103564>
- Nganje, W. E., Kaitibie, S., Wilson, W. W., Leistritz, F. L., & Bangsund, D. A. (2004). Economic impacts of Fusarium head blight in wheat and barley: 1993–2000. In *Agribusiness & Applied Economics Report No. 538*. <https://doi.org/10.22004/ag.econ.13627>
- Owen W. Griffith. (1980). Determination of Glutathione and Glutathione Disulfide Using Glutathione Reductase and 2-Vinylpyridine. *Analytical Biochemistry*, 106, 207–212. [https://doi.org/10.1016/0003-2697\(80\)90139-3](https://doi.org/10.1016/0003-2697(80)90139-3)
- Pan, Y., Liu, Z., Lecomteau, H., Fauteux, F., Wang, Y., McCartney, C., & Ouellet, T. (2018). Resistance gene dynamics associated with resistance and susceptibility against fusarium head blight in four wheat genotypes. *BMC Genomics*, 19(1), 1–26. <https://doi.org/10.1186/S12864-018-5000-3/FIGURES>
- Pancho, P., Miller, A. J., & Giri, J. (2021). Organic acids: Versatile stress-response roles in plants. *Journal of Experimental Botany*, 72(11), 4038–4052. <https://doi.org/10.1093/jxb/erab119>
- Pandey, P., Singh, J., Achary, S. M. M., & Mallireddy Reddy, K. (2015). Redox homeostasis via gene families of ascorbate-glutathione pathway. *Frontiers in Environmental Science*, 3, 133465. <https://doi.org/10.3389/FENVS.2015.00025/XML/NLM>
- Paranidharan, V., Abu-Nada, Y., Hamzehzarghani, H., Kushalappa, A. C., Mamer, O., Dion, Y., Rioux, S., Comeau, A., & Choiniere, L. (2008). Resistance-related metabolites in wheat against Fusarium graminearum and the virulence factor deoxynivalenol (DON). *Botany*, 86(10), 1168–1179. <https://doi.org/10.1139/B08-052>

- Pasquali, M., Beyer, M., Logrieco, A., Audenaert, K., Balmas, V., Basler, R., Boutigny, A. L., Chrpová, J., Czembor, E., Gagkaeva, T., González-Jaén, M. T., Hofgaard, I. S., Köycü, N. D., Hoffmann, L., Levic, J., Marin, P., Miedaner, T., Migheli, Q., Moretti, A., Müller, M. E. H., Munaut, F., Päivi, P., Pallez-Barthel, M., Picot, D., Scauflaire, J., Scherm, B., Stanković, S., Thrane, U., Uhlig, S., Vanheule, A., Tapani, Z. M., Vogelgsang, S. (2016). A European database of *Fusarium graminearum* and other culmorum tricothecene genotypes. *Frontiers in Microbiology*, 7. <https://doi.org/10.3389/fmicb.2016.00406>
- Paul, M. J., & Foyer, C. H. (2001). Sink regulation of photosynthesis. *Journal of Experimental Botany*, 52(360), 1383–1400. <https://doi.org/10.1093/jexbot/52.360.1383>
- Peng, J. H., Sun, D., & Nevo, E. (2011). Domestication evolution, genetics and genomics in wheat. *Molecular Breeding*, 28(3), 281–301. <https://doi.org/10.1007/s11032-011-9608-4>
- Peng, Y., Yang, J., Li, X., & Zhang, L. (2011). Salicylic Acid: Biosynthesis and Signaling. *Annual Review of Plant Biology*, 72, 461–489. <https://doi.org/10.1146/annurev-arplant-081320-092855>
- Perincherry, L., Lalak-Kozłowska, J., & Stępień, Ł. (2019). Fusarium Produced Mycotoxins in Plant-Pathogen Interactions. *Toxins*, 11(11), 661. <https://doi.org/10.3390/toxins11110664>
- Peršić, V., Požinić, I., Vranica, I., Babić, J., & Spanić, V. (2023). Impact of Fusarium Head Blight on Wheat Flour Quality: Examination of Amylase Activity, Technological Quality and Rheological Properties. *Agronomy*, 13(3), 1–23. <https://doi.org/10.3390/agronomy13030662>
- Picot, D., Thomasova-Pénichon, V., Pons, S., Maréchal, G., Barreau, C., Pinson-Gadais, L., Roucolle, J., Daveau, F., Cordon, D., & Richard-Forget, F. (2013). Maize kernel antioxidants and their potential involvement in fusarium ear rot resistance. *Journal of Agricultural and Food Chemistry*, 61(14), 3389–3395. <https://doi.org/10.1021/jf4000033>
- Pieterse, C. M. J., Leon-Reyes, A., Van Der Ent, S., & Van Wees, S. C. M. (2009). Networking by small-molecule hormones in plant immunity. *Nature Chemical Biology*, 5(5), 308–316. <https://doi.org/10.1038/nchembio.164>
- Pirgozliev, S. R., Edwards, S. G., Hare, M. C., & Jenkinson, P. (2003). Strategies for the control of Fusarium head blight in cereals. *European Journal of Plant Pathology*, 109(7), 731–742. <https://doi.org/10.1023/A:1026034509247>

- Pistol, G. C., Gras, M. A., Marin, D. E., Israel-Roming, F., Stancu, M., & Taranu, I. (2014). Natural feed contaminant zearalenone decreases the expressions of important pro- and anti-inflammatory mediators and mitogen-activated protein kinase (NF- κ B) signalling molecules in pigs. *British Journal of Nutrition*, 111(3), 452–464. <https://doi.org/10.1017/S0007114513002675>
- Pleadin, J., Vahčić, N., Perši, N., Ševelj, D., Markov, K., & Frece, J. (2013). Fusarium mycotoxins' occurrence in cereals harvested from Croatian fields. *Food Control*, 32(1), 49–54. <https://doi.org/10.1016/j.foodcont.2012.12.002>
- Pokotylo, I., Kravets, V., & Ruelland, E. (2019). Salicylic acid binding proteins (SABPs): The hidden forefront of salicylic acid signalling. *International Journal of Molecular Sciences*, 20(18), 1–20. <https://doi.org/10.3390/ijms201818425>
- Popovski, S., & Celar, F. A. (2013). The impact of environmental factors on the infection of cereals with *Fusarium* species and mycotoxin production - A review. *Acta Agriculturae Slovenica*, 101(1), 105–117. <https://doi.org/10.2478/acas-2013-0002>
- Powell, J. J., Carere, J., Fitzgerald, T. L., Still, J., Covarelli, L., Xu, C., Guider, F., Colgrave, M. L., Gardiner, D. M., Monneret, J. M., Henry, R. J., & Kazan, M. (2017). The *Fusarium crown rot* pathogen *Fusarium pseudograminearum* triggers a suite of transcriptional and metabolic changes in bread wheat (*Triticum aestivum* L.). *Annals of Botany*, 119(5), 852–867. <https://doi.org/10.1093/aob/mbx027>
- Powell, J. J., Carere, J., Salok, G., Fitzgerald, T. L., Still, J., Colgrave, M. L., Gardiner, D. M., Monneret, J. M., Vogel, J. P., Henry, R. J., & Kazan, M. (2017). Transcriptome analysis of rhizopodium during fungal pathogen infection reveals both shared and distinct defense responses with wheat. *Scientific Reports*, 7(1), 1–14. <https://doi.org/10.1038/s41598-017-17454-4>
- Pritsch, C., Muehlbauer, G. J., Bushnell, W. R., Somers, D. A., & Vance, C. P. (2000). Fungal development and induction of defense response genes during early infection of wheat spikes by *Fusarium graminearum*. *Molecular Plant-Microbe Interactions*, 13(2), 159–169. <https://doi.org/10.1094/MPMI.2000.13.2.159;CTYPE:STRING:JOURNAL>
- Pritsch, C., Vance, C. P., Bushnell, W. R., Somers, D. A., Hohn, T. M., & Muehlbauer, G. J. (2001). Systemic expression of defense response genes in wheat spikes as a response to *Fusarium graminearum* infection. *Physiological and Molecular Plant Pathology*, 58(1), 1–12. <https://doi.org/10.1006/pmpp.2000.0308>
- Qi, G., Chen, J., Chang, M., Chen, H., Hall, K., Korin, J., Liu, F., Wang, D., & Fu, Z. Q.

- (2018). Pandemonium Breaks Out: Disruption of Salicylic Acid-Mediated Defense by Plant Pathogens. *Molecular Plant*, 11(12), 1427–1439. <https://doi.org/10.1016/j.molp.2018.10.002>
- Qi, L. L., Pumphrey, M. O., Friebe, B., Chen, P. D., & Gill, B. S. (2008). Molecular cytogenetic characterization of alien introgressions with gene Tbh3 for resistance to Fusarium head blight disease of wheat. *Theoretical and Applied Genetics*, 117(7), 1155–1166. <https://doi.org/10.1007/s00122-008-0853-9>
- Qi, P. F., Balcerzak, M., Rocheleau, H., Leung, W., Wei, Y. M., Zheng, Y. L., & Ouellet, T. (2016). Jasmonic acid and abscisic acid play important roles in host-pathogen interaction between Fusarium graminearum and wheat during the early stages of fusarium head blight. *Physiological and Molecular Plant Pathology*, 93(2016), 39–48. <https://doi.org/10.1016/j.pmpp.2015.12.004>
- Qi, P. F., Jiang, Y. F., Guo, Z. R., Chen, Q., Ouellet, T., Zong, L. J., Wei, Z. Z., Wang, Y., Zhang, Y. Z., Xu, B. J., Kong, X., Deng, M., Wang, J. R., Chen, G. Y., Jiang, T., Lan, X. J., Li, W., Wei, Y. M., & Zheng, Y. L. (2019). Transcriptional reference map of hormone responses in wheat spikes. *BMC Genomics*, 20(1), 1–13. <https://doi.org/10.1186/s12864-019-0726-x>
- Qi, P. F., Johnston, A., Balcerzak, M., Rocheleau, H., Harris, L. J., Leung, X. Y., Wei, Y. M., Zheng, Y. L., & Ouellet, T. (2012). Effect of salicylic acid on Fusarium graminearum, the major causal agent of fusarium head blight in wheat. *Fungal Biology*, 116(3), 413–427. <https://doi.org/10.1016/j.funbio.2012.01.001>
- Qi, P. F., Zhang, Y. Z., Liu, C. H., Chen, Q., Guo, Z. R., Wang, Y., Xu, B. J., Jiang, Y. F., Zheng, T., Gong, X., Luo, C. H., Wu, X., Kong, X., Deng, M., Ma, J., Lan, X. J., Jiang, T., Wei, Y. M., Wang, J. R., & Zheng, Y. L. (2019). Functional analysis of FgNahG clarifies the contribution of salicylic acid to wheat (*Triticum aestivum*) resistance against fusarium head blight. *Toxins*, 11(2). <https://doi.org/10.3390/toxins11020059>
- Quarta, A., Mita, G., Haidukowski, M., Cantino, A., Mulè, G., & Visconti, A. (2005). Assessment of trichothecene chemotypes of Fusarium culmorum occurring in Europe. *Food Additives and Contaminants*, 22(4), 309–315. <https://doi.org/10.1080/02652030500058361>
- R Core Team. (2021). *R: A language and environment for statistical computing*. R Foundation for Statistical Computing.
- Racker, E. (1955). Glutathione reductase from bakers' yeast and beef liver. *The Journal of Biological Chemistry*, 217(2), 855–865. [https://doi.org/10.1016/s0021-9258\(18\)65950-2](https://doi.org/10.1016/s0021-9258(18)65950-2)

- Rai, A., Das, M., & Tripathi, A. (2020). Occurrence and toxicity of a fusarium mycotoxin, zearalenone. *Critical Reviews in Food Science and Nutrition*, 60(16), 2710–2729. <https://doi.org/10.1080/10408398.2019.1655388>
- Ramaroson, M. L., Koutouan, C., Helesbeux, J. J., Le Clerc, V., Mamam, L., Geocheleau, E., & Briard, M. (2022). Role of Phenylpropanoids and Flavonoids in Plant Resistance to Pests and Diseases. *Molecules*, 27(23), 8371. <https://doi.org/10.3390/MOLECULES27238371>
- Ren, J., Wang, Z., Du, Z., Che, M., Zhang, Y., Quan, W., Wang, Y., Wang, X., & Zhang, Z. (2019). Detection and validation of a novel major QTL for resistance to Fusarium head blight from *Triticum aestivum* in the terminal region of chromosome 7DL. *Theoretical and Applied Genetics*, 132(1), 241–255. <https://doi.org/10.1007/s00122-018-3213-4>
- Reynolds, M. P., & Braun, H.-J. (2022). Wheat Improvement. In *Wheat Improvement: Food Security in a Changing Climate* (Springer). https://doi.org/10.1007/978-3-030-62673-3_9
- Ribichich, K. F., Lopez, S. E., & Vege, A. C. (2000). Histopathological sporelet changes produced by *Fusarium graminearum* in susceptible and resistant wheat cultivars. *Plant Disease*, 84(7), 794–802. <https://doi.org/10.1094/PDIS.2000.84.7.794>
- Riewe, D., Jeon, J. J., Lisec, J., Heuermann, M. C., Schmeichel, J., Seyfarth, M., Meyer, R. C., Willmitzer, L., & Altmann, T. (2016). A naturally occurring promoter polymorphism of the Arabidopsis FUM2 gene causes expression variation, and is associated with metabolic and growth traits. *The Plant Journal*, 88(5), 826–838. <https://doi.org/10.1111/TPJ.13303>
- Riewe, D., Kohn, M., Lisec, J., Pfeiffer, M., Heuermann, R., Schmeichel, J., Willmitzer, L., & Altmann, T. (2012). A tyrosine aminotransferase involved in tocopherol synthesis in Arabidopsis. *The Plant Journal*, 71(5), 850–859. <https://doi.org/10.1111/J.1365-3113.2012.05035.X>
- Rocheleau, H., Al-harthi, R., & Guellet, T. (2019). Degradation of salicylic acid by *Fusarium graminearum*. *Fungal Biology*, 123(1), 77–86. <https://doi.org/10.1016/j.funbio.2018.11.002>
- Rommens, C. M., & Kishore, G. M. (2000). Exploiting the full potential of disease-resistance genes for agricultural use. *Current Opinion in Biotechnology*, 11(2), 120–125. [https://doi.org/10.1016/S0958-1669\(00\)00083-5](https://doi.org/10.1016/S0958-1669(00)00083-5)
- Ropejko, K., & Twarużek, M. (2021). Zearalenone and Its Metabolites—General

- Overview, Occurrence, and Toxicity. *Toxins*, 13(1).
<https://doi.org/10.3390/TOXINS13010035>
- Rybecky, A. I., Chulze, S. N., & Chiotta, M. L. (2018). Effect of water activity and temperature on growth and trichothecene production by *Fusarium merisioense*. *International Journal of Food Microbiology*, 285, 69–73.
<https://doi.org/10.1016/j.ijfoodmicro.2018.07.028>
- Sahu, P. K., Jayalakshmi, K., Tilgam, J., Gupta, A., Nagaraju, Y., Kumar, A., Hamid, S., Singh, H. V., Minkina, T., Rajput, V. D., & Rajawat, M. S. (2022). ROS generated from biotic stress: Effects on plants and alleviation by endophytic microbes. *Frontiers in Plant Science*, 13, 1042936.
<https://doi.org/10.3389/FPLS.2022.1042936> ML/NL
- Salgado, J. D., Madden, L. V., & Paul, P. A. (2014). Efficacy and economics of integrating in-field and harvesting strategies to manage fusarium head blight of wheat. *Plant Disease*, 98(10), 1407–1421. <https://doi.org/10.1094/PDIS-01-14-0093-RE>
- Salgado, J. D., Wallhead, M., Madden, L. V., & Paul, P. A. (2011). Grain harvesting strategies to minimize grain quality losses due to fusarium head blight of wheat. *Plant Disease*, 95(11), 1448–1455. <https://doi.org/10.1094/PDIS-07-11-0309>
- Šarkanj, B., Warth, D., Schlig, A., Abia, W. A., Sulyok, M., Knap, T., Jurska, R., & Banjari, I. (2013). UHPLC analysis reveals high deoxynivalenol exposure in pregnant women from Croatia. *Food and Chemical Toxicology*, 62, 231–237.
<https://doi.org/10.1016/j.fct.2013.08.043>
- Sarver, B. A., Wood, T. J., Gale, L. R., Brice, K., Cobby-Kinder, H., Aoki, T., Nicholson, Carter, J., & McDonnell, K. (2011). Novel Fusarium head blight pathogens from Nepal and Louisiana revealed by multilocus genealogical concordance. *Fungal Genetics and Biology*, 48(12), 1106–1107. <https://doi.org/10.1016/j.fgb.2011.09.002>
- Schoeder, H. W., & Christensen, J. J. (1963). Factors affecting resistance of wheat to scab caused by *Gibberella zeae*. *Phytopathology*, 53, 831–838.
<https://www.cabdigitalibrary.org/doi/full/10.5555/19641602012>
- Seybold, H., Trempel, F., Ranf, S., Scheel, D., Romeis, T., & Lee, J. (2014). Ca²⁺ signalling in plant immune response: From pattern recognition receptors to Ca²⁺ decoding mechanisms. *New Phytologist*, 204(4), 782–790. <https://doi.org/10.1111/nph.13031>
- Shewry, P. R., & Hey, S. J. (2015). The contribution of wheat to human diet and health. *Food and Energy Security*, 4(3), 178–202. <https://doi.org/10.1002/FES3.64>

- Shi, S., Zhao, J., Pu, L., Sun, D., Han, D., Li, C., Feng, X., Fan, D., & Hu, X. (2020). Identification of new sources of resistance to crown rot and fusarium head blight in wheat. *Plant Disease*, 104(7), 1979–1985. <https://doi.org/10.1094/PDIS-10.19-2254-RE>
- Shigeoka, S., Ishikawa, T., Tamoi, M., Miyagawa, Y., Takeda, T., Yabuta, Y., & Yoshimura, K. (2002). Regulation and function of ascorbate peroxidase isoenzymes. *Journal of Experimental Botany*, 53(372), 1305–1319. <https://doi.org/10.1093/JEXBOT/53.372.1305>
- Siegel, B. Z., & Galston, A. W. (1967). The isoperoxidases of *Pisum sativum*. *Plant Physiology*, 42(2), 221–226. <https://doi.org/10.1104/pp.42.2.221>
- Siranidou, E., Kang, Z., & Buchenauer, H. (2002). Studies on Symptom Development, Phenolic Compounds and Morphological Defence Responses in Wheat Cultivars Differing in Resistance to Fusarium Head Blight. *Journal of Phytopathology*, 150(4–5), 200–208. <https://doi.org/10.1046/j.1439-0434.2002.00738.x>
- Slowikowski, K. (2021). *ggrepel: Automatically Position Non-Overlapping Text Labels with “ggplot2”* (R package version 0.9.1.).
- Snijders, C. H. A., & Peckowski, J. (1990). Effects of head blight caused by *Fusarium culmorum* on toxin content and weight of wheat kernels. *Phytopathology*, 80(6), 566–570.
- Sorahinobar, M., Niknam, V., Ebrahimzadeh, H., Soltanloo, H., Bahmanesh, M., & Enferadi, S. T. (2016). Central Role of Salicylic Acid in Resistance of Wheat Against *Fusarium graminearum*. *Journal of Plant Growth Regulation*, 35(2), 477–491. <https://doi.org/10.1007/s00344-015-9355-1>
- Sorahinobar, M., Niknam, V., Ebrahimzadeh, H., Soltanloo, H., Moradi, B., & Bahram, M. (2016). Lack of association between *Fusarium graminearum* resistance in spike and crude extract tolerance in seedling of wheat. *European Journal of Plant Pathology*, 144(3), 525–538. <https://doi.org/10.1007/s10658-015-0792-7>
- Sorahinobar, M., Safaie, N., & Mojtahedi, B. (2022). Salicylic Acid Seed Priming Enhanced Resistance in Wheat Against *Fusarium graminearum* Seedling Blight. *Journal of Plant Biology*, 65(5), 423–434. <https://doi.org/10.1007/s12374-021-09329-y>
- Španić, V. (2016). *Pšenica* (T. Ledenčan (ed.); 1st edition). Agricultural Institute Osijek.
- Španić, V. (2023). *Sitno, ali moćno zrno pšenice* (M. Josipovic (ed.); 1st edition). Agricultural Institute Osijek.

- Spanic, V., Katanic, Z., Sulyok, M., Krska, R., Puskas, K., Vida, G., Drezner, G., & Šarkanj, B. (2020). Multiple fungal metabolites including mycotoxins in naturally infected and fusarium-inoculated wheat samples. *Microorganisms*, 8(4). <https://doi.org/10.3390/microorganisms8040578>
- Spanic, V., Lemmens, M., & Drezner, G. (2010). Morphological and molecular identification of *Fusarium* species associated with head blight of wheat in East Croatia. *European Journal of Plant Pathology*, 128(4), 511–519. <https://doi.org/10.1007/s10658-010-9682-1>
- Spanic, V., Maricevic, M., Ikic, I., Sulyok, M., & Sarcevic, H. (2023). Three-Year Survey of *Fusarium* Multi-Metabolites/Mycotoxins Contamination in Wheat Samples in Potentially Epidemic FHB Conditions. *Agronomy*, 13(2). <https://doi.org/10.3390/agronomy13030805>
- Spanic, V., & Sarcevic, H. (2023). Evaluation of Effective System for Tracing FHB Resistance in Wheat: An Editorial Commentary. *Agronomy*, 13(8), 13–16. <https://doi.org/10.3390/agronomy13082016>
- Spanic, V., Viljevac Vuletic, M., Irbic, M., & Marcek, T. (2017). Early response of wheat antioxidant system with special reference to *Fusarium* head blight stress. *Plant Physiology and Biochemistry*, 115, 34–43. <https://doi.org/10.1016/j.plaphy.2017.03.010>
- Spanic, V., Zdunic, Z., Drezner, G., & Sarkanj, B. (2019). The presence of fusarium diseases and correlation with mycotoxins in the wheat grain and malt. *Toxins*, 11(4). <https://doi.org/10.3390/toxins11040198>
- Spanic, V., Zdunic, Z., Drezner, G., & Viljevac Vuletic, M. (2020). Differences in physiological traits at the initial stage of *Fusarium* head blight infection in wheat. *Biotropica Plantarum*, 64, 174–181. <https://doi.org/10.32615/bp.2020.014>
- Stanciu, O., Banc, R., Cozma, A., Filip, L., Miere, D., Mañes, J., & Loghin, F. (2015a). Occurrence of fusarium mycotoxins in wheat from Europe - a review. *Acta Universitatis Cibiniensis - Series E: Food Technology*, 19(1), 35–60. <https://doi.org/10.1515/aucft-2015-0005>
- Stanciu, O., Banc, R., Cozma, A., Filip, L., Miere, D., Mañes, J., & Loghin, F. (2015b). Occurrence of *Fusarium* Mycotoxins in Wheat from Europe – A Review. *Acta Universitatis Cibiniensis. Series E: Food Technology*, 19(1), 35–60. <https://doi.org/10.1515/aucft-2015-0005>
- Stanciu, O., Juan, C., Miere, D., Loghin, F., & Mañes, J. (2017). Occurrence and co-

- occurrence of *Fusarium* mycotoxins in wheat grains and wheat flour from Romania. *Food Control*, 73, 147–155. <https://doi.org/10.1016/j.foodcont.2016.07.042>
- Steiner, B., Buerstmayr, M., Michel, S., Schweiger, W., Lemmens, M., & Buerstmayr, H. (2017). Breeding strategies and advances in line selection for *Fusarium* head blight resistance in wheat. *Tropical Plant Pathology*, 42(3), 165–174. <https://doi.org/10.1007/s40858-017-0127-7>
- Stenglein, S. A., Dinolfo, M. I., Barros, G., Bongiorno, F., Chulze, S. N., & Moreno, M. V. (2014). *Fusarium poae* pathogenicity and mycotoxin accumulation on selected wheat and barley genotypes at a single location in Argentina. *Plant Disease*, 98(12), 1733–1738. <https://doi.org/10.1094/PDIS-02-14-0182-RE>
- Stępień, Ł., Lalak-Kańczugowska, J., Witaszak, P., & Urbaniak, M. (2020). *Fusarium* Secondary Metabolism Biosynthetic Pathways: So Close but So Far Away. In *Reference Series in Phytochemistry*. https://doi.org/10.1007/978-3-319-96397-6_28
- Strasser, R. J., Tsimilli-Michael, M., & Srivastava, A. (2004). *Analysis of the Chlorophyll a Fluorescence Transient*. 321–362. https://doi.org/10.1007/978-1-4020-3212-9_12
- Streit, E., Schatzmayr, G., Fassis, A., Tzika, E., Marin, D., Tarantola, I., Gabuc, C., Nicolau, A., Aprodu, I., Puel, C., & Oswald, I. P. (2012). Current situation of mycotoxin contamination and co-occurrence in animal feed for Europe. *Toxins*, 4(10), 788–809. <https://doi.org/10.3390/toxins4100788>
- Su, Z., Bernadillo, R., Tian, B., Chen, H., Wang, S., Li, H., Li, S., Liu, D., Zhang, D., Li, T., Black, P., St. Amand, P., Yu, J., Zhang, L., & Bai, G. (2019). A deletion mutation in TaHRC confers Fhb1 resistance to *Fusarium* head blight in wheat. *Nature Genetics*, 51(7), 1099–1105. <https://doi.org/10.1038/s41588-019-0425-8>
- Sun, R., & McKeown, P. C. (2015). Moving toward a comprehensive map of central plant metabolism. *Annual Review of Plant Biology*, 66, 187–210. <https://doi.org/10.1146/annurev-arplant-043014-114720>
- Sulyok, M., Stadler, D., Steiner, H., & Krska, R. (2020). Validation of an LC-MS/MS-based dilute-and-shoot approach for the quantification of > 500 mycotoxins and other secondary metabolites in food crops: challenges and solutions. *Analytical and Bioanalytical Chemistry*, 412(11), 2607–2620. <https://doi.org/10.1007/s00216-020-02489-9>
- Syman, K., Turpanova, R., Nazarova, G. A., Berdenkulova, A. Z., Tulindinova, G. K., Korogod, N. P., Izbassarova, Z. Z., Aliyeva, Z. G., & Utegaliyeva, R. (2024). Role of

- oxidative stress enzymes in abiotic and biotic stress. *Caspian Journal of Environmental Sciences*, 22(2), 521–528. <https://doi.org/10.22124/CJES.2024.7744>
- Tadesse, W., Amri, A., Ogbonnaya, F. C., Sanchez-Garcia, M., Sohail, Q., & Baum, M. (2015). Wheat. In *Genetic and Genomic Resources for Grain Cereals Improvement*. <https://doi.org/10.1016/B978-0-12-802000-5.00002-2>
- Taheri, P. (2018). Cereal diseases caused by *Fusarium graminearum*: from biology of the pathogen to oxidative burst-related host defense response. *European Journal of Plant Pathology*, 152(1), 1–20. <https://doi.org/10.1007/s10658-017-1111-2>
- Takahashi, K., Kasai, K., & Ochi, K. (2004). Identification of the bacterial alarmone guanosine 5'-diphosphate 3'-diphosphate (ppGpp) in plants. *Proceedings of the National Academy of Sciences of the United States of America*, 101(12), 4320–4324. <https://doi.org/10.1073/pnas.0308555101>
- Thapa, G., Gunupuru, L. R., Hehir, J. G., Fahla, A., Mullins, E., & Doohan, F. (2018). A pathogen-responsive leucine rich receptor like kinase contributes to *Fusarium* resistance in cereals. *Frontiers in Plant Science*, 9, 326624. <https://doi.org/10.3389/fpls.2018.00367/XML/NLM>
- Trail, F. (2009). For blighted waves of grain: *Fusarium graminearum* in the postgenomic era. *Plant Physiology*, 149(1), 103–110. <https://doi.org/10.1104/pp.108.129684>
- Uarrota, V., Steier, P. L. V., Leolato, L. S., Gindoff, D. M., & Merling, D. (2018). Polyketide Carotenoids and Their Role in Plant Stress Responses: From Biosynthesis to Plant Signaling Mechanisms During Stress. In D. Gupta, J. Palma, & F. Corpas (Eds.), *Antioxidants and Antioxidant Enzymes in Higher Plants* (pp. 207–232). Springer International Publishing. https://doi.org/10.1007/978-3-319-75088-0_10
- Uhlir, S., Eriksen, G. S., Hofgaard, A. E., Krska, R., Beltrán, E., & Sulyok, M. (2013). Faces of a Changing Climate: Semi-Quantitative Multi-Mycotoxin Analysis of Grain Grown in Exceptional Climatic Conditions in Norway. *Toxins* 2013, Vol. 5, Pages 1682-1697, 5(10), 1682–1697. <https://doi.org/10.3390/TOXINS5101682>
- Ullah, C., Chen, Y. H., Ortega, M. A., & Tsai, C. J. (2023). The diversity of salicylic acid biosynthesis and defense signaling in plants: Knowledge gaps and future opportunities. *Current Opinion in Plant Biology*, 72, 102349. <https://doi.org/10.1016/j.pbi.2023.102349>
- van der Fels-Klerx, H. J., de Rijk, T. C., Booij, C. J. H., Goedhart, P. W., Boers, E. A. M.,

- Zhao, C., Waalwijk, C., Mol, H. G. J., & van der Lee, T. A. J. (2012). Occurrence of Fusarium Head Blight species and Fusarium mycotoxins in winter wheat in the Netherlands in 2009. *Food Additives and Contaminants - Part A*, 29(11), 1716–1726. <https://doi.org/10.1080/19440049.2012.685891>
- Vanacker, H., Carver, T. L. W., & Foyer, C. H. (2000). Early H₂O₂ accumulation in mesophyll cells leads to induction of glutathione during the hypersensitive response in the barley-powdery mildew interaction. *Plant Physiology*, 123(4), 1289–1300. <https://doi.org/10.1104/pp.123.4.1289>
- Vaughan, M., Backhouse, D., & Del Ponte, E. M. (2016). Climate change impacts on the ecology of Fusarium graminearum species complex and susceptibility of wheat to Fusarium head blight: A review. *World Mycotoxin Journal*, 9(5), 685–700. <https://doi.org/10.3920/WMJ2016.2053>
- Venske, E., dos Santos, R. S., Farias, D. da R., Rother, V., da Maia, L. C., Pegoraro, C., & Costa de Oliveira, A. (2019). Meta-analysis of the QTLome of fusarium head blight resistance in bread wheat: Refining the current puzzle. *Frontiers in Plant Science*, 10, 1–19. <https://doi.org/10.3389/fpls.2019.00727>
- Verhage, A., van Wees, C. M., & Pieterse, C. M. J. (2010). Plant immunity: It's the hormones talking, but what do they say? *Plant Physiology*, 152(3), 536–540. <https://doi.org/10.1104/pp.110.161570>
- Verma, S., & Dubey, R. S. (2003). Lead toxicity induces lipid peroxidation and alters the activities of antioxidant enzymes in growing rice plants. *Plant Science*, 164(4), 645–655. [https://doi.org/10.1016/S0168-9052\(03\)00220-0](https://doi.org/10.1016/S0168-9052(03)00220-0)
- Vishwakarma, K., Upadhyay, N., Kumar, N., Yadav, P., Singh, J., Mishra, R. K., Kumar, V., Sharma, R., Upadhyay, R. G., Pandey, M., & Sharma, S. (2017). Absciscic acid signaling and abiotic stress tolerance in plants: A review on current knowledge and future prospects. *Frontiers in Plant Science*, 8, 1–12. <https://doi.org/10.3389/fpls.2017.00001>
- Walter, S., Nicholson, P., & Doohan, M. (2010). Action and reaction of host and pathogen during Fusarium head blight disease. *New Phytologist*, 185(1), 54–66. <https://doi.org/10.1111/j.1469-8137.2009.03041.x>
- Wang, L., Liu, H., Yin, Z., Li, Y., Lu, C., Wang, Q., & Ding, X. (2022). A Novel Guanine Elicitor Stimulates Immunity in Arabidopsis and Rice by Ethylene and Jasmonic Acid Signaling Pathways. *Frontiers in Plant Science*, 13, 841228. <https://doi.org/10.3389/FPLS.2022.841228/BIBTEX>

- Wang Ma, F., & Cheng, L. (2004). Exposure of the shaded side of apple fruit to full sun leads to up-regulation of both the xanthophyll cycle and the ascorbate-glutathione cycle. *HortScience*, 39(4), 887A – 887. <https://doi.org/10.21273/HORTSCI.39.4.887A>
- Wang, Y. Z., & Miller, J. D. (1988). Effects of *Fusarium graminearum* Metabolites on Wheat Tissue in Relation to *Fusarium* Head Blight Resistance. *Journal of Phytopathology*, 122(2), 118–125. <https://doi.org/10.1111/J.1439-0414.1988.tb00998.X>
- Weber, J., Vaclavikova, M., Wiesenberger, G., Haider, M., Hametner, C., Fröhlich, J., Berthiller, F., Adam, G., Mikula, H., & Fruhmant, C. (2018). Chemical synthesis of culmorin metabolites and their biologic role in culmorin and acetyl-culmorin treated wheat cells. *Organic and Biomolecular Chemistry*, 16(12), 2043–2048. <https://doi.org/10.1039/c7ob02460f>
- Wickham, H., & Sievert, C. (2009). *ggplot2: elegant graphics for data analysis*.
- Wipfler, R., McCormick, S. P., Proctor, K. J., Teresi, J. M., Hao, G., Ward, T. J., Alexander, N. J., & Vaughan, M. M. (2020). Synergistic Phytotoxic Effects of Culmorin and Trichothecene Mycotoxins. *Toxins*, 11, 555. <https://doi.org/10.3390/toxins1110555>
- Withers, J., & Dong, X. (2016). Posttranslational Modifications of PRR1: A Single Protein Playing Multiple Roles in Plant Immunity and Physiology. *PLoS Pathogens*, 12(8), 1–9. <https://doi.org/10.1371/journal.ppat.1005707>
- Woelflingseder, L., Adam, G., & Marko, D. (2020). Suppression of Trichothecene-Mediated Immune Response by the *Fusarium* Secondary Metabolite Butenolide in Human Colon Epithelial Cells. *Frontiers in Nutrition*, 7, 1–13. <https://doi.org/10.3389/fnut.2020.00127>
- Woelflingseder, L., Warth, B., Viehheilig, I., Schwartz-Zimmermann, H., Hametner, C., Nagl, V., Novak, B., Šarkanj, B., Berthiller, F., Adam, G., & Marko, D. (2019). The *Fusarium* metabolite culmorin suppresses the in vitro glucuronidation of deoxynivalenol. *Archives of Toxicology*, 93(6), 1729–1743. <https://doi.org/10.1007/s00204-019-02459-w>
- Wu, F., Zhou, Y., Shen, Y., Sun, Z., Li, L., & Li, T. (2022). Linking Multi-Omics to Wheat Resistance Types to *Fusarium* Head Blight to Reveal the Underlying Mechanisms. *International Journal of Molecular Sciences*, 23(4). <https://doi.org/10.3390/ijms23042280>
- Wu, L., He, X., He, Y., Jiang, P., Xu, K., Zhang, X., & Singh, P. K. (2022). Genetic sources and loci for *Fusarium* head blight resistance in bread wheat. *Frontiers in Genetics*,

- 13(September), 1–12. <https://doi.org/10.3389/fgene.2022.988264>
- Xu, X. M., Monger, W., Ritieni, A., & Nicholson, P. (2007). Effect of temperature and duration of wetness during initial infection periods on disease development, fungal biomass and mycotoxin concentrations on wheat inoculated with single or combinations of *Fusarium* species. *Plant Pathology*, 56(6), 943–956. <https://doi.org/10.1111/j.1365-3059.2007.01650.x>
- Xu, X. M., Nicholson, P., Thomsett, M. A., Simpson, D., Cooke, B. M., Doohan, F. M., Brennan, J., Monaghan, S., Moretti, A., Mule, G., Hornok, L., Giczey, G., Ritieni, A., & Edwards, S. G. (2008). Relationship between the fungal complex causing *Fusarium* head blight of wheat and environmental conditions. *Phytopathology*, 98(1), 69–78. <https://doi.org/10.1094/PHYTO-98-1-0069>
- Xu, X. M., Parry, D. W., Nicholson, P., Thomsett, M. A., Simpson, D., Edwards, S. G., Cooke, B. M., Doohan, F. M., Brennan, J. M., Moretti, A., Tocco, G., Mule, G., Hornok, L., Giczey, G., & Tatnell, J. (2005). Predominance and association of pathogenic fungi causing *Fusarium* head blight in wheat in four European countries. *European Journal of Plant Pathology*, 112(2), 143–154. <https://doi.org/10.1007/s10658-005-2446-7>
- Yang, H., & Luo, P. (2021). Changes in photosynthesis could provide important insight into the interaction between wheat and fungal pathogens. *International journal of molecular sciences*, 22(16), 8865. <https://doi.org/10.3390/ijms22168865>
- Yang, S., Li, Y., Chen, Y., Liu, T., Zhong, S., Ma, L., Zhang, Y., Zhang, H., Yu, D., & Luo, P. (2020). Wheat resistance to *Fusarium* head blight is associated with changes in photosynthetic parameters. *Plant Disease*, 104(4), 841–852. <https://doi.org/10.1094/PDIS-04-14-0398-17>
- Yemaliyev, T. M., Nurbekova, Z., Mukiyanova, G., Akbassova, A., Sutula, M., Zhagazin, S., Bari, A., Tleukuleva, Z., Shamekova, M., Masalimov, Z. K., & Omarov, R. T. (2016). The involvement of ROS producing aldehyde oxidase in plant response to *Tombusvirus* infection. *Plant Physiology and Biochemistry*, 109, 36–44. <https://doi.org/10.1016/j.plapny.2016.09.001>
- Yli-Mattila, T. (2011). Detection of trichothecene-producing *Fusarium* species in cereals in northern Europe and Asia. *Agronomy Research*, 9, 521–526.
- Yli-Mattila, Tapani, Rämö, S., Hietaniemi, V., Hussien, T., Carlobos-Lopez, A. L., & Cumagun, C. J. R. (2013). Molecular quantification and genetic diversity of toxigenic *Fusarium* species in northern Europe as compared to those in southern

- europa. *Microorganisms*, 1(1), 162–174.
<https://doi.org/10.3390/microorganisms1010162>
- Yusuf, M. A., Kumar, D., Rajwanshi, R., Strasser, R. J., Tsimilli-Michael, M., Choudhury, S., & Sarin, N. B. (2010). Overexpression of γ -tocopherol methyl transferase gene in transgenic *Brassica juncea* plants alleviates abiotic stress: Physiological and chlorophyll a fluorescence measurements. *Biochimica et Biophysica Acta Bioenergetics*, 1797(8), 1428–1438. <https://doi.org/10.1016/j.bbabio.2010.02.002>
- Zadoks, J. C., Chang, T. T., & Konzak, C. F. (1974). A decimal code for the growth stages of cereals. *Weed Research*, 14(6), 415–421.
- Zander, M., La Camera, S., Lamotte, O., Métraux, J. P., & Gatzwiler, C. (2010). Arabidopsis thaliana class-II TGA transcription factors are essential activators of jasmonic acid/ethylene-induced defense responses. *The Plant Journal*, 61(2), 200–210.
<https://doi.org/10.1111/j.1365-3113.2009.04044.x>
- Zechmann, B. (2020). Subcellular Roles of Glutathione in Mediating Plant Defense during Biotic Stress. *Plants*, 9(9), 1067. <https://doi.org/10.3390/plants9091067>
- Zeier, J. (2013). New insights into the regulation of plant immunity by amino acid metabolic pathways. *Plant, Cell & Environment*, 36(12), 2085–2093.
<https://doi.org/10.1111/pce.12122>
- Zhang, G. L., Feng, L. L., Song, J. L., & Zhou, X. S. (2018). Tricaraleone: A Mycotoxin With Different Toxic Effect in Domestic and Laboratory Animals' Granulosa Cells. *Frontiers in Genetics*, 9(December), 1–8. <https://doi.org/10.3389/fgene.2018.00667>
- Zhang, Y., Terrero, M. J., Lassner, M., & Li, W. (2003). Knockout Analysis of Arabidopsis Transcription Factors TGA2, TGA5, and TGA6 Reveals Their Redundant and Essential Roles in Systemic Acquired Resistance. *Plant Cell*, 15(11), 2647–2653.
<https://doi.org/10.1105/tpc.014601>
- Zhao, J., Cheng, T., Xu, W., Han, X., Zhang, J., Zhang, H., Wang, C., Fanning, S., & Li, F. (2021). Natural co-occurrence of multi-mycotoxins in unprocessed wheat grains from China. *Food Control*, 130. <https://doi.org/10.1016/j.foodcont.2021.108321>
- Zhu, Z., Hao, Y., Mergoum, M., Bai, G., Humphreys, G., Cloutier, S., Xia, X., & He, Z. (2019). Breeding wheat for resistance to Fusarium head blight in the Global North: China, USA, and Canada. *Crop Journal*, 7(6), 730–738.
<https://doi.org/10.1016/j.cj.2019.06.003>

Web sources

<https://www.fao.org/faostat/en/#home> (accessed on February 3rd 2025)

Ocjena rada
u tieku

Ocjena rada
u tijeku

7. SUMMARY

Wheat today represents one of the most extensively cultivated crops globally and one of the most adaptable cereals, growing in multiple environments. Climate change in recent years has heightened the risk of biotic stress by expanding larger pathogen populations, more frequent disease outbreaks, and enhanced spread of disease to new areas. Fusarium head blight (FHB), as one of the most destructive and extensively studied fungal diseases, affects wheat on a worldwide scale. It is particularly dangerous due to significant reductions in grain yield and degradation of grain quality during epidemic years. Apart from the deterioration of wheat grain yield and quality, wheat food or feed can often be contaminated with mycotoxins produced by *Fusarium* fungi. Since resistance to FHB is a quantitatively inherited trait affected by environmental factors, the effective management of FHB cannot be accomplished with only one control method. Thus, breeding for resistance combined with other control measures could be the most sustainable solution. This study aimed to determine the impact of FHB on winter wheat genotypes that differ in the level of resistance to FHB. The aim was achieved through the determination of the impact of the disease on the synthesis of mycotoxins and polar metabolites in wheat grain from field experiments at two experimental locations, Osijek and Tovarnik, as well as through the determination of the biochemical, physiological, and molecular response of wheat spikes to FHB in the controlled conditions. Results from the field experiments showed that the experimental location, Tovarnik, exhibited higher precipitation and temperatures during the winter wheat flowering stage compared to the experimental location, Osijek. Consequently, the epidemic FHB conditions, induced by artificial inoculations, resulted in more pronounced disease symptoms and elevated levels of *Fusarium* metabolites at the experimental location Tovarnik. Nevertheless, elevated mycotoxin levels were higher in genotypes susceptible to FHB compared to the moderately resistant and resistant genotypes at both experimental locations. Furthermore, it can be concluded that culmorin (CUL) may play a certain role in *Fusarium* virulence. This was supported by the fact that increased CUL and hydroxyculmorin levels were observed in winter wheat genotypes with higher deoxynivalenol concentrations. Metabolomic analysis of polar metabolites in wheat grain resulted in the identification of 18 metabolites which varied among treatments at both experimental locations together. Following principal component analysis (PCA) of metabolite profiles, metabolites observed near the moderately resistant and resistant genotypes on the PCA biplot belonged to the functional groups of carbohydrates and derivatives, amino acids and derivatives, and polyphenols and derivatives. Based on these results, it can be

concluded that these metabolites impact FHB resistance. Since photosynthesis functions as a basis for signal transduction in plant immune defence, chlorophyll *a* fluorescence and photosynthetic pigments were measured. Results showed that severe FHB stress adversely impacted photosynthetic efficiency in wheat spikes in almost all genotypes studied, particularly in those susceptible to FHB, which was evident as a more pronounced decrease of quantum yield of primary photochemistry and performance index on absorption basis. In addition, the main photosynthetic pigments (chlorophyll *a* and *b*) did not show a uniform trend of response to inoculation. However, the increase of carotenoids caused by more pronounced stress in FHB-susceptible genotypes might imply the utilisation of alternative defence mechanism against the pathogen attack. Measurement of oxidative stress indicators, lipid peroxidation level and hydrogen peroxide (H₂O₂) content showed the highest increase in lipid peroxidation and H₂O₂ content in FHB-susceptible genotypes, indicating more cellular damage than in moderately resistant and resistant genotypes. Stress induced by artificial inoculations resulted in decreased activities of catalase, ascorbate peroxidase, monodehydroascorbate reductase (MDHAR), and dihydroascorbate reductase (DHAR) in FHB-susceptible genotypes. This may imply a more important role of glutathione peroxidase (GPx) in reactive oxygen species (ROS) scavenging, which maintained high activity levels in almost all genotypes studied. In addition, decreased MDHAR and DHAR activities in susceptible genotype may imply insufficient ascorbate recycling. Increased glutathione S-transferase (GST) activity in all genotypes except the most susceptible one might imply that GST plays an important role in detoxifying *Fusarium* mycotoxins. Although moderately resistant and resistant genotypes also reduced certain enzyme activities in FHB-inoculated spikes, this could be explained by their earlier activation immediately after inoculations. Despite increased glutathione reductase activity, significantly increased oxidised glutathione concentrations in nearly all genotypes might indicate that GSH is not successfully recycled, while increased glutathione (GSH) levels in FHB-susceptible genotypes may result from *de novo* GSH synthesis, implying higher GSH consumption and elevated cytosolic oxidation. Furthermore, increased GSH consumption could also be a consequence of GSH participation in direct or the indirect removal of ROS in wheat cells, as well as in maintaining other antioxidants, such as AsA and α -tocopherol, in a reduced state. Furthermore, enzymes such as glyoxalase I, glutathione peroxidases, and GST, also use GSH in their detoxification reactions. Almost each of these reactions, with the exception of reactions catalyzed by GST and glyoxalase I, results in

the formation of GSSG. Increased abscisic acid (ABA) levels in FHB-susceptible genotypes may indicate that ABA accumulation likely lowers FHB tolerance, while inconsistent salicylic acid (SA) levels in the studied genotypes could indicate that SA plays a crucial role in the very early stages of FHB infection, following the activation of jasmonic acid-mediated pathway. Except the biochemical level, the wheat response was monitored at the molecular level, too. Relative expression of *PR1*, *PR3*, and *PR5* genes was increased in all genotypes, expression of *TGA2* only in susceptible genotypes, and expression of *NPR1* gene only in resistant genotype. Since it has been shown that *NPR3*, which promotes *NPR1* degradation, has a low affinity for SA, low SA levels should reduce *NPR1* degradation. Lower SA levels in resistant genotype in the current study might be the reason why there was an increase of *NPR1* in resistant genotype even on 10 dpi. This research contributes to characterising and better understanding of the defence mechanisms of winter wheat genotypes resistant to FHB. It also contributes to gaining deeper insight into mycotoxins and polar metabolites, as well as detection of physiological, biochemical, and molecular processes of wheat related to resistance or susceptibility to FHB. Better understanding of metabolic, biochemical, and physiological mechanisms in response to FHB stress will contribute to the improvement of breeding programmes for FHB resistance in the early stages of selection.

Ocjena rada
u tijeku

8. SAŽETAK

Pšenica danas predstavlja jedan od najšire uzgajanih usjeva u svijetu i jednu od najprilagodljivijih žitarica koja raste u različitim okolišnim uvjetima. Klimatske promjene posljednjih godina povećavaju rizik od biotičkog stresa širenjem većine populacija patogena, češćim razvojem i pojačanim širenjem bolesti na nova područja. Fuzarijska palež klasa (FHB), kao jedna od najdestruktivnijih i najopsežnije proučavanih gljivičnih bolesti pšenice, pogađa pšenicu u čitavom svijetu. Bolest je osobito opasna zbog značajnih smanjenja uroda zrna, te degradacije kvalitete zrna tijekom epidemijske godina. Osim pogoršanja uroda i kvalitete zrna pšenice, ljudska ili stočna psionična krmna često može biti kontaminirana mikotoksinima koje proizvode vrste poput *Fusarium*. Budući da je otpornost na FHB kvantitativno nasljedno svojstvo na koje utječu čimbenici okoliša, učinkovito suzbijanje ove bolesti ne može se postići samo jednom metodom kontrole. Stoga bi oplemenjivanje na otpornost u kombinaciji s drugim mjerama kontrole moglo predstavljati najodrživije rješenje. Cili ovog istraživanja bio je utvrditi utjecaj FHB na genotipove ozime pšenice koji se razlikuju po stupnju otpornosti na FHB. Cilj je postignut utvrđivanjem utjecaja bolesti na sintezu mikotoksina i polarnih metabolita u zrnu pšenice iz poljskih pokusa na dvije lokacije, Osijek i Tovarnik, kao i određivanje mikotoksičkog, fiziološkog i molekularnog odgovora klasova pšenice na FHB u kontroliranim uvjetima. Rezultati poljskih pokusa pokazali su da je lokacija Tovarnik imala veće temperature i više temperature u blizini ozime pšenice u odnosu na lokaciju Osijek. Kao posljedica toga uvijek epidemije FHB izazvane umjetnim infekcijama, rezultirali su izraženijim simptomima bolesti i povišenim razinama *Fusarium* metabolita na lokaciji Tovarnik. Ipak, razine mikotoksina bile su više kod genotipova osjetljivih na FHB u usporedbi s umjereno otpornim i otpornim genotipovima na obje lokacije. Nadalje, može se zaključiti da kulorin (CUL) može imati određenu ulogu u virulenciji *Fusariuma*. Ovakvi zaključci potkrijepljeni su činjenicom da su povećane razine CUL i hidrksikulmorina uočene u genotipovima ozime pšenice s višim koncentracijama deoksivalenola. Analiza polarnih metabolita u zrnu pšenice rezultirala je identifikacijom 18 metabolita koji su varirali među tretmanima na obje lokacije. Nakon analize glavnih komponenti (PCA), metaboliti uočeni u blizini umjereno otpornih i otpornih genotipova na PCA biplotu pripadali su funkcionalnim skupinama ugljikohidrata i njihovim derivatima, aminokiselinama i njihovim derivatima te polifenola i njihovim derivatima. Na temelju ovih rezultata može se zaključiti da takvi metaboliti utječu na otpornost na FHB. Budući da fotosinteza predstavlja osnovu za prijenos signala u imunološkoj obrani biljaka, mjerena je fluorescencija klorofila *a* te fotosintetski

pigmenti. Rezultati su pokazali da je jak FHB stres nepovoljno utjecao na fotosintetsku učinkovitost u klasovima pšenice u gotovo svim proučavanim genotipovima, posebno u onima osjetljivim na FHB, što je vidljivo kao izraženije smanjenje maksimalnog kvantnog prinosa primarne fotokemije i indeksa učinkovitosti na bazi apsorpcije. Glavni fotosintetski pigmenti (klorofil *a* i *b*) nisu pokazali ujednačen trend odgovora na inokulacije, povećanje karotenoida uzrokovano izraženijim stresom kod genotipova osjetljivih na FHB može upućivati na korištenje alternativnih obrambenih mehanizama protiv napada patogena. Mjerenje pokazatelja oksidativnog stresa, razine lipidne peroksidacije i sadržaja vodikovog peroksida (H_2O_2) pokazalo je najveći porast lipidne peroksidacije i sadržaja H_2O_2 kod genotipova osjetljivih na FHB, što ukazuje na veća oštećenja stanica nego kod umjereno otpornih i otpornih genotipova. Stres izazvan umjetnim inokulacijama rezultirao je smanjenom aktivnošću katalaze, askorbat peroksidaze, monodehidroaskorbat reduktaze (MDHAR) i dehidroaskorbat reduktaze (DHAR) u genotipovima osjetljivim na FHB. Takvi rezultati mogu upućivati na važniju ulogu enzima gvajakol peroksidaze (GPOR) u uklanjanju reaktivnih kisikovih vrst (ROS-a) koji je zadržao slične aktivnosti u gotovo svim proučavanim genotipovima. Osim toga, smanjene aktivnosti MDHAR i DHAR u osjetljivim genotipovima mogu značiti nedovoljno recikliranje askorbata (AsA) povećana aktivnost glutation S-transferaze (GST) kod svih genotipova osim kod najosjetljivijeg može značiti da GST igra važnu ulogu u detoksikaciji mikotoksina. Iako su umjereno otporni i otporni genotipovi kod smanjenja određene aktivnosti enzima inokuliranim klasovima, takva smanjenja mogu se objasniti ranijom aktivnošću enzima antioksidativnog sustava, neposredno nakon inokulacije. Unatoč povećanoj aktivnosti glutation reduktaze (GR), značajno povećane koncentracije oksidiranog glutationa (GSSG) u gotovo svim genotipovima mogu ukazivati na činjenicu da GSH nije uspješno recikliran, dok povećane razine reduciranog glutationa (GSH) u genotipovima osjetljivim na FHB mogu biti rezultat *de novo* sinteze GSH te ukazivati na veću potrošnju GSH i posljedično povećanu oksidaciju citosola. Nadalje, povećana potrošnja GSH također može biti posljedica sudjelovanja GSH u izravnom ili neizravnom uklanjanju ROS-a u stanicama pšenice, kao i u održavanju drugih antioksidansa, poput AsA i α -tokoferola, u reduciranom stanju. Nadalje, enzimi kao što su glioksalaza I, glutation peroksidaze i GST, također koriste GSH u svojim reakcijama detoksikacije. Gotovo svaka od ovih reakcija, s izuzetkom reakcija kataliziranih GST-om i glioksalazom I, dovodi do stvaranja GSSG-a. Povećane razine apscizinske kiseline (ABA) u genotipovima osjetljivim na FHB mogle bi

značiti da nakupljanje ABA vjerojatno smanjuje toleranciju na FHB, dok su različite razine salicilne kiseline (SA) u proučavanim genotipovima vjerojatno posljedica ključne uloge SA u vrlo ranim fazama infekcije FHB, nakon čega je uslijedila inokulacija puta posredovanog jasmonskom kiselinom. Osim na biokemijskoj razini, odgovor pšenice praćen je i na molekularnoj razini. Relativna ekspresija gena *NPR1*, *PR3* i *PR5* bila je povećana kod svih genotipova, ekspresija *TGA2* samo kod osjetljivih genotipova, a ekspresija gena *NPR1* samo kod otpornog genotipa. Budući da je pokazano da *NPR3* koji potiče razgradnju *NPR1* ima nizak afinitet za SA, niske razine SA smanjuju razgradnju *NPR1*. Niže razine SA u otpornom genotipu u trenutnom ispitivanju mogu biti razlog zašto je došlo do povećanja *NPR1* u otpornom genotipu čak i deseti dan nakon inokulacija. Ovo istraživanje pridonosi karakterizaciji i boljem razumijevanju obrambenih mehanizama genotipova ozime pšenice otpornih na FHB. Također doprinosi stjecanju dubljeg uvida u mikotoksine i polarne metabolite, kao i detekciji fizioloških, biokemijskih i molekularnih procesa pšenice povezanih s otpornošću ili osjetljivošću na FHB. Bolje razumijevanje metaboličkih, biokemijskih i fizioloških mehanizama kao odgovor na stres uzrokovan FHB doprinit će poboljšanju programa oplemenjivanja na otpornost na FHB u ranim fazama selekcije.

Ocjena rada
u tijeku

9. SUPPLEMENTARY MATERIAL

Supplementary table 1. Spearman correlation matrix of 18 wheat metabolites in grain and root resistance to *Fusarium*. Marked correlations are significant at $p < 0.05$ (N=48).

	Guanosine	Piperidine-2-carboxylic acid	3-hydroxydodecanoic acid	2-hydroxyhippuric acid	Secologanin	2-deoxyguanosine	5,7-dihydroxyflavone	Histidine	3-hydroxyflavone	3-(2,4-dihydroxyphenyl)-propanoic acid	α-tocopherol acetate	Lactic acid dimer	Pyrrrole-2-carboxylic acid	4-hydroxybenzoic acid	Resistance	Sophorose	5-hydroxytryptophan	Cellobiitol	Turanose
Guanosine	1																		
Piperidine-2-carboxylic acid	0.3544122	1																	
3-hydroxydodecanoic acid	0.396085	0.3356687	1																
2-hydroxyhippuric acid	0.2738975	0.3726912	0.1668704	1															
Secologanin	0.01192093	0.2114998	-0.02762011	0.3590677	1														
2-deoxyguanosine	0.05373191	0.2610325	0.2880574	-0.1376538	0.1996795	1													
5,7-dihydroxyflavone	0.145499	0.2695766	0.1298751	0.1510146	0.1129221	0.1743712	1												
Histidine	-0.3919653	-0.4179789	-0.255545	-0.1881008	-0.2828012	-0.2107621	0.923046	1											
3-hydroxyflavone	-0.4402726	-0.4418074	-0.2857259	-0.2474742	-0.2599805	-0.1466587	0.009451	0.92995 ***	1										
3-(2,4-dihydroxyphenyl)-propanoic acid	-0.4557103	-0.3551278	-0.335442	-0.1467561	-0.1620638	-0.0000000	-0.207141	0.9479 ***	0.927212 ***	1									
α-tocopherol acetate	-0.3495683	-0.3756042	-0.2968856	-0.1196632	-0.1930639	-0.1852445	0.09364222	0.1836 ***	0.9065164 ***	0.9154563 ***	1								
Lactic acid dimer	-0.3007982	-0.1738812	-0.4098352	-0.1239068	-0.2871000	0.1443041	0.0000039	-0.08348265	0.06386445	-0.08487416	0.074342	1							
Pyrrrole-2-carboxylic acid	-0.3925391	0.1045514	-0.1568958	0.01963713	-0.07571972	0.0372709	-0.1150000	-0.02739317	-0.08699902	0.04911623	0.07779407	0.3200000	1						
4-hydroxybenzoic acid	-0.1138357	0.156368	0.02096687	-0.04485072	-0.1397061	-0.0000014	0.08296208	-0.2040079	-0.2150947	-0.1457745	0.2131664	0.3200000	0.3842853	1					
Resistance	-0.2935481	-0.3048723	-0.349392	-0.2825700	-0.3300000	-0.3048556	0.3610762	0.3170849	0.3073900	0.2849100	0.289356	0.1812067	0.2425049	0.2766107	1				
Sophorose	0.5227081 ***	-0.316354	-0.2040617	0.0200016	-0.0140000	-0.0711370	-0.0124647	0.2642037	0.2710341	0.2900000	0.2830000	0.3824224	0.0000000	0.2425049	0.2766107	1			
5-hydroxytryptophan	0.534354 ***	-0.2723397	-0.0000000	-0.0000000	-0.0000000	-0.0000000	-0.1086248	0.3113277	0.0000000	0.0000000	0.0000000	0.0000000	0.3059379	0.2344124	0.3310449	0.8038604 ***	1		
Cellobiitol	0.5550024 ***	-0.353417	-0.1916366	-0.0000000	-0.0000000	-0.08537066	-0.089388	-0.1750749	0.2306268	0.2000000	0.168376	0.2000000	0.1757538	0.2749416	0.3181873	0.7643542 ***	0.6725451 ***	1	
Turanose	-0.398755	-0.3124563	-0.0390400	-0.1880000	-0.103075	-0.08570278	-0.165066	0.2110000	0.2039000	0.2190000	0.1699497	0.0000000	0.1605455	0.1892843	0.2218451	0.7772384 ***	0.7666021 ***	0.7994533 ***	1

Ocjena rada
u tijeku

10. CURRICULUM VITAE

Katarina Šunić Budimir was born on August 21, 1994, in Slavonski Brod. In 2013, she graduated from "Matija Mesić" High School in Slavonski Brod. After completing high school, she enrolled in the undergraduate program in Biology at the Department of Biology at Josip Juraj Strossmayer University of Osijek. She earned her Bachelor of Science in Biology in 2016. In the same year, she continued her education by enrolling in the graduate program in Biology at the same university. She graduated in 2017, earning the title of Master of Science in Biology. During her studies, she was a member of the ZOA student association and she participated in various science popularization activities. At the end of March 2021, Katarina was employed at the Department of Breeding and Genetics of Small Grain Cereals at the Agriculture Institute in Osijek. She worked on the project "Response of Winter Wheat to Biotic and Abiotic Stresses Caused by Climate Change," led by Dr. Valentina Španić. In the 2022-2023 academic year, she enrolled in a postgraduate interdisciplinary university study of Molecular Biosciences. In 2021, she completed a two-week professional training program at the Department of Molecular Genetics at the Leibniz Institute of Plant Genetics and Crop Plant Research (IPK Gatersleben) in Gatersleben, Germany. In 2023, as part of the ERASMUS+ mobility program, she completed two months of traineeship at Helmholtz Zentrum Munich, Germany. In 2024, she participated in two additional programs: a two-week internship at the Helmholtz Zentrum in Munich, Germany, and a five-day visit to the Universitaire de Technologie de Béthune (UT) in Béthune, France, as part of the ERASMUS+ Blended Intensive Program.

She has participated in several scientific conferences and has published four papers as the first author in journals indexed in the Current Contents database. Additionally, she has co-authored seven papers and contributed a chapter to a monograph as a co-author. She is a member of the Alumni Association of the Department of Biology at Josip Juraj Strossmayer University of Osijek (Alumni BiolOs) and the European Association for Research on Plant Breeding (Eucarpia). She received the 2023 the State Science Award in the category Annual Award for the Young Researchers/Scientists for biotechnical sciences.

Ocjena rada
u tijeku

11. PUBLICATION LIST

Original scientific and review articles

1. Španić, Valentina; Duvnjak, Jurica; **Šunić Budimir, Katarina**; Drenjančević, Luka; Jukić, Goran; Varnica, Ivan. Measuring the Effects of Different Sowing Dates of Winter Wheat // *International Journal of Plant Production*, 19 (2025), 2; 1, 8.
2. Španić, Valentina; **Šunić Budimir, Katarina**; Duvnjak, Jurica; Lukić, Zvonimir; Drenjančević, Luka; Jukić, Goran; Varnica, Ivan. DUS Testing Characteristics Related with Agro-morphological and Quality Traits of Winter Wheat // *Agronomski glasnik*, 5 (2024), 5, 147-152.
3. **Šunić, Katarina**; Španić, Valentina. Genetic Biofortification of Winter Wheat with Selenium (Se) // *Plants*, 13 (2024), 1816, 15.
4. Španić, Valentina; Duvnjak, Jurica; **Šunić, Katarina**; Jukić, Goran; Varnica, Ivan. The Effects of Different Sowing Dates on Winter Wheat // *Poljoprivreda (Osijek)*, 29 (2023), 2; 16-21.
5. **Šunić, Katarina**; D'Auria, John Charles; Sarkar, Bojan; Španić, Valentina. Metabolic Profiling Identifies Changes in the Winter Wheat Grain Following *Fusarium* Treatment at Two Locations in Croatia // *Plants*, 12 (2023), 911, 11.
6. Španić, Valentina; **Šunić, Katarina**; Duvnjak, Jurica; Yin Gang, Lu; Katanić, Zorana. Chlorophyll *a* fluorescence during flag leaf senescence of field-grown winter wheat plants under drought conditions // *Journal of applied biology*, 10 (2023), 1; 86-92.
7. **Šunić, Katarina**; Brkijčić, Lidija; Vuković, Rosemary; Katanić, Zorana; Salopek-Sondi, Branka; Španić, Valentina. *Fusarium* Head Blight Infection Induces Responses of Six Winter Wheat Varieties in Ascorbate-Glutathione Pathway, Photosynthetic Efficiency and Stress Hormones // *Plants*, 12 (2023), 21; 2020, 20.
8. Španić, Valentina; **Šunić, Katarina**; Duvnjak, Jurica; Babić, Jurislav; Drezner, Georg. Winter wheat grain yield response to fungicide application at different stages and fusarium head blight is rather influenced by variety and year // *Romanian agricultural research*, 40 (2023), 1-13.
9. Vuković, Rosemary; Štolfa Čamagajevac, Ivna; Vuković, Ana; **Šunić, Katarina**; Begović, Lidija; Mlinarić, Selma; Sekulić, Ramona; Sabo, Nikolina; Španić, Valentina. Physiological, Biochemical and Molecular Response of Different Winter Wheat Varieties under Drought Stress at Germination and Seedling Growth Stage // *Antioxidants*, 11 (2022), 4; 1-26.

10. Španić, Valentina; **Šunić, Katarina**; Zdunić, Zvonimir; Drezner, Georg. Genetic Ability and Seedling Drought Characterization of Winter Wheat Lines in Croatia // *Agronomski glasnik*, 83 (2021), 5-6; 281-294.

11. **Šunić, Katarina**; Kovač, Tihomir; Lončarić, Ante; Babić, Jurislav; Sulyok, Michael; Krska, Rudolf; Drezner, Georg; Španić, Valentina. *Fusarium* Secondary Metabolite Content in Naturally Produced and Artificially Provoked FHB Pressure in Winter Wheat // *Agronomy*, 11 (2021), 2239, 19.